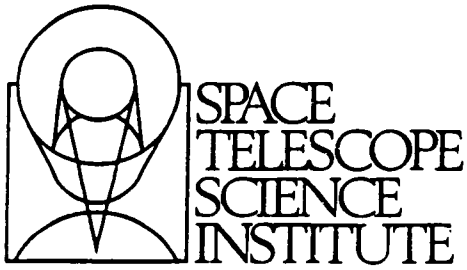

NASA-CR-189749
19920008941

Hubble Space Telescope

Goddard High Resolution Spectrograph Instrument Handbook

Version 2.1

May 1990

Revision History

Handbook Version 1.0	October 1985; written by Dennis Ebbets
Handbook Version 2.0	May 1989; written by Douglas K. Duncan & Dennis Ebbets
Handbook Version 2.1	May 1990; revised by Douglas K. Duncan

The Space Telescope Science Institute is operated by the Association of Universities for Research in Astronomy, Inc., for the National Aeronautics and Space Administration.

SCREEN IMAGE USER=>EBB SESSION=T20BR08 4/15/92-10:09:20-AM

DISPLAY 92N18183/2

92N18183># ISSUE 9 PAGE 1553 CATEGORY 89 RPT#: NASA-CR-189749 NAS 1.26:189749 CNT#: NAS5-26555 90/05/00 103 PAGES UNCLASSIFIED DOCUMENT

Revised

TITL: Hubble Space Telescope: Goddard high resolution spectrograph instrument handbook, Version 2.1

AUTH: A/DUNCAN, DOUGLAS K.; B/EBBETS, DENNIS PAA: B/(Ball Aerospace Systems Div., Boulder, CO.)

CORP: Space Telescope Science Inst., Baltimore, MD.

SAP: Avail: NTIS HC/MF A06

CIO: UNITED STATES

MAJS: /*ASTRONOMY/*HANDBOOKS/*HUBBLE SPACE TELESCOPE/*IMAGING TECHNIQUES/*SATELLITE-BORNE INSTRUMENTS/*ULTRAVIOLET SPECTROMETERS

MINS: / CHROMOSPHERE/ COMETS/ CORONAS/ FEASIBILITY/ HIGH RESOLUTION/ INTERSTELLAR MATTER/ PLANETARY ATMOSPHERES/ STELLAR EVOLUTION/ STELLAR WINDS/ TEMPORAL RESOLUTION

ABA: Author

ABS: The Goddard High Resolution Spectrograph (GHRS) is an ultraviolet spectrometer which has been designed to exploit the imaging and pointing capabilities of the Hubble Space Telescope. It will obtain observations of astronomical sources with greater spectral, spatial and temporal resolution than has been possible with previous space-based instruments.

ENTER: MORE

SCREEN IMAGE USER=*EOB SESSION=120BR08 4/15/92-10:09:49-AM

DISPLAY 92N18183/2

Data from the GHRS will be applicable to many types of scientific investigations, including studies of the interstellar medium, stellar winds, chromospheres and coronae, the byproducts and endproducts of stellar evolution, planetary atmospheres, comets, and many kinds of extragalactic sources. This handbook is intended to introduce the GHRS to potential users. The main purpose is to provide enough information to explore the feasibility of possible research projects and to plan, propose and execute a set of observations. An overview of the instrument performance, which should allow one to evaluate the suitability of the GHRS to specific projects, and a somewhat more detailed description of the GHRS hardware are given. How observing programs will be carried out, the various operating modes of the instrument, and the specific information about the performance of the instrument needed to plan an observation are discussed.

ENTER:

GODDARD
HIGH RESOLUTION SPECTROGRAPH
INSTRUMENT HANDBOOK

Version 2.1

Douglas K. Duncan
Space Telescope Science Institute
3700 San Martin Drive, Baltimore, MD 21218

and

Dennis Ebbets
Ball Aerospace Systems Division
Boulder, Colorado

TABLE OF CONTENTS

LIST OF FIGURES

LIST OF TABLES

1.0 INTRODUCTION TO THE HIGH RESOLUTION SPECTROGRAPH

The GHRS is an ultraviolet spectrometer which has been designed to exploit the imaging and pointing capabilities of the Hubble Space Telescope. It will obtain observations of astronomical sources with greater spectral, spatial and temporal resolution than has been possible with previous space-based instruments. Data from the GHRS will be applicable to many types of scientific investigations, including studies of the interstellar medium, stellar winds, chromospheres and coronae, the byproducts and endproducts of stellar evolution, planetary atmospheres, comets, and many kinds of extragalactic sources.

This handbook is intended to introduce the GHRS to potential users. The main purpose is to provide enough information to explore the feasibility of possible research projects and to plan, propose and execute a set of observations. Chapter 2 presents an overview of the instrument performance, which should allow one to evaluate the suitability of the GHRS to specific projects. Chapter 3 presents a somewhat more detailed description of the GHRS hardware. It describes how observing programs will be carried out and defines the various operating modes of the instrument. Chapter 4 provides the specific information about the performance of the instrument needed to plan an observation. Chapter 5 outlines how to specify the program on HST proposal forms. There is a large literature of more detailed information about the hardware, software, operations, and data analysis available at the ST ScI. References to other available documents are also contained in Chapter 5. The data products which an astronomer can expect will be described in Chapter 6, along with an overview of the calibration and data reduction procedures.

This handbook was written in the spring of 1989; replacing the First Edition of 1985. The performance characteristics reported here are based on the results of an extensive program of testing and calibration at Ball Aerospace in Boulder, Colorado, and testing in Vacuum at Lockheed Missiles and Space Division in Sunnyvale, California. Most of the important properties will be measured and calibrated again during the post-launch Science Verification period. Quantities such as absolute photometric sensitivity, scattered light effects, precision of the wavelength scales, and instrumental overhead times will be subject to revision. We intend to maintain this handbook with updates to these and other important properties as the post-launch experience warrants. First notification of important changes will usually be given in the ST ScI *Institute Newsletter.*

Version 2.1, released in the spring of 1990 fixes a few typographical errors of version 2.0, and incorporates more recent timing estimates for ground system operations.

2.0 AN OVERVIEW OF THE IMPORTANT PERFORMANCE CHARACTERISTICS OF THE GHRS

2.1 SPECTRAL RANGE

The GHRS operates in the vacuum ultraviolet, in the wavelength range 1050 A to 3200 A. Shortward of 1200 A the efficiency is hampered by the magnesium fluoride coatings on the telescope mirrors and on the internal optics of the GHRS itself. The quantum efficiency of the CsTe detector decreases rapidly for wavelengths longer than 3200 A. For bright stars, some observations may be made out to 3400 A where ground based spectroscopy becomes possible.

2.2 SPECTRAL RESOLUTION

Three resolving powers are available with the GHRS. A low resolution grating can provide spectra with $R = \frac{\lambda}{\Delta\lambda} = 2000$ in the wavelength range 1050 A to 1800 A. Four separate medium resolution gratings will provide spectra with a resolving power of 20000 over the entire range of 1050 A to 3200 A. The highest spectral resolution, R = 100000, is achieved in two Echelle configurations which together cover the entire spectral range of the instrument.

2.3 WAVELENGTH SCALES

The optical and mechanical designs produce a simple and very stable spectral format, which can be calibrated to assign wavelengths with a routine accuracy of $\pm$ 1 pixel. This corresponds to uncertainties in radial velocity of approximately 150, 15, and 3 km s^{-1} in the low, medium, and high resolution configurations, respectively. If a scientific application requires greater precision, a special calibration exposure can be requested. In the Echelle configurations approximately 1 km s^{-1} accuracy can be achieved.

2.4 SENSITIVITY

The large collecting area of the telescope and the high efficiency of the optics and detectors contribute to the high sensitivity of the GHRS. As an example, consider an observation which achieves a signal to noise ratio of 10 with an exposure time of 1000 seconds. For a flux distribution resembling that of a lightly reddened B0V star, observations made between 1200 Å and 1500 Å can reach stars with visual magnitudes of approximately 19, 16 and 14 in the three GHRS resolving powers. Many galactic OB stars, white dwarfs and sub-dwarfs, luminous hot stars in the Magellanic Clouds, and even in nearby galaxies such as M31 and M33, will be observable with the GHRS.

2.5 PHOTOMETRIC ACCURACY

The design of the instrument, and much of the calibration effort has endeavored to maximize the photometric accuracy of the data. There are four basic characteristics which are recognized. (1) The absolute photometric calibration will be based on observations of standard stars. We expect that the accuracy of absolute flux measurements will be ~10% initially. (2) The relative accuracy of fluxes measured at widely different wavelengths should be substantially better, 2–5% initially. (3) The relative accuracy of fluxes measured over very narrow spectral regions, such as measurements of line profiles and central depths, should be 2–5% initially. As knowledge of the scattered light and small scale detector non-uniformities improves, accuracies of 1% or better should be realized. (4) The signal to noise ratio of the

data should be dominated by photon statistics for values up to about 60. At higher signal levels, small non-uniformities in the detector will have to be corrected for carefully. With care, signal to noise ratios of 100 or more should be achievable.

2.6 LINEARITY AND DYNAMIC RANGE

The GHRS uses Digicon detectors to record the spectrum. These are photon-counting detectors with no readout noise. One of the primary advantages of this type of device is the enormous dynamic range, limited by the extremely low background dark count at the faint end, and saturation of the pulse counting electronics at the bright end. In the GHRS these limits are approximately 3×10^{-4} and 150000 counts per channel per second, giving a dynamic range in excess of 10^7. The counts are accumulated into buffers with a capacity of 2^{16}, or 65535 counts per channel for a single observation.

2.7 TIME RESOLUTION

In its most common mode of operation, referred to as Accumulation Mode, the GHRS can obtain spectra with time resolution of approximately 10 seconds. However, by sacrificing certain operating features the time between observations can be made as short as 50 milliseconds in the Rapid Readout Mode. The GHRS itself does not impose any upper limit on the length of an observation. Exposures will be limited in practice by the duration of target visibility, and other external scheduling constraints.

2.8 SPATIAL RESOLUTION AND APERTURE MAPPING

The spatial resolution is determined by which of two entrance apertures is used. There is a Large Science Aperture (LSA; also called the **2.0** aperture), whose dimensions on the sky are 2 by 2 arc seconds square, and a Small Science Aperture (SSA; also called the **0.25** aperture), which is a one quarter arc second square. These apertures allow precise isolation of sources in crowded fields, rejection of light from brighter neighboring objects, and fine spatial definition for observations of extended sources. The GHRS has the ability to "map" its apertures, in typically 1/8 by 1/8 arc second steps, by scanning a small diode across them. The relation between the GHRS and ST coordinate systems is shown in Figure 2-1.

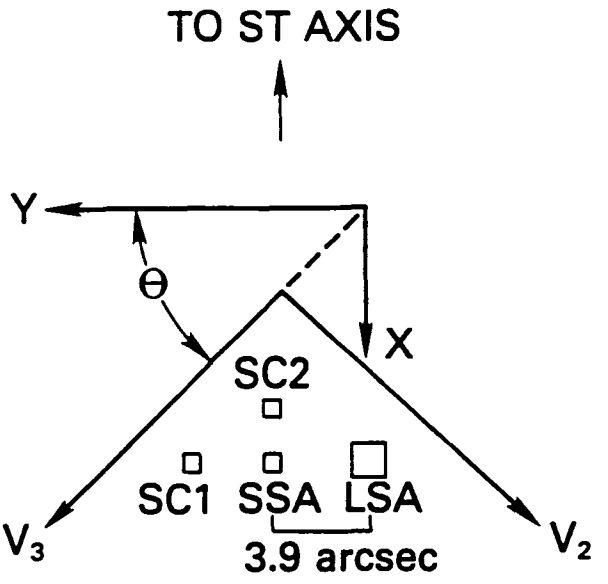

Figure 2-1. Relation between the GHRS and ST Coordinate Systems
V_2, V_3 and the ST coordinate system are illustrated in the *Call for Proposals*. The X-axis is the direction of dispersion of the GHRS. The GHRS apertures are located off the ST optical axis by approximately 5.55 arc-minutes in V_2 and 5.55 arc-minutes in V_3. (The WF/PC is the only on-axis instrument).

3.0 A DESCRIPTION OF THE DESIGN, CONSTRUCTION AND THE OPERATION OF THE GHRS

3.1 DESIGN AND CONSTRUCTION

3.1.1 Optics

The GHRS is basically a Czerny-Turner spectrograph. The excellent images provided by the HST allow the use of a very small entrance aperture. The Small Science Aperture is matched to the image of a point source, and allows the full resolving power of the instrument to be achieved. An off-axis parabolic collimator collects the light and directs it to a plane diffraction grating, in the process correcting the astigmatism which arises from the placement of the GHRS off the optical axis of HST. Dispersion is provided by one of six gratings, which are mounted on a rotating carousel. The desired optical element is positioned in the collimated beam by rotating this mechanism to the appropriate angle. The diffracted beam is then directed to one of four focusing optics. For the low and medium resolution gratings, two parabolic camera mirrors are used. Each grating directs its light to one of these mirrors, as determined by the alignment. There is one Echelle grating on the carousel. Its output can be directed to either of two concave cross-disperser gratings. One selects the orders containing the short wavelength spectral region (1050 A to 1700 A), while the other handles the orders containing the 1700 A to 3200 A region. The focusing optic directs the dispersed image to the photocathode of one of the two detectors. The detector associated with each camera and cross-disperser is fixed by the alignment, and is not user selectable.

In addition to these dispersive elements there are four optical plane elements which are used for target acquisition purposes. These have various sizes and reflectivities and project an undispersed image of the entrance apertures onto the detectors. The four elements allow a range of approximately 18 stellar magnitudes to be detected without saturating a detector. They are also mounted on the carousel, and are selected by positioning that mechanism to the appropriate angle.

There is no way to adjust the optical focus of the GHRS. All of the internal components were carefully aligned and focused during the assembly and testing, and are rigidly mounted on the optical bench. The focus of the telescope will be monitored and adjusted periodically to ensure that the entrance apertures of the GHRS, and of the other instruments as well, are properly illuminated.

As a reference for those who are interested in details, the numerical values of certain relevant design parameters are presented in Table 3-1. These values can be used with the grating equation and other optical relationships to predict the image size, linear dispersion, etc. The nominal scale of the HST focal plane is $3.58''$/mm.

3.1.1.1 Designation of the Spectral Element

The convention for naming a grating on the Science Institute's proposal forms is a five character word, of the form GWWWR. The prefix G identifies the element as a diffraction grating. The number WWW is the approximate center of its wavelength range in units of nanometers (Angstoms divided by 10). The suffix R indicates the relative resolving power, with L = "low," and M = "medium." The two high resolution Echelle configurations will be referred to simply as ECH-A and ECH-B. Some older documents use different grating designations. The four target acquisition mirrors are referred to as N1, N2, A1 and A2.

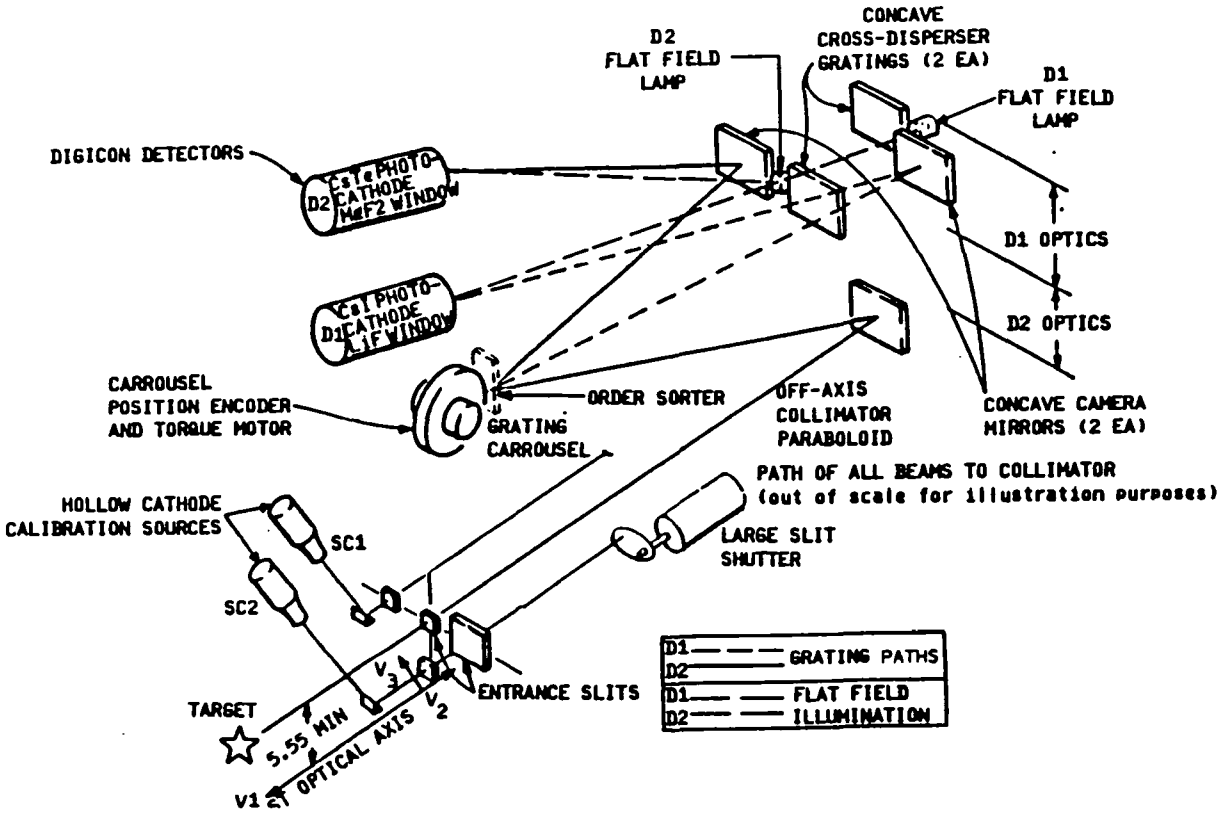

Figure 3-1 GHRS Optical Concept

TABLE 3-1

HRS Optical Design Parameters

Component	Clear Aperture mm	Focal Length mm	Grating Constant mm^{-1}	Blaze Angle Degrees	Order of Diffraction	Incidence Angle α degrees	Diffraction Angle β degrees	Deviation Angle $2\,\delta$ degrees	Detector	Description
LSA	0.559	–	–	–	–	–	–	–	D1,D2	Large Science Aperture
SSA	0.067	–	–	–	–	–	–	–	D1,D2	Small Science Aperture
Collimator	80	1850	–	–	–	–	–	–	D1,D2	
G140L	80	–	600	2.6	1	9.0 – 10.3	-5.3 – -4.0	14.25	D1	R=2000 grating
G140M	80	–	6000	23*	1	26 – 38	11 – 24	14.25	D1	R=20000 grating
G160M	80	–	4960	19*	1	21 – 33	14 – 27	6.25	D2	R=20000 grating
G200M	80	–	4320	26*	1	23 – 34	17 – 28	6.25	D2	R=20000 grating
G270M	80	–	3600	28*	1	27 – 38	20 – 32	6.25	D2	R=20000 grating
ECH-A	80	–	316	63.4	33–53	68 – 74	54 – 61	13.25	D1	R=100000 Echelle
ECH-B	80	–	316	63.4	17–33	63 – 72	58 – 66	5.75	D2	R=100000 Echelle
N2	80	–	–	–	–	–	–	–	D2	Most sensitive mirror
N1	80	–	–	–	–	–	–	–	D1	2nd most sensitive mirror
A2	20	–	–	–	–	–	–	–	D2	3rd most sensitive mirror
A1	20	–	–	–	–	–	–	–	D1	least sensitive mirror
Cam-A	84	1425	–	–	–	–	–	–	D1	camera for G140L, G140M, N1, A1
Cam-B	86	1350	–	–	–	–	–	–	D2	camera for G160M, G200M, 270M, N2, A2
CD-A	80	1460	195	0.75	1	–	–	–	D1	ECH-A cross disperser
CD-B	80	1340	86	0.54	1	–	–	–	D2	ECH-B cross disperser
D1	22 x 28	–	–	–	–	–	–	–	D1	LiF + CsI photocathode
D2	22 x 28	–	–	–	–	–	–	–	D2	MgF_2 + CsTe photocathode

* The holographic gratings do not have a true blaze angle, but are optimized for best performance in a restricted wavelength region. If this angle is used as a blaze angle, it predicts the center of the optimum region.

Those with the prefix N have "normal" reflectivity, and are used to acquire faint targets. Those with the letter A are "attenuated" to image brighter objects safely. Those with the number 1 work with detector D1, while the number 2 refers to detector D2.

3.1.2 Detectors

The GHRS contains two magnetically focused, photon counting digicon detectors, which differ only in the nature of their photocathodes. Each detector contains a digicon tube, a permanent magnet to provide a focusing field, a high voltage power supply to produce a 23kv accelerating field, magnetic deflection coils to direct the electron image to an array of silicon diodes, and a set of charge sensitive preamplifiers to detect the pulses produced when photoelectrons strike the diodes. Detector D1 has a CsI photocathode deposited on a LiF window. This tube has good quantum efficiency from 1050 A to about 1700 A, with a peak of 15% or so near 1300 A. It is extremely insensitive to longer wavelength light and is thus said to be "solar blind." The second detector, called D2, has a CsTe cathode on a MgF_2 window. Its sensitivity extends from 1150 to 3200 A.

The photoelectrons are detected by a linear array of 500 silicon diodes. Twelve additional diodes can be used for measuring background light, producing two dimensional images to assist with target acquisition, and monitoring the high energy charged particle environment in orbit. More details about the detectors are given in Section 4.4, and about the diode array in Section 4.4.5.

3.1.3 Calibration Lamps

There are four on-board lamps to assist with calibration needs. Two are Pt-Ne hollow cathode lamps, which produce a rich spectrum of emission lines. Each has its own aperture adjacent to the two science apertures. They are referred to as SC1 and SC2 for "spectral calibration" lamps 1 and 2. The light follows the same optical path through the instrument as that from the target star, and provides a precise fiducial for wavelength calibration. Both hollow cathode lamps can be used with all optical configurations and both detectors. The other two lamps are "flat-field" sources, which are used to calibrate the deflection coils, the discriminator threshold levels, and the small spatial irregularities in the detector sensitivity. Each flat field lamp is aligned to produce a uniform illumination of one of the detector photocathodes. They are identified as FF1 and FF2. Their light does not pass through any of the dispersive optics. These lamps radiate primarily in the 1470 A resonance line of Xe.

3.1.4 Mechanisms

The GHRS requires only two moving parts in routine operation. The primary mechanism is the carousel on which the gratings, Echelle, and target acquisition mirrors are mounted. Its rotation is controlled by brushless dc torque motors, and measured by 16 bit encoders. The other mechanism used routinely is a shutter which can cover the Large Science Aperture. Usually when a target is positioned in the Small Science Aperture, this shutter is closed to minimize stray light. There is no shutter to block the small aperture; however, stray light from this aperture will rarely be a problem.

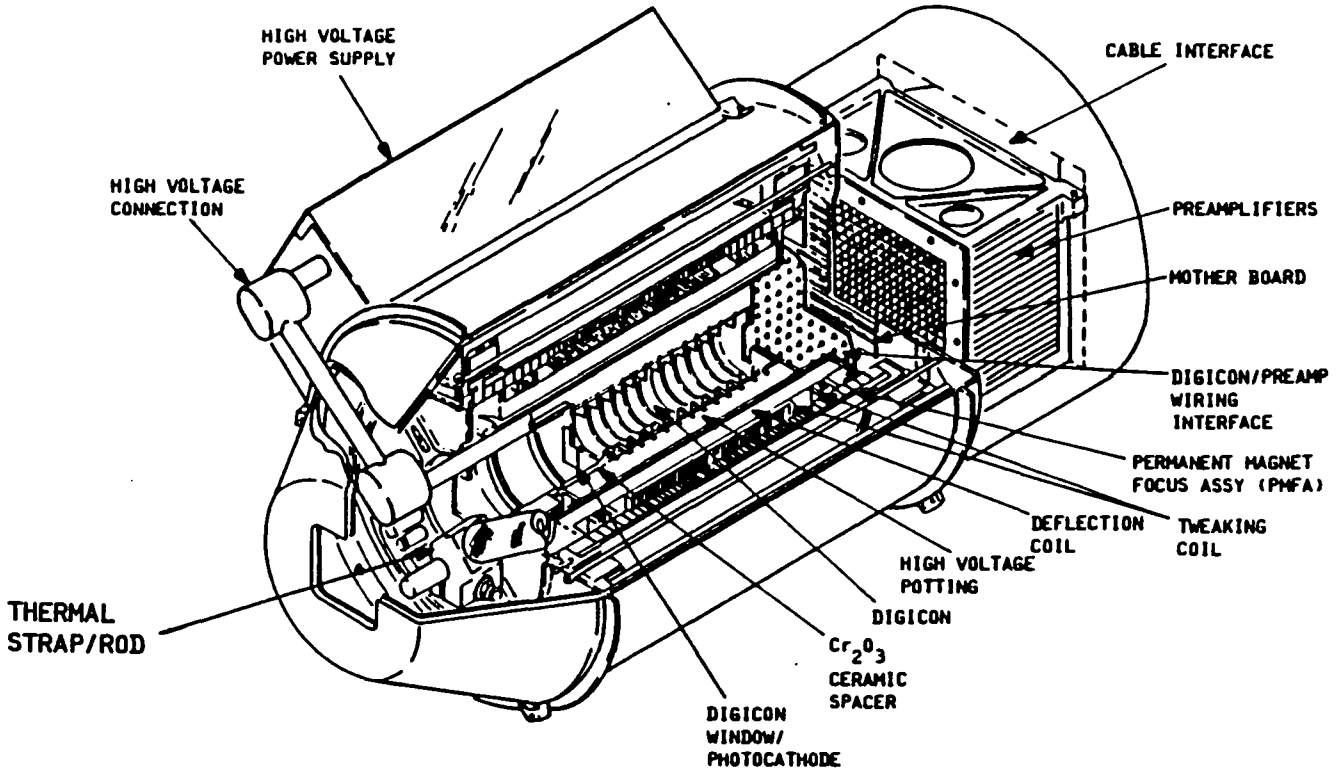

Figure 3-2. Anatomy of a Digicon Detector

3.1.5 Structures

The entrance apertures, all of the optical elements, the carousel, and the detectors are mounted on an optical bench. The bench is made of graphite epoxy which is light-weight, stiff, and very insensitive to temperature variations. It is temperature controlled to 21 ± 4C. Furthermore, it is designed to maintain the focus and alignment of the spectrograph during all of the ground-based activities, through launch, and in the presence of a variable thermal environment during orbital operations. The optical bench is attached to the focal plane structure of the telescope with a set of mechanical latches. The optical bench is surrounded by an enclosure which provides some additional mechanical strength, thermal isolation, and stray light control.

3.1.6 Control and Communication

The GHRS does not have its own microprocessor. The flight software is resident in the spacecraft Science Instrument Control and Data Handling computer. Commands are uplinked to the computer either as discrete instructions or as tables of parameters. A long series of related observations can be defined by an Observation Sequence Table (OST). The astronomer will define the observations on the proposal forms. The actual OST will be constructed by the operations ground system and loaded into memory at the appropriate time for execution by the flight software. There are five tasks which can be controlled automatically: (1) target acquisition, (2) instrument configuration, (3) data acquisition and exposure control, (4) science data readout, and (5) monitoring and ensuring the health and safety of the instrument. The software can perform real-time data quality control by detecting and rejecting counts due to a high radiation environment, cosmic ray "hits," and electrical noise. It can handle interruptions due to occultation of the target by the Earth, loss of Fine Guidance Sensor lock, or passage of the spacecraft through the South Atlantic Anomaly. The duration of an observation can be controlled by an "exposure meter" capability. Finally, the software allows for real-time interaction with the observer whenever a communications link is available.

3.2 OPERATIONAL CONCEPTS

3.2.1 Proposal Submission

The GHRS is a complex instrument, with dozens of selectable or programmable features. Many of these items have standard values, which are determined by calibration and engineering experience. Most observers will have to make only a minimal choice of optical and exposure control parameters, allowing others to be set at their default values. The default values of most items can be overridden though, and as users become more experienced they may wish to tailor their observation descriptions to take more complete advantage of the power and sophistication of the GHRS. For proposals which have been granted observing time the details of most of these parameters will be addressed during a Phase II. A Host Scientist from the Institute will consult with the GO in an effort to clarify requirements and optimize use of the available time.

The *Phase II Proposal Instructions*, which are distributed to successful proposers after selection by the Time Allocation Committee, supplement the material contained in the *Proposal Instructions.* They allow the user to specify more details than the original (Phase I) proposal submission. *GHRS Target Acquisitions Guidelines* will also be distributed to successful proposers during Phase II.

3.2.2 Target Acquisition

The GHRS can perform three types of target acquisition: Onboard, Early, or Interactive (Real-time). Advice and details about the process are given in the "GHRS Target Acquisition Guidelines" manual. Many targets will be relatively easy to acquire and the process is expected to be accomplished automatically by the flight software. For stationary point sources with well known ultraviolet fluxes and positions, Onboard Acquisition should be successful. Complicated objects, such as moving targets, crowded fields, extended sources, and objects with variable or poorly known brightness may require an Interactive Acquisition. An image of the field surrounding the target can be acquired either with the Wide Field/Planetary Camera, or with a "field map" capability of the GHRS itself. The observer can then visually identify the correct target. If at all possible, this should be done well before the actual observation (Early Acquisition). The image will be obtained several weeks or months prior to the scheduled science observation, allowing the analysis to be carried out in a leisurely manner. If it must be done at the time of observation, it is an Interactive Acquisition. This mode of operation obviously requires the presence of the observer in the control center during the observation. If any of the objects on the target list are likely to be acquired this way, the nature of the potential problem, and a request that an Interactive Acquisition be scheduled must be explicitly stated on the Phase I proposal submission. Real-time interaction with HST is a limited resource, available only about 20% of the time, and it should be called for only when needed.

3.2.3 Science Data Acquisition

After the target has been centered in the appropriate aperture, the instrument will be configured, and a sequence of observations will be executed according to the specifications made on the proposal forms. For routine observations the entire sequence can be performed with no intervention by the astronomer. If the exposure time will be longer than 5 to 10 minutes it is advisable to break the observation into a series of shorter integrations. This protects against a catastrophic loss of data and allows the astronomer, if present, to monitor the progress of the observation.

3.2.4 Transmission of Data to ST ScI

When the exposure is finished, the science data, accompanied by a concise set of engineering data and log information will be read out. The data can either be sent directly to the ground station, or be stored on the onboard science data tape recorder for transmission at a later time. The data follow a somewhat circuitous path through several communications satellites and ground systems, and arrive at the Science Institute within several minutes of the conclusion of the observation. Data is entered into the standard data reduction "pipeline," and it should become available to the astronomer for display, analysis, or further processing within one day of the observation.

3.2.5 Constraints, Interruptions and Limitations

There are several operational limitations imposed by the low earth orbit of the HST and the lack of continuous contact between the spacecraft and the control center.

(1) A block of observing time allocated to the GHRS will begin and end at predetermined absolute times. There is no way to extend an observation for "just a few more minutes" when the end of observing time arrives. Within the allotted block of time though,

individual observations may begin and end at times which are not rigidly determined in advance.

(2) All large maneuvers of the telescope will occur at preplanned times. An observer does not have the flexibility to slew to new targets at arbitrary times. There is no way to say "I don't like this object, let's go on to the next one right now."

(3) Most targets will rise and set, just as they do when observed from the ground. A target will typically be visible for about one hour per orbit. Long exposures that span several orbits will be broken up into shorter segments. During occultation of the target the flight software will suspend the exposure and idle until the object is again visible. The target will then be reacquired and the observation will continue.

(4) The spacecraft will pass through the South Atlantic Anomaly (SAA) several times each day. This is a region of the trapped radiation belts of the earth's magnetosphere which dips to lower than usual altitudes off the east coast of South America. The background noise in the detectors may be higher than usual during the passage. The GHRS is equipped with both hardware and software capabilities to identify and suppress counts caused by the radiation environment. After these mechanisms are fully calibrated, it should be possible for the GHRS to continue to observe during SAA passages without serious degradation of the data quality.

3.2.6 Real-Time Capabilities

Making observations with the HST in general, and the GHRS in particular, is a more automated process than using most ground-based telescopes. For the most part, observations must be fully specified months ahead of time, will usually be made without the observer being present, and will not require intervention by the operations staff. If the astronomer is present it is possible to participate in the process to a limited extent. It is expected during these opportunties that the following kinds of activities will be possible:

(1) One can examine target acquisition images of the field to identify a target, and to verify that the object is centered correctly in the aperture.

(2) One can display spectra shortly after they are read out. A quick-look facility allows a crude wavelength calibration to be applied, and some simple measurements to be made.

(3) One can alter the sequence of observations of a given target in the previously defined set via a mechanism called the Ground Control Observation Sequence Table (GCOST). This does not mean making up new observations "on the fly," but rather choosing which of several pre-planned observations is to be carried out (on the same target).

3.3 PRINCIPAL MODES OF OPERATION

The GHRS has several distinct operational modes which can be used for target acquisition and science data acquisition. The observer must select which of these modes to use, and must specify certain other information during the proposal process. This section provides additional information about these modes, and defines many of the terms used on the proposal forms. Sensitivity curves and other performance data needed to make specific calculations are presented in chapter 4.

3.3.1 Target Acquisition Mode

As outlined in section 3.2.2 and the *GHRS Target Acquisition Guidelines* Manual, there are several ways to accomplish a target acquisition depending on the location, brightness, complexity and motion of the object. It is necessary that the observer be aware of the different acquisition strategies, and the circumstances under which each might be needed. Target acquisition observations must be explicitly identified and defined on the Exposure Logsheet forms of the Phase II proposal. There are four types of target acquisition processes.

3.3.1.1 GHRS Onboard Acquisition and Spiral Search

If the target position and brightness can be specified accurately the flight software can be configured to perform an autonomous onboard target acquisition. This process can be completely automatic, requiring no interaction with the observer. The software can execute a series of operations designed to search for, identify, locate and center up on a properly defined object. It is intended that this will become the standard acquisition procedure, particularly for targets that have been observed previously. This section describes the sequence of processes involved, and explains what information the observer must supply. In some older documents Onboard Acquisition is called a "Mode II" target acquisition.

An onboard target acquisition observation consists of distinct phases, which will be executed in ascending numerical order. Phases 1 and 2 perform initialization and internal calibration functions, and need not concern the observer. The third phase is called Target Search. The flux coming through the Large Science Aperture is measured, and compared to a pair of upper and lower limits. If the measured value falls between these limits the target is assumed to be within the aperture. If the target is not detected at the initial pointing a series of small angle maneuvers, called a "spiral search," will be initiated to search an area of the sky up to 10 by 10 arc seconds, centered on the initial position. Once the correct flux level is detected the search stops. The observer may request that a field map be generated at each dwell point, by means of the MAP optional parameter. One should be aware, though, that approximately two minutes is required for each map, and that up to twenty-five pointings may be made during the search. If one intends to analyze the maps in real time, the search phase must be done as the Interactive Acquisition described in section 3.3.1.3.

After the target is detected, the fourth phase, known as Target Locate, is performed. This process measures the precise location of the target within the aperture, and requests a small angle maneuver to move it to the center. After centering a second maneuver will translate the image to the Small Science Aperture if that is the aperture to be used for the observation. The large aperture shutter may be closed at this time. As an option, a field map of the Large Science Aperture may be made before and/or after the centering maneuver is performed. One subtlety to be aware of is that the algorithm detects the center of light, and is not sensitive to the detailed shape of the image. If target is not a point-source, centering may not be perfect. Consult the *GHRS Target Acquisition Guidelines* Manual, which also gives more details on the time required for target acquistion. The fifth phase is called Peakup, and is used to fine tune the centering in the Small Science Aperture.

Phases 6 and 7 were designed to allow an offset under the control of the GHRS. Such an offset is now directly controlled by HST. The eighth and final phase is a Flux Measurement, in which the flux entering the GHRS through the final target aperture is measured and inserted into the data.

If your target is extended, part of a multiple system, or faint, you might acquire a nearby star for offset purposes. If your Phase II Proposal Forms specify a target acquisition *for* a particular Exposure Logsheet line, and the coordinates given on that line are different than those on the target acquisition line, the telescope will automatically perform the offset.

The coordinates of the object relative to the offset star must be known with an uncertainty less than half the diameter of the aperture if one is to be confident that the object will end up in the aperture. Measuring accurate offset coordinates would be a good justification for requesting a WF/PC Early Acquisition image.

Several items of information must be provided to fully specify an onboard target acquisition. These will be requested in Phase II (only of successful proposers):

(1) Which acquisition mirror to use—N1, N2, A1, A2. Guidelines for estimating count rates are presented in Chapter 4.
(2) Lower and Upper flux limits for the Target Search comparison.
(3) How large a spiral search pattern to execute. The maximum possible is a 5x5 point grid spaced on 2 arc second centers.
(4) Whether or not to produce a field map at each search point.
(5) If a map is to be made, the exposure time and certain other options.
(6) The aperture in which to center the object.
(7) If the initial target is an offset star, the offset coordinates in right ascension and declination.

3.3.1.2 WF/PC Assisted Target Acquisition

For many kinds of difficult targets an image obtained with the WF/PC will be essential to the acquisition process. The following types of problems might qualify a target for this approach:

(1) The uncertainty in the coordinates is greater than a few arc sec in either declination or right ascension. The target could be outside the largest area that the GHRS can search in its onboard procedure.
(2) The object is a moving target whose coordinates cannot be predicted with $\pm$ 5 arc sec accuracy when the proposal is written. Features in the atmosphere of a planet, and comets are examples.
(3) Objects with poorly known or unpredictably variable ultraviolet fluxes.
(4) Targets with nearby neighbors of similar brightness—the onboard search process could center up on the wrong object.
(5) Objects with a spatial extent greater than two arc seconds. The automatic centering algorithms are designed to work on point sources, and may not produce acceptable results on objects which fill the Large Science Aperture.

If one wishes to obtain a WF/PC image, it is necessary to enter a line on the Exposure Logsheet requesting the observation. Either the Wide Field (WF) or Planetary Camera (PC) may be used with any available filter. Details such as exposure times and readout formats should be specified in accordance with the guidelines presented in the WF/PC Instrument Handbook. It should be noted on the proposal that the image is intended to assist with target acquisition. It should be stated as a Special Requirement whether the image may be an Early Acquisition or whether an Interactive Acquisition is required. When an Interactive Acquisition is performed the observer must be present at the Observation Support

System (OSS) Station at the Science Institute. One should be prepared to inspect the image and identify the target in a timely fashion. Note that if the same guide stars are to be used for the WF/PC and GHRS observations, the effective area within which the guide star must lie is decreased (see the HST focal plane diagram in the *Call for Proposals*). Real-time observations are subject to many constraints and are difficult to schedule (occasionally impossible). Early Acquisition should therefore be chosen in prefertence to Interactive Acquisition whenever possible. The HST (Phase I) Proposal Forms request justification of requests for real-time observation.

3.3.1.3 GHRS Interactive Acquisition

In some cases an acquisition image will be helpful, but the field of view of the WF/PC is not needed. Stationary point sources in crowded but recognizable fields would be examples. The GHRS has its own "field map" capability which will produce an image of the sky as seen through the Large Science Aperture. Each map is a square array of 22 × 22 pixels, covering 2 × 2 arc seconds with 1/8 arc second spatial resolution. If an area larger than 2 × 2 arc seconds must be imaged, a "Spiral Search," consisting of a series of small "step and dwell" maneuvers of the telescope can be issued, with a map being created at each dwell point. The GHRS can request maneuvers through its flight software to map an area up to 10 by 10 arc seconds ("5 × 5 spiral search"), centered on the initial pointing. The data will be sent to the ground, where the images will be reconstructed for display and inspection.

A single field map requires a minimum of two minutes to take the data and send it to the ground, and much longer if each point in a Spiral Search is mapped. One WF/PC image requires from three to five minutes, but covers a much larger area of the sky. As a practical matter, if more than one field map would be needed, a WF/PC image would be a more efficient choice.

If the observer desires to use the field map option in an Interactive Acquisition, an observation must be defined on the Exposure Logsheet. The instrument mode will be called ACQ, the aperture is the 2.0 arc second Large Science Aperture, and the spectral element is MIRROR. The Science Institute will decide which of the four acquisition mirrors should be used if the observer has not specified a choice. Generally, one image with a two minute exposure time will be sufficient. The optional parameter MAP and the special requirement Interactive Acquisition should be stated. In some cases a field map may be acquired as an Early Acquisition, although the small field of view will hinder its usefulness. For cross-reference purposes, we note that an Interactive Acquisition is called a "Mode I" target acquisition in some HST documents. This terminology is not used on the proposal forms, however.

3.3.1.4 Blind Pointing

This fourth method of target acquisition may be used in cases where the position of the target is known to much greater precision than the field of view of the instrument, and the initial pointing of the telescope is guaranteed to be adequate. This will almost always be true for the cameras. For the GHRS, this method may be used for extended objects when precise centering is not required, or for repeated observations where a previously calibrated guide star pair can be used.

3.3.2 Science Data Acquisition Modes

There are several modes of science data acquisition, including Accumulation Mode, Rapid Readout Mode, and Image Mode. Each of these modes may be used in conjunction with any of the optical configurations described earlier.

3.3.2.1 Accumulation Mode

Accumulation Mode is the normal way of obtaining spectral data with the GHRS. The name refers to the fact that data can be accumulated in the onboard computer during a long exposure. All of the features of the flight software are available in this mode, making it the most powerful, flexible and automatic way to use the GHRS. There are four general benefits which one can expect by using the flight software in Accumulation Mode.

The first is the ability to make long duration observations with effective and automatic control of the process. The time varying Doppler shift caused by the orbital velocity of the spacecraft is compensated for automatically. The software constantly monitors a set of data quality criteria and can flag, reject, or reobserve individual integrations that fail the tests. Finally, the software can suspend the observation during scheduled or unexpected interruptions, such as occultation of the target by the Earth, passage through the South Atlantic Anomaly, and resume when the interruption ends. The very low background dark rate and absence of readout noise in the Digicons make exposures of hours duration feasible, though it is suggested that these be broken into shorter segments to aid in scheduling and protect against catastrophic data loss in the event of an unexpected problem.

The second capability is the flexible way in which the duration of an observation can be controlled. There are three methods, any or all of which can be implemented for a given observation. The most straightforward way is to specify the actual elapsed time—number of seconds,minutes, etc.—required for the exposure. There is an exposure meter capability which monitors the data as they accumulate, and can terminate an observation if the count rate is less than a specified threshold or when the cumulative counts per diode reach a specified upper limit. An observation can thus be controlled either by exposure time or by the number of counts actually obtained.

The third category of benefits results from the ability of the software to perform patterns of integrations at closely spaced positions on the photocathode, a process which is referred to as substepping. There are four purposes for this. At the beginning of an observation the software can execute a procedure called Spectrum Y Balance to find the optimum centering of the image on the diode array. This compensates for minor changes in the image location due to thermal or electrical drifts. The second use is to make multiple (2 or 4) samples per resolution element (1 diode width) to ensure that the digital data satisfy the Nyquist sampling criterion. This is important when the ultimate spectral resolution of narrow features is required. Thirdly, the background adjacent to the spectrum or in the Echelle interorder region can be measured. Finally, substepping allows the effect of small diode-to-diode sensitivity variations to be minimized and eliminates the holes in the data due to a few inoperative channels. When substepping is used to define the detailed sampling of the spectrum and background, the data obtained at each step are accumulated into one of up to seven distinct "bins" in the memory of the onboard computer.

The fourth important capability of the accumulation mode is the ability to execute long sequences of observations automatically. Typically, one will wish to observe more than the very limited spectral region recorded by the diode array. Sequences of observations at

adjacent regions, or even observations with different spectral elements can be easily specified. Observations of the onboard wavelength calibration lamps can be inserted into the sequence, as can measurements of the sky background. One may specify more observations than is expected can be done, under Meter-mode control, so that if some observations finish early, extra observations are taken, and no telescope time is wasted.

This overview of the flight software features is not exhaustive, but summarizes those capabilities which are immediately relevant to the acquisition of spectra in accumulation mode. Several items, namely substepping and exposure control, require the observer to specify certain parameters. These will be described in more detail in the next chapter of this handbook.

3.3.2.2 Rapid Readout Mode (sometimes called Direct Downlink)

Rapid Readout Mode is intended to provide very fast time resolution. The Sample Time can be between 50 ms and 12.75 seconds, in increments of 50 milliseconds (1 to 255 times 50 ms). At the end of each integration the data are read out, either directly to the TDRSS satellite or to the spacecraft science data tape recorder. It is not possible for the flight software to execute all of its functions and still allow readouts every 50 ms. When the rapid readout mode is entered, substepping, data quality checks and exposure control features are deactivated. The primary factor governing the choice between these two modes is time resolution. In accumulation mode the time between exposures can be as short as somewhat less than one minute. If higher time resolution is required, if the source is bright enough to give useful counts in a shorter integration, and if one is willing to sacrifice the flight software control, then direct downlink is a useful alternative.

3.3.2.3 Image Mode

Images may be obtained in this mode by deflecting the image of the photocathode over the $1/8 \times 1/8$ arc second focus diodes. The result can be a map similar to that obtainable during Target Acquisition (without an Acquisition being performed), or, if a grating rather than a mirror is chosen as the optical element, high spectral purity images of emission-line sources can be obtained.

3.3.2.4 OSCAN and WSCAN modes

These are really modifications of the ACCUMulation mode designed for higher efficiency in multiple observations, and they may be requested during Phase II of the proposal process. WSCAN obtains a series of spectra within a given order, incrementing by a specified wavelength increment between each. OSCAN works with the echelle, and uses the magnetic deflection of the Digicon to obtain spectra in adjacent echelle orders. The grating carousel is not rotated, and spectra are obtained at equal values of $m\lambda$, where m is the echelle order.

4.0 DETAILED PERFORMANCE CHARACTERISTICS

The rationale behind the construction of the GHRS was described in previous chapters. In this chapter specific and detailed information is presented regarding the actual performance. These data should be used in making the calculations required to plan an observing program. The majority of the results are based on measurements made during the ground based calibration, rather than on calculations, models, or design goals. Most of these characterisitics will be calibrated again during the post-launch "Science Verification" activities. This handbook will be updated accordingly as new results become available, and results of immediate interest published in the ST ScI *Institute Newsletter.*

4.1 TARGET ACQUISITION CAPABILITIES

4.1.1 Sensitivity Curves

The four target acquisition mirrors were designed to allow objects with a range of over 18 stellar magnitudes to be detected without saturating a detector. They accomplish this with combinations of physical diameter (cf. Table 3-1), spectral reflectivity, and detector quantum efficiency. The net efficiency at each wavelength can be combined with the throughput of the telescope to produce an effective area. Table 4-1 and Figure 4-1 present the effective areas for each mirror which were estimated from ground based calibration data.

If the spectrum of the target is known, these tables can be used to estimate the count rate produced by each mirror. First interpolate the effective areas onto the same wavelength grid as the spectrum. Convert the flux spectrum into units of photons/cm^2 sec Å. Multiply the area times the flux times the wavelength interval, and sum over all wavelengths.

$$\dot{C} = \sum_{\lambda} A_\lambda F_\lambda \Delta\lambda \text{ counts/sec} \qquad (4-1)$$

Ideally, the count rate should be between about 1000 and 100000 cts/sec. Lower signal levels will require longer integration times and may produce inaccurate centroiding. High count rates will saturate the counting electronics and will cause numerical problems in the software.

4.1.2 Response to Stellar Point Sources

Ultraviolet spectra of stars observed with IUE were combined with these effective areas to predict how each mirror will respond to stars of different visual magnitude V, unreddened color index (B-V), and color excess E(B-V).

The results are summarized in Figure 4-2, which may be used as follows. Estimate the unreddened color index from the observed (B-V) and E(B-V). Read the count rates for each of the four mirrors from the figure. The plot is normalized to V=0, so the count rate must be scaled to the magnitude of the target

$$\dot{C}_V = \dot{C}_0 * 10^{-(\frac{V}{2.5})} \qquad (4-2)$$

If the star has significant interstellar extinction, use a corrected visual magnitude, V - 3E(B-V) in this formula. Since extinction severely attenuates the ultraviolet spectrum, the countrates must then be adjusted for its effect. The following formulae give a good estimate:

$$N_1, A1 \qquad \dot{C}_{V,E(B-V)} = \dot{C}_V * 10^{-3.6E(B-V)} \qquad (4-3)$$

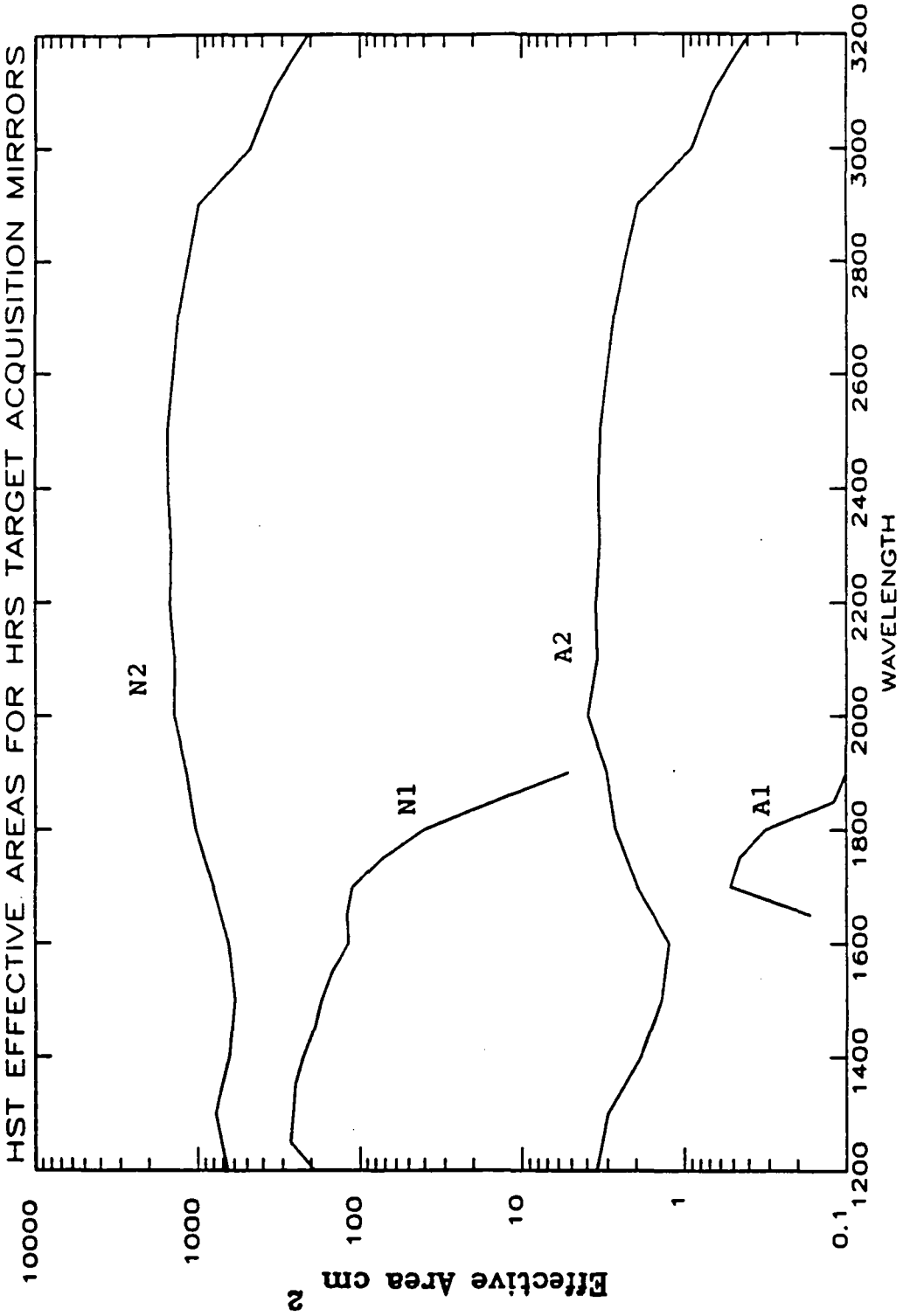
HST EFFECTIVE AREAS FOR HRS TARGET ACQUISITION MIRRORS
N2
N1
A2
A1
Effective Area cm 2
10000
1000
100
10
1
0.1
1200
1400
1600
1800
2000
2200
2400
2600
2800
3000
3200
WAVELENGTH

FIGURE 4-1

TABLE 4-1
TARGET ACQUISITION EFFECTIVE AREAS (cm^2)

WAVELENGTH	N2	N1	A2	A1
1200	657	191	3.5	
1250		268		
1300	775	257	3.0	
1350		249		
1400	638	222	1.9	
1450		190		
1500	588	172	1.4	
1550		147		
1600	643	117	1.3	
1650		118		0.17
1700	800	110	2.0	0.52
1750		72		0.46
1800	1023	40	2.7	0.31
1850		15		0.12
1900	1159	5	3.0	0.04
2000	1393		3.9	
2100	1384		3.4	
2200	1469		3.5	
2300	1447		3.4	
2400	1507		3.4	
2500	1524		3.3	
2600	1401		3.0	
2700	1301		2.7	
2800	1136		2.3	
2900	980		1.9	
3000	478		0.9	
3100	346		0.7	
3200	207		0.4	

$$N_2, A2 \qquad \dot{C}_{V,E(B-V)} = \dot{C}_V * 10^{-3.2E(B-V)} \qquad (4-4)$$

Again, a mirror which results in countrates between 1000–100000 cts/sec is desirable.

4.1.3 Power Law Spectra

If the ultraviolet spectrum may be approximated by a power law, a rough estimate of the count rate may be obtained from Figure 4-4, which shows estimated count rates for each mirror normalized to V=0 and E(B-V) = 0. The procedure is identical to the previous example. Determine the countrate suggested by the spectral parameter α, and scale for V and E(B-V). The power law index α indicates the slope of the flux distribution:

$$\frac{df}{d\lambda} \sim \lambda^{-\alpha} \qquad (4-5)$$

or

$$\frac{df}{d\nu} \sim \nu^{\alpha-2} \qquad (4-6)$$

4.1.4 Predicted Count Rates for Selected Targets

Count rates have been estimated for many targets which will be observed during the in-orbit calibration tests. The calculations followed the precepts of the previous sections. Table 4-2 shows the predictions, and gives a general idea of the target acquisition sensitivities for different types of objects.

4.1.5 Field Maps

In section 3.3.1.3 the use of field maps for interactive target acquisition was described. The standard size map is produced with a pixel spacing of 0.125 arc sec, and covers the entire 2×2 arc second Large Science Aperture. As an option, the pixel spacing can be reduced to 0.062 or 0.031 arc sec. The 22×22 pixel map then covers an area approximately 1.4 or 0.7 arc sec on a side.

The maximum count rate expected on the mapping diodes is approximately 0.15 times the count rate discussed in the previous sections, since maps are done with the focus diodes, which are smaller than the main array diodes. The maps are produced by rastering the aperture field with two small diodes. The standard integration time for each dwell point is 0.2 seconds. A normal 484 pixel map requires 242 dwells, or 96.8 seconds. If integration times longer than 0.2 seconds are required, the total time required for the map is increased proportionately. The maximum possible dwell time is 12.75 seconds. An additional 8 seconds is required to read out the data.

4.1.6 Time Requirements

Times required to complete the various target acquisition functions are itemized in Table 4-3. A typical acquisition sequence might include the following elements: Initialize, Calibrate Deflections, Spiral Search with 9 Dwell Points, a Field Map, Center in LSA, Translate to SSA, Peakup and Flux Measurement. The total time required is approximately 10 minutes.

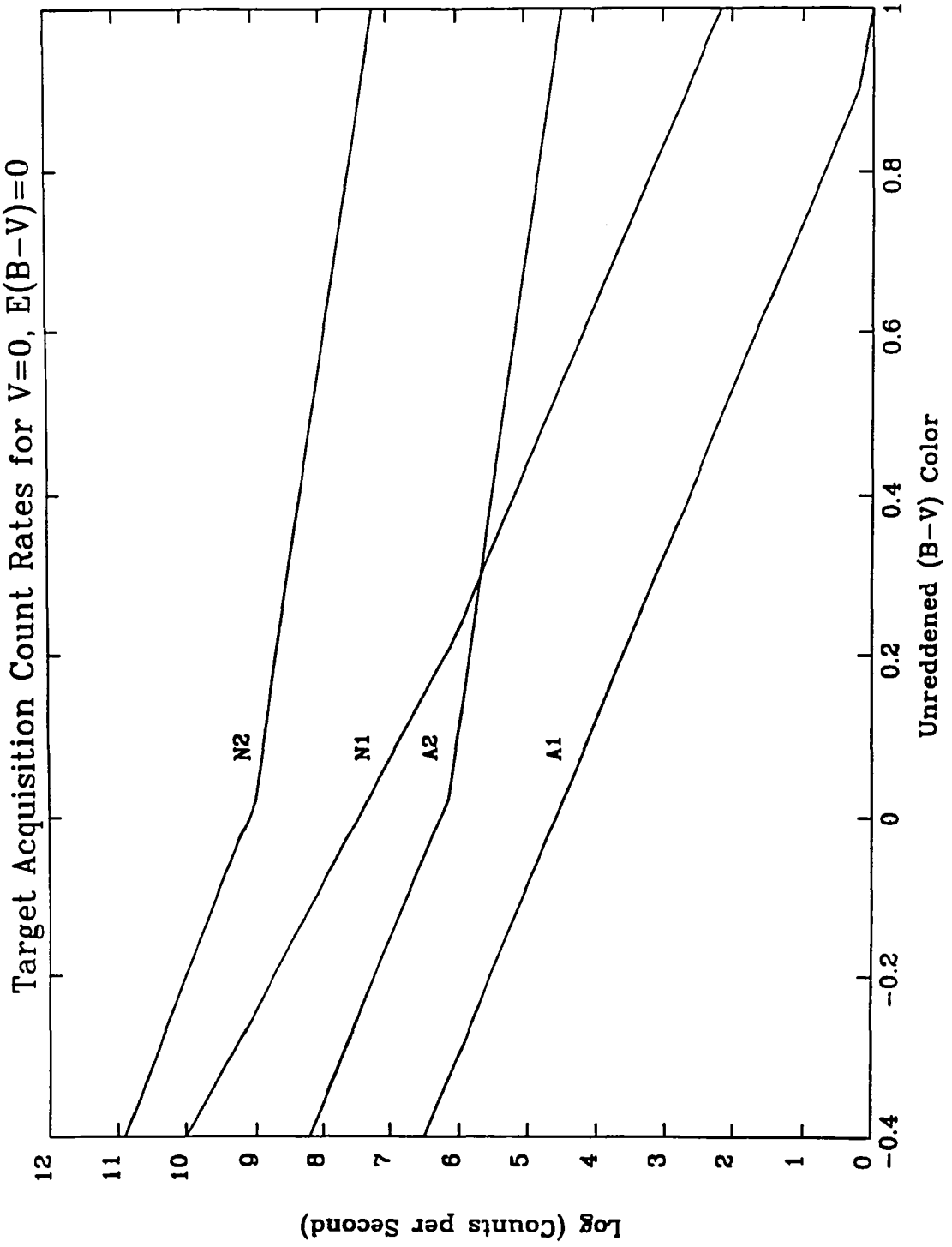
Target Acquisition Count Rates for V=0, E(B−V)=0
Log (Counts per Second)
Unreddened (B−V) Color
N2
N1
A2
A1
12
11
10
9
8
7
6
5
4
3
2
1
0
−0.4
−0.2
0
0.2
0.4
0.6
0.8
1

Figure 4-2

NOT USED IN THIS EDITION

Figure 4-3

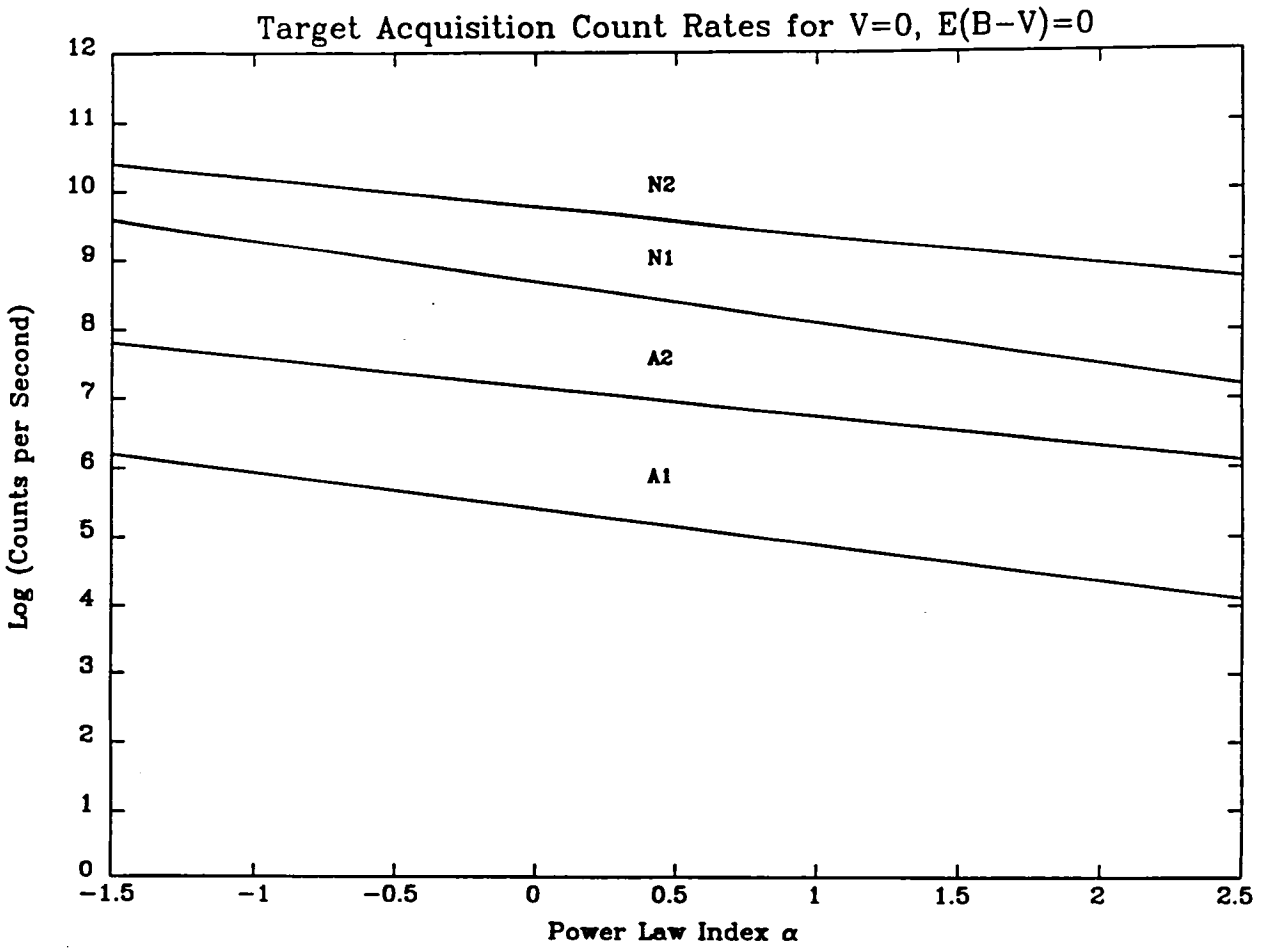

Figure 4-4

TABLE 4-2

ESTIMATED TARGET ACQUISITION COUNT RATES

Object	Spt	V	B-V	E(B-V)	N2	N1	A2	A1
Unreddened Hot Stars								
βCen	B1 II	0.62	-0.24	0	6.4E9	6.1E8	1.7E7	3.0E5
μCol	09V	5.16	0.29	0.01	1.6E8	1.7E7	3.8E5	6.7E3
HD93521	09V	7.04	-0.28	0.03	2.4E7	2.6E6	5.8E4	1.0E3
BD+75°325	SdO	9.54	-0.37	0	4.7E6	7.8E5	1.4E4	2.5E2
HZ44	SdO	11.71	-0.27	0	4.1E5	4.3E4	9.7E2	1.7E1
HZ21	D	14.22	-0.36	0	6.3E4	1.E4	1.9E2	3.4E0
Reddened Hot Stars								
ζOph	09.5V	2.56	+0.02	0.3	2.0E8	1.6E7	4.6E5	7.5E3
ζSco	BIIa	4.73	+0.49	0.6	3.2E5	9.7E3	7.2E2	8.9E0
HD93129A	03If	7.3	+0.22	0.5	5.9E5	3.9E4	1.3E3	1.8E1
Unreddened Neutral Stars								
αLyr	AOV	0.04	0.00	0	9.8E8	3.8E7	2.3E6	4.7E4
BD+70°5824	DA3	12.87	-0.09	0	1.5E4	7.8E2	3.6E1	6.3E-1
Cool Stars								
αOri	M2Ia	0.5	+1.85		1.2E6	2.2E1	2.4E3	1.8E-1
16Cygβ	G5V	6.2	+0.66	0	1.2E5	5.0E1	2.4E2	9.0E-2
TTauri	KO	10			5.0E3	1.1E2	1.1E1	7.6E-2
Non-Stellar Objects								
3C273	QSO	12.8	+0.21		3.4E4	2.5E3	8.6E1	1.5E0
NGC4151	Seyfert	13.5			1.6E4	1.0E3	3.9E1	6.2E-1

TABLE 4-3
***Approximate* Target Acquisition Time Requirements**

Function	Time	Comments
Initialization and Setup	120 sec	Always performed
Deflection Calibration	60 sec	Required
Spiral Search	n×12 sec	Each search point
Field Map	100 sec	Minimum dwell time
Center in LSA	120 sec	Average time
Translate to SSA	12 sec	Optional
Peakup in SSA	120 sec	Average time
Flux Measurement	0.2 sec	Always performed

4.2 ENTRANCE APERTURES

4.2.1 Effective Areas

The Large Science Aperture has dimensions of 2×2 arc sec on the sky, with an effective area of 4.0 square arc sec.

The Small Science Aperture has dimensions of 0.25×0.25 arc sec on the sky, with an effective area of 0.0625 square arc sec.

4.2.2 Transmission of Light from a Point Source

The Small Science Aperture accepts only the central peak of the OTA point spread function. Light which falls in the outer wings of the image is lost. Even the LSA will fail to pass some light which has undergone scattering due to dust and mirror microroughness. Table 4-4 of the first edition of the HRS Handbook gave rough estimates of the transmission of the small aperture relative to the large aperture. These have been superseded by better calculations based on models of the OTA image structure, which include scattering due to small scale mirror irregularities, and the amount of dust projected to have settled on the mirror by launch. They are uncertain by perhaps 10% and will be replaced by measured transmissions after launch. The transmission calculations have been incorporated into the sensitivity curves and tables given later in this chapter.

4.3 GRATING AND ECHELLES

4.3.1 Wavelength Coverage

The grating which produces a resolving power of R = 2000 is referred to as G140L. This ruled, plane diffraction grating is used in conjunction with dectector D1. It is blazed to be most efficient in first order, and is used in the region 1050 Å to 1800 Å. The second and higher orders of diffraction are not used. The zero order image is used as target acquisition mirror N1. Because of its lower dispersion and high efficiency, G140L is the most sensitive dispersive optic, and can be used to observe the faintest objects.

There are four gratings which provide a resolving power of R = 20000. Together they cover the entire spectral range of the GHRS. Each is a plane holographically manufactured

diffraction grating, optimized for best sensitivity over a restricted wavelength interval. All are used in first order. G140M is used with detector D1. It is intended for use at the shortest wavelengths, 1050 to 1500 Å. Gratings G160M, G200M and G270M all work with detector D2. Together they cover the region 1200 to 3200 Å with good sensitivity and resolving power. A quartz window is mounted in front of G270M and serves as an order sorting filter. Since the grating is used in first order and since the detector is sensitive to wavelengths as short as 1150 Å, this filter is needed to block the second order spectrum.

The diode array records only a small segment of the total spectral region of each grating at one time. For the low resolution grating, approximately 285 Å is recorded at each setting. For the medium resolution gratings, the coverage varies between 25 and 45 Å. The linear reciprocal dispersion (usually called simply the dispersion) varies with wavelength as well. Table 4-5 contains a summary of these properties for each first order grating. The limits on the wavelength range indicate the region of optimum performance, but are not hard limits. Beyond these points the image quality and sensitivity deteriorate. The ranges on the spectral coverage, dispersion and resolving power refer to values near the short and long wavelength limits.

TABLE 4-5
Properties of the First Order Gratings

Grating	Wavelength Range (Å)	Dispersion Å/diode	Spectral Coverage (Å)
G140L	1050–1800	.572–.573	286–287
G140M	1050–1700	.056–.052	28–26
G160M	1200–2000	.072–.066	36–33
G200M	1600–2400	.081–.075	41–38
G270M	2200–3200	.096–.087	48–44

In Echelle configuration ECH-A orders 53 through 33, containing the spectral region 1060 A to 1700 A, are detected by digicon D1. Echelle configuration ECH-B, using detector D2, covers the region 1700 A to 3200 A in orders 33 through 18. All of the orders are present on the photocathode simultaneously, separated from each other in the direction perpendicular to dispersion. Any order can be selected, but only one order, together with the background adjacent to it, is contained in one observation. As with the first order gratings, only a short segment of the spectral range of any order can be recorded at one time. A longer spectral range may be scanned by making observations at several carousel positions, and/or recording several orders at each position. Figures 4-5 and 4-6 are handy schematics of the Echelle Formats. They show which wavelengths are present in the various orders for each value of $m\lambda$ (m the echelle order). The arrows at the top of the figures indicate the fraction of an order recorded by the diode array in a single observation. Tables 4-6 and 4-7 provide for the Echelles the same basic information about spectral range and dispersion that Table 4-5 provides for the first order gratings. The significance of the Scattered Light column is described in section 4.3.5.

The quantities listed in Tables 4-5, 4-6 and 4-7 are directly relevant to planning observations. Optical parameters which describe the design were presented in Table 3-1.

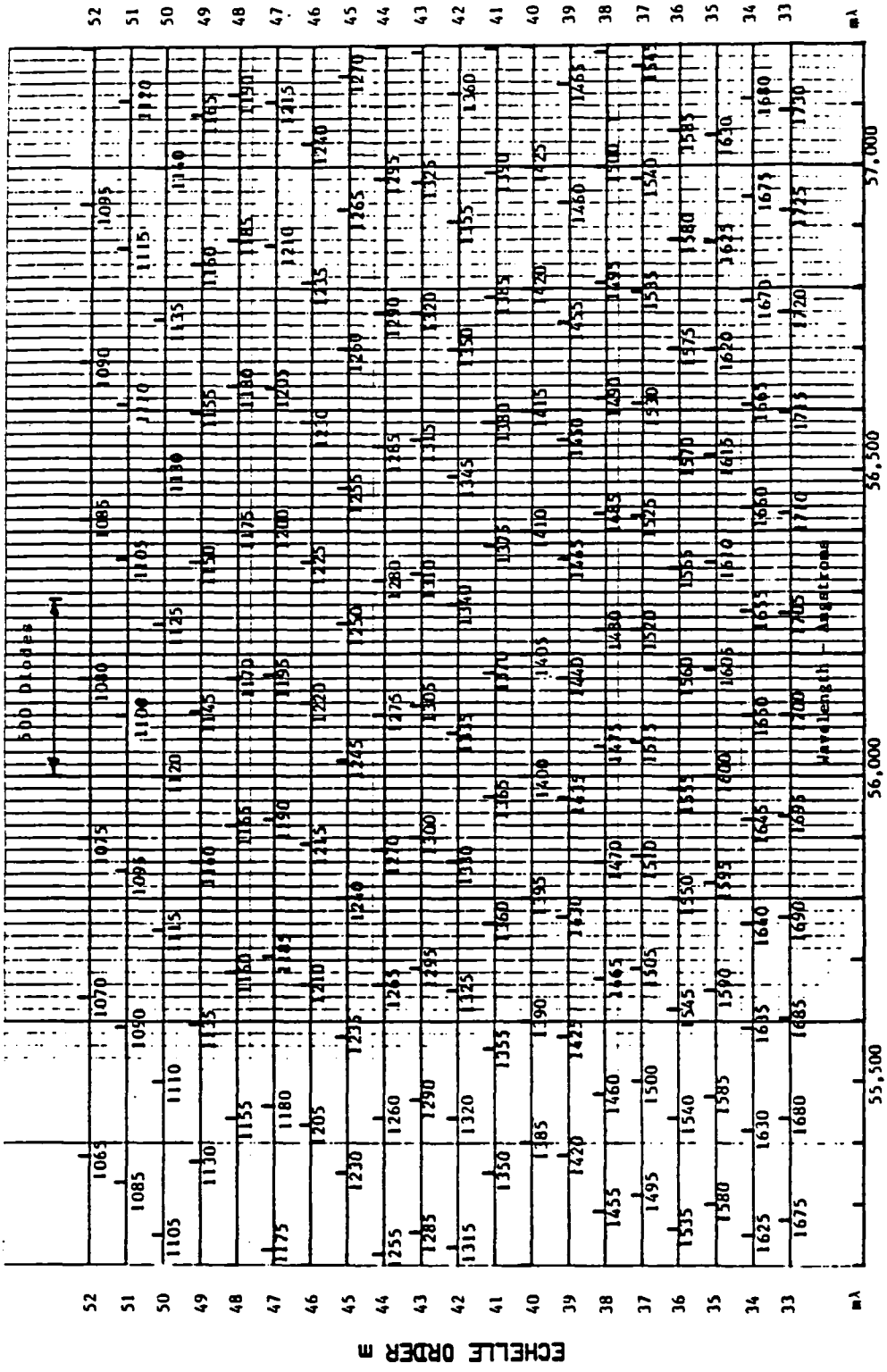

Figure 4-5. ECH-A Spectral Format

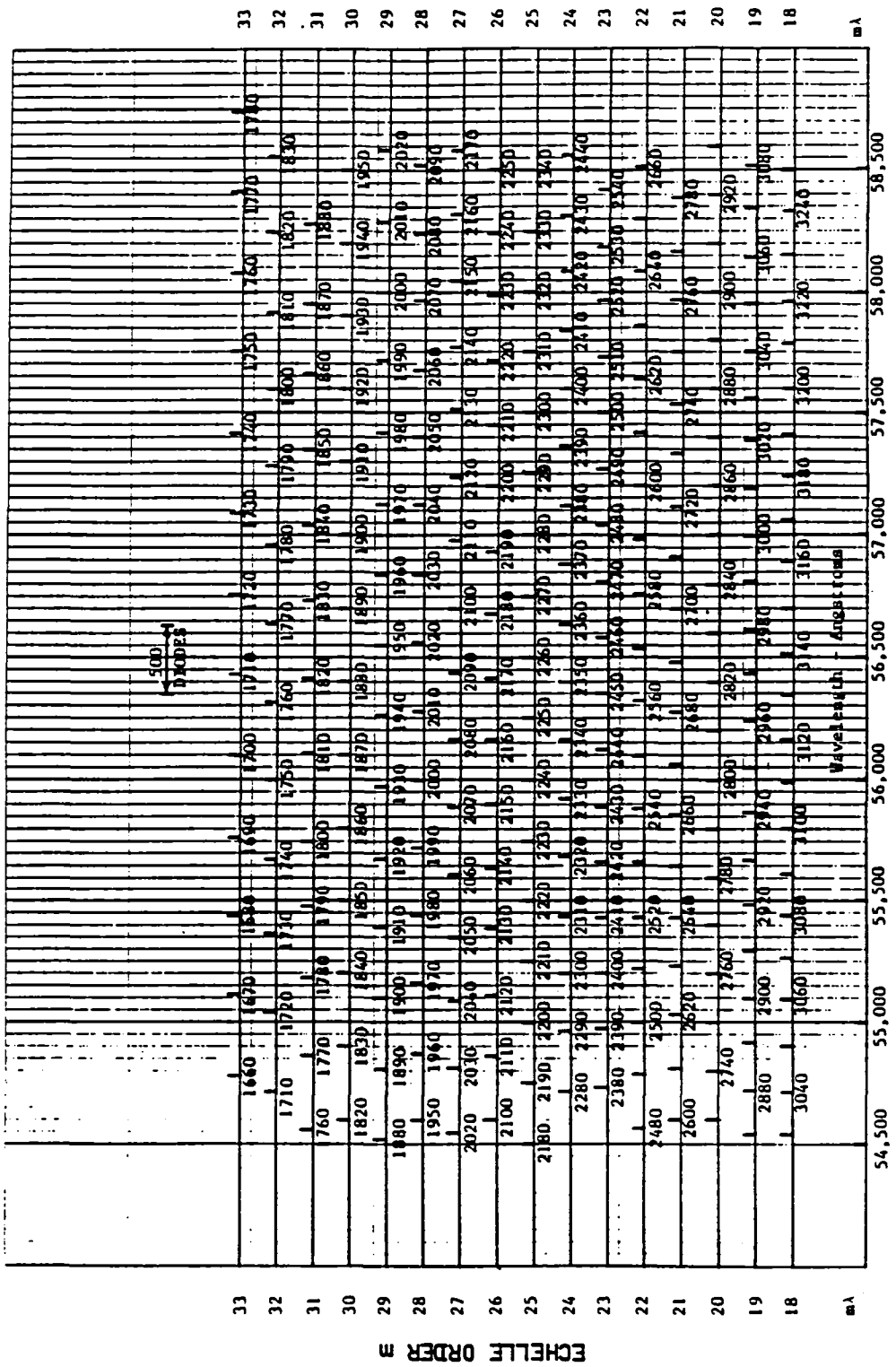

Figure 4-6. ECH–B Spectral Format

TABLE 4-6
Properties of Echelle A

Order m	λ_c (Å)	Free Spectral Range (Å)	Dispersion Å/Diode	Spectral Coverage (Å)	Scattered Light
53	1060	1050–1070	.0114–.0107	5.69–5.35	–
52	1081	1070–1091	.0116–.0109	5.80–5.45	–
51	1102	1091–1113	.0118–.0111	5.90–5.55	–
50	1124	1113–1135	.0121–.0113	6.05–5.65	–
49	1147	1135–1159	.0123–.0115	6.15–5.75	.50
48	1171	1159–1183	.0125–.0118	6.25–5.90	.43
47	1196	1183–1209	.0128–.0120	6.40–6.00	.38
46	1222	1209–1235	.0131–.0122	6.55–6.10	.30
45	1249	1235–1263	.0134–.0125	6.70–6.25	.26
44	1277	1263–1292	.0137–.0128	6.85–6.40	.22
43	1307	1292–1322	.0141–.0131	7.05–6.55	.20
42	1338	1322–1354	.0144–.0134	7.20–6.70	.17
41	1371	1354–1387	.0148–.0137	7.40–6.85	.14
40	1405	1387–1423	.0151–.0140	7.55–7.00	.11
39	1441	1423–1460	.0156–.0144	7.80–7.20	.10
38	1479	1460–1498	.0160–.0148	8.00–7.40	.09
37	1519	1498–1539	.0165–.0151	8.25–7.55	.09
36	1561	1539–1583	.0169–.0155	8.45–7.75	.08
35	1606	1583–1629	.0174–.0159	8.70–7.95	.08
34	1653	1629–1677	.0179–.0164	8.95–8.20	.07
33	1703	1677–1729	.0185–.0168	9.25–8.40	.06

TABLE 4-7
Properties of Echelle B

Order m	λ_c (Å)	Free Spectral Range (Å)	Dispersion Å/Diode	Spectral Coverage (Å)	Scattered Light
33	1703	1677–1729	.0186–.0168	9.3– 8.4	.36
32	1756	1729–1784	.0191–.0172	9.6– 8.6	.23
31	1813	1784–1842	.0198–.0178	9.9– 8.9	.18
30	1873	1842–1905	.0205–.0183	10.3– 9.2	.14
29	1938	1905–1971	.0213–.0189	10.7– 9.5	.11
28	2007	1971–2043	.0221–.0196	11.1– 9.8	.10
27	2082	2043–2120	.0229–.0202	11.5–10.1	.07
26	2162	2120–2203	.0238–.0209	11.9–10.5	.06
25	2248	2203–2293	.0248–.0217	12.4–10.9	.05
24	2342	2293–2391	.0259–.0225	13.0–11.3	.04
23	2444	2390–2497	.0271–.0234	13.6–11.7	.03
22	2555	2497–2613	.0284–.0243	14.2–12.2	.03
21	2676	2613–2740	.0298–.0254	14.9–12.7	.02
20	2810	2740–2880	.0314–.0266	15.8–13.3	.02
19	2958	2880–3036	.0334–.0278	16.7–13.9	.02
18	3122	3036–3209	.0352–.0292	17.6–14.6	.02

4.3.2 Wavelength Calibration

Since the spectral format of the GHRS is geometrically simple, and appears to be very stable, the assignment of precise wavelengths is a fairly straightforward procedure. Each data point is assigned a coordinate on the detector focal plane (*i.e.*, on the photocathode) called "sample" and "line" for directions parallel and perpendicular to dispersion. The detector deflection settings and the diode numbers are used to calculate the sample and line positions via a mapping function which is a standard detector calibration. Emission lines in the spectra of the Pt lamps are identified, and a regression formula relates the wavelengths to the sample coordinates. The coefficients of the formula, which is usually a simple quadratic polynomial, are called the dispersion constants and are themselves functions of the carousel position. Since the Pt lamps have apertures adjacent to the science apertures, small wavelength dependent adjustments are made to refer the dispersion constants to the science apertures. Vacuum wavelengths are used in the calibration. For each stellar spectrum, the dispersion constants are used to convert sample numbers to wavelengths. An adjustment is made to produce air wavelengths for $\lambda > 2000$Å. Doppler shifts introduced by the orbital motion of the spacecraft and the Earth are then removed to result in a heliocentric wavelength scale.

4.3.2.1 Routine Accuracy

A detailed error analysis suggests the following uncertainties. Errors in carousel positioning typically will amount to about $\pm$ 1/4 diode width. If no calibration had ever been obtained at exactly the same carousel position, using interpolated dispersion constants will cause about $\pm$ 1/2 diode width error. Varying thermal conditions are known to cause another few tenths of a diode width image motion. There are no significant uncertainties in the laboratory wavelengths of the Pt lines, the vacuum to air adjustment or the heliocentric correction. Therefore, if a special Pt lamp calibration is not obtained, the wavelengths will have an uncertainty of about $\pm$ 1 full diode width. This calibration is maintained by the *Institute*, and it is expected to suffice for many, if not most, observers. If it does, you will not need to make any wavelength calibration observations yourself.

4.3.2.2 Better Accuracy

If you need better accuracy than about $\pm$ 1 diode, it can be achieved by taking a spectral calibration (Pt lamp) observation immediately before a science observation, without moving the grating carousel. If the science observation lasts longer than about 30 minutes, you may want to take a lamp observation both before and after. Either spectral calibration lamp may generally be used. It is recommended that you specify "SEQUENCE WITHIN 15 MIN" (*cf* the *Phase II Proposal Instructions*) to insure that your object and calibration spectra are taken close together in time.

4.3.2.3 Best Accuracy

A final, very small, source of wavelength inaccuracy arises if the target and spectral calibration lamps are not centered in their respective apertures. This, of course, would produce a small offset between the object and reference spectra. The GHRS Digicons are magnetically defected in discrete steps which are 1/8 diode width in size. The centering of the spectral calibration lamp in its aperture will typically have errors of this order, and the

centering of the target in the Small Science Aperture may also not be perfect. However, the positions in the aperture can be measured.

The recommended procedure is to take two Accumulation mode observations in the mirror mode used for target acquisition, and use them to measure the relative offset between the target and one of the spectral calibration lamps. The first observation, of the target, should use one of the four acquisition mirrors and an exposure time which will give about 1000 counts (*cf* Section 4.1.1). The second, of the lamp, must follow immediately and use the same mirror. Exposure times should be 200 seconds for mirrors A1 or A2, and 2 seconds for mirrors N1 or N2. One then procedes with the calibrations given in Section 4.3.2.2. Obviously, the "best accuracy" sequence takes extra time, and should only be done when the last small improvement in wavelength accuracy is essential.

4.3.3 Image Quality and Resolving Power

The resolving power of a spectrograph is determined by the quality of the optical image, the linear dispersion of the grating, and the pixel size of the detector. To facilitate measurements, a figure of merit was adopted based on the observed profiles of narrow emission lines. The parameter $R = \lambda / \Delta\lambda$ is called the resolving power, where λ is the wavelength and $\Delta\lambda$ is the full width at half maximum intensity. The pre-launch measurements were made with an optical system which overfilled the small science aperture. The width of the monochromatic image, $\Delta\lambda$, is therefore the convolution of the aperture image with the detector diode response. During flight the image width will be determined by the point spread function of the telescope, and is likely to be somewhat narrower than the entrance aperture. The resolving power for spectra of point sources will likely be better than the data shown here indicate. Figure 4-7 shows contour plots of narrow emission line images produced by grating G140M and ECH-A. They are representative of the images produced by all other optical configurations as well. The slightly elliptical isophotes and twisted major axes are features of the off-axis configuration of the camera mirrors and detectors. The profiles of these images as measured by the diode array are shown in Figure 4-8. The full width at half maximum intensity was used to produce the plots of resolving power vs. wavelength shown in Figures 4-10 to 4-14, and 4-16. For all first order gratings the instrumental profile is sensibly Gaussian. The Echelle profiles have noticeably extended wings which will influence the critical interpretation of narrow line profiles. The broadening function is currently being analyzed.

4.3.4 Coarse Track vs. Fine Lock

The default HST guiding mode used with the GHRS is called "Coarse Track," and is expected to have tracking accuracy better than 20 milli-arc seconds (0.020″). This corresponds to 0.08 diode width (4 microns) at the GHRS Digicons. In the very rare case this is thought not to be accurate enough, one may specify a Guiding Tolerance of less than 20 milli-arc seconds, and the guiding mode "Fine Lock" may be invoked. This has an expected tracking accuracy of about 7 milli-arc seconds. Acquiring Guide Stars in the Fine Lock mode is expected to take about twice as long as in Coarse Track mode. Further information is contained in the *Phase II Proposal Instructions.*

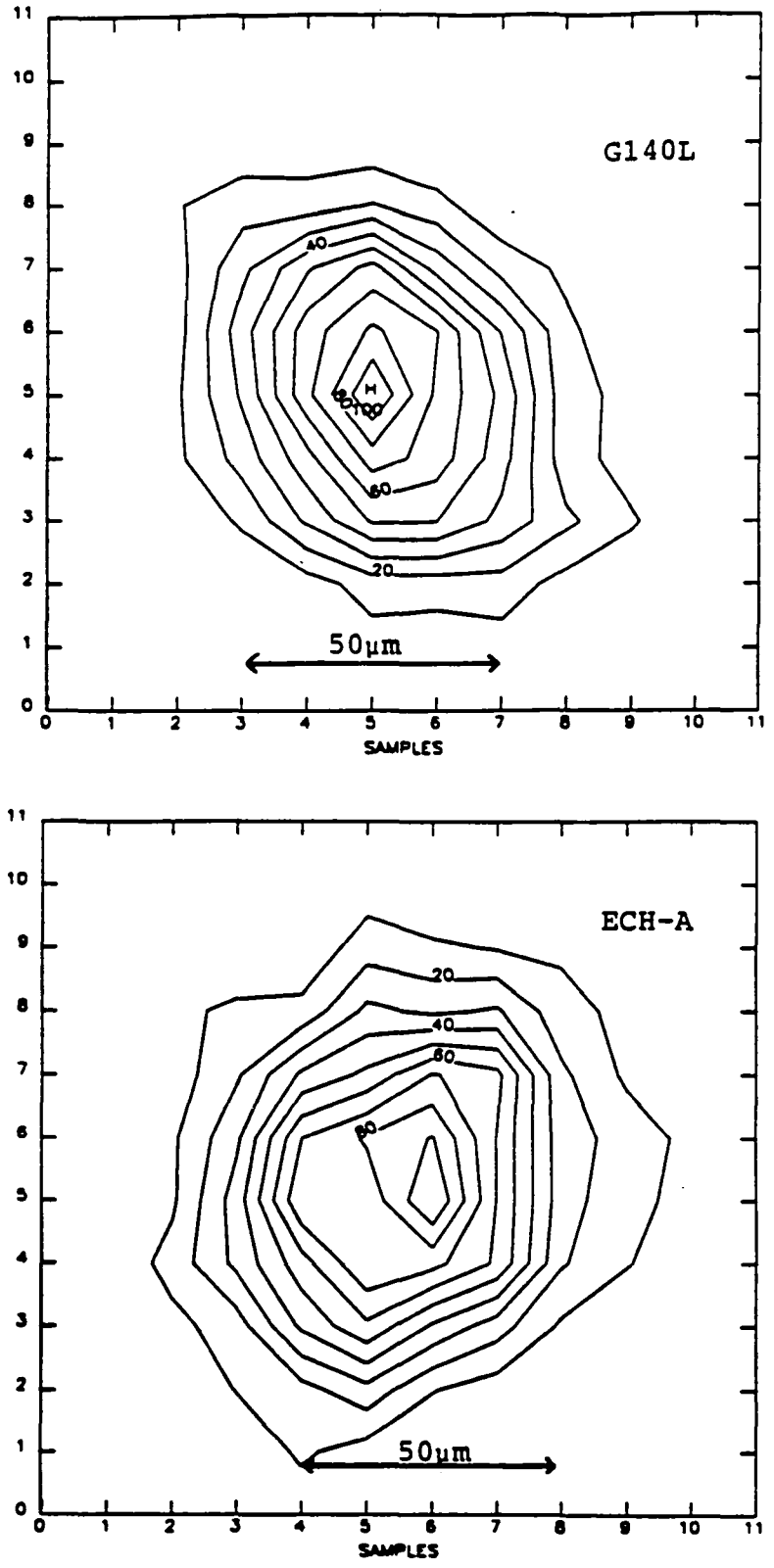

Figure 4-7. Contours of Emission Line Images

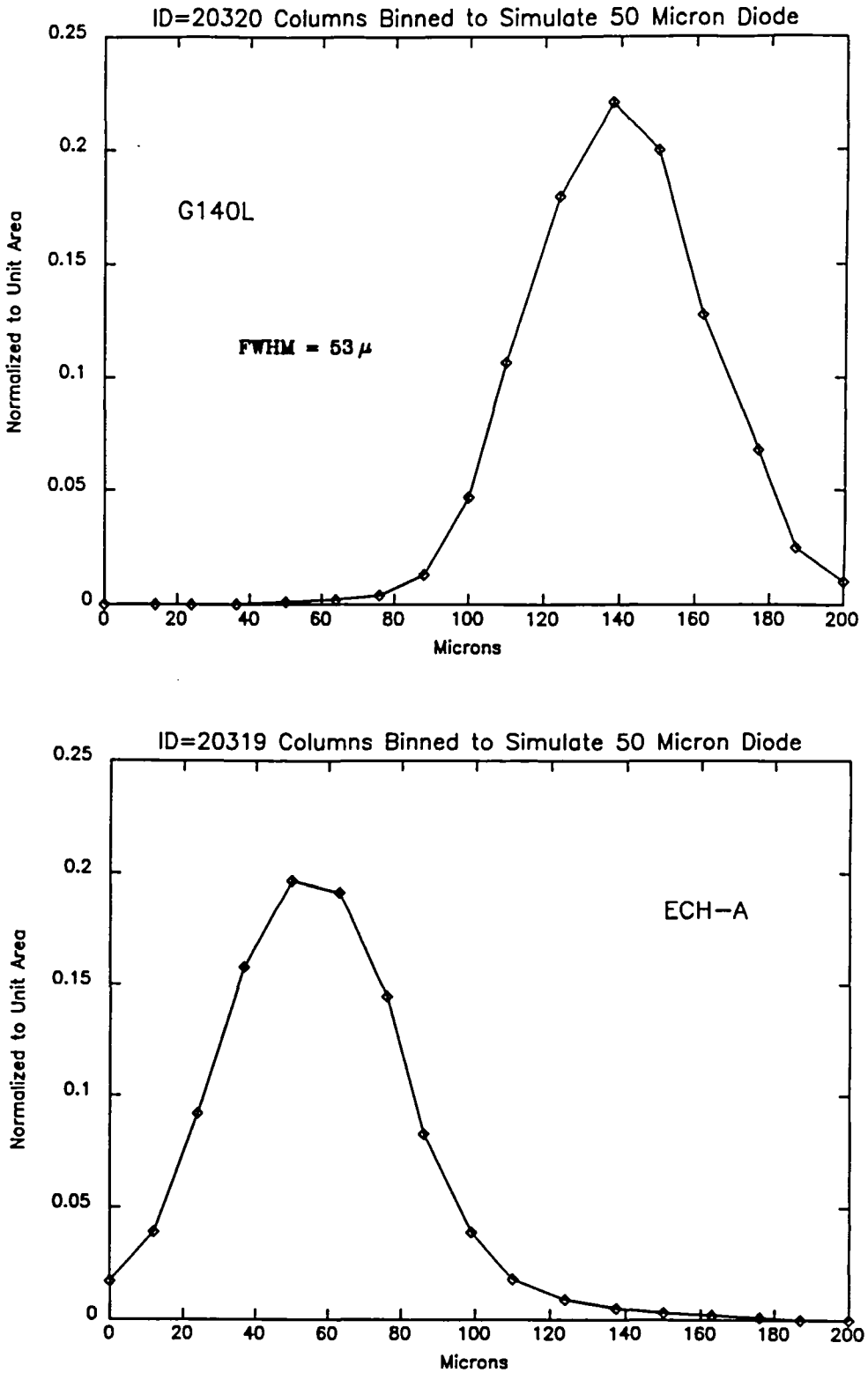

Figure 4-8. Emission Line Profiles

4.3.5 Sensitivity

During the pre-launch testing, the photometric sensitivity of each optical configuration was calibrated. This measured GHRS efficiency was combined with the expected throughput of the telescope to estimate the combined HST and GHRS sensitivity. This quantity is designated S_λ, and has units of counts per diode per second/ergs per square centimeter per second per Angstrom. The sensitivity varies as a function of wavelength for each grating. If the flux from the target is known, multiplying it by the appropriate value of S_λ will yield an estimate of the count rate to be expected in a particular grating configuration at the chosen wavelength. Sensitivity curves for each grating and Echelle are shown in Figures 4-9 through 4-16. The digital values are presented on Tables 4-8 through 4-14.

The data presented here was prepared in December 1986. It is the most accurate available today, incorporating final corrections derived from the thermal-vacuum testing at Lockheed, and utilizing the estimated transmission of the HRS apertures based on calculations of the HST point-spread function done by Dan Schroeder in January 1986.

There are seven tables with two parts each. The first ("a") tables give the calibration for the Large Science Aperture (LSA), which is 2.0 arcsec square, while the second ("b") give the calibration for the Small Science Aperture (SSA), which is 0.25 arcsec square. The echelle tables 4–13 and 4–14, are for the mid-points of each order in echelles A and B, respectively. The efficiency of the GHRS alone is given in column 2 of the tables, while columns 3 and 4 give the sensitivity of the combined OTA + aperture + GHRS system.

In the echelle configurations the sensitivity varies rapidly with wavelength across each order. This behavior is charatcteristic of all Echelle spectrographs, and is called the "Ripple Function." The basic nature of the variation with wavelength is quite similar for all orders, and can be parameterized in terms of the product $m\lambda$. The shape of the blaze function, normalized to a peak value of unity, and plotted as a function of $m\lambda$ is shown in Figure 4–16. The sensitivity at any wavelength in any order can be estimated by multiplying the peak response of the order shown in Figure 4–15 by the relative response shown in Figure 4–16.

The HRS efficiencies reported here are very poorly known shortward of 1300 Å . For example, the large variations in efficiency shortward of 1300 Å may be due to an artificial depression near 1220 Å or an artificial rise near 1170 Å . Despite these uncertainties, potential HRS observers are asked to use the sensitivities reported here in estimating exposure times. Linear interpolation between adjacent points can be used to estimate the sensitivity at a particular wavelength. Once the sensitivity of the HRS is better determined after in-orbit calibration, requested exposure times may be adjusted to ensure that appropriate signal-to-noise ratios are achieved.

In each table, the columns have the following meanings:

Column 1: wavelength in Angstroms.

Column 2: **efficiency of the HRS alone** in counts photon^{-1}, without taking into account the efficiency of the OTA or the size of the HRS aperture used.

Column 3: sensitivity in (counts diode^{-1} s^{-1}) (photon cm^{-2} s^{-1} Å $^{-1}$)$^{-1}$ of the combined OTA + aperture + HRS system.

Column 4: sensitivity in (counts diode^{-1} s^{-1}) (erg cm^{-2} s^{-1} Å $^{-1}$)$^{-1}$ of the combined OTA + aperture + HRS system.

Table 4–8a
Grating G140M, 2.0 Aperture

λ	Eff.	Sens.	Sens.
(Å)		(photons)	(flux)
1160	2.12E−02	12.9	7.56E+11
1180	1.45E−02	9.25	5.49E+11
1200	1.14E−02	7.81	4.72E+11
1220	6.96E−03	5.00	3.07E+11
1240	5.96E−03	4.41	2.75E+11
1260	2.43E−02	18.4	1.17E+12
1280	2.72E−02	20.7	1.33E+12
1300	2.12E−02	16.2	1.06E+12
1320	1.78E−02	13.6	9.06E+11
1340	1.48E−02	11.3	7.65E+11
1360	1.18E−02	9.05	6.20E+11
1380	9.94E−03	7.62	5.30E+11
1400	1.01E−02	7.76	5.47E+11
1420	1.07E−02	8.15	5.82E+11
1442	1.06E−02	8.08	5.87E+11
1460	1.05E−02	7.94	5.84E+11
1480	1.03E−02	7.76	5.79E+11
1502	9.90E−03	7.44	5.62E+11
1520	9.50E−03	7.01	5.37E+11
1600	5.80E−03	4.14	3.33E+11
1700	3.30E−03	2.36	2.02E+11
1800	8.00E−04	0.66	5.95E+10
1900	1.00E−04	0.04	4.22E+09

Table 4–9a
Grating G160M, 2.0 Aperture

λ	Eff.	Sens.	Sens.
(Å)		(photons)	(flux)
1150	9.38E−03	7.67	4.44E+11
1175	1.18E−02	9.38	5.55E+11
1200	8.30E−03	7.12	4.30E+11
1225	6.90E−03	6.27	3.87E+11
1250	9.04E−03	8.71	5.48E+11
1275	2.12E−02	20.9	1.34E+12
1300	1.66E−02	16.4	1.07E+12
1324	1.29E−02	12.7	8.50E+11
1350	1.02E−02	10.2	6.91E+11
1375	8.17E−03	8.07	5.58E+11
1400	7.76E−03	7.67	5.40E+11
1424	9.50E−03	9.36	6.72E+11
1450	9.70E−03	9.48	6.92E+11
1475	9.30E−03	9.06	6.72E+11
1501	9.20E−03	8.88	6.71E+11
1525	1.01E−02	9.62	7.38E+11
1550	1.12E−02	10.5	8.23E+11
1575	1.19E−02	11.1	8.83E+11
1600	1.23E−02	11.3	9.11E+11
1626	1.23E−02	11.1	9.11E+11
1650	1.17E−02	10.4	8.63E+11
1675	1.13E−02	10.2	8.63E+11
1700	1.14E−02	10.5	8.95E+11
1725	1.13E−02	10.6	9.19E+11
1750	1.15E−02	10.9	9.64E+11
1775	1.14E−02	11.2	1.00E+12
1800	1.10E−02	11.1	1.01E+12
1825	1.03E−02	10.7	9.84E+11
1850	9.70E−03	10.3	9.60E+11
1900	8.30E−03	9.28	8.88E+11
2000	6.00E−03	7.42	7.47E+11
2101	5.00E−03	6.58	6.96E+11

Table 4–10a
Grating G200M, 2.0 Aperture

λ	Eff.	Sens.	Sens.
(Å)		(photons)	(flux)
1501	8.40E−03	9.6	7.30E+11
1601	9.90E−03	10.8	8.70E+11
1650	1.06E−02	11.2	9.28E+11
1680	1.00E−02	10.8	9.12E+11
1710	1.00E−02	11.1	9.53E+11
1741	1.15E−02	12.9	1.13E+12
1770	1.31E−02	15.2	1.36E+12
1800	1.36E−02	16.3	1.48E+12
1831	1.33E−02	16.5	1.52E+12
1860	1.24E−02	15.9	1.48E+12
1891	1.12E−02	14.9	1.42E+12
1921	1.02E−02	13.9	1.34E+12
1950	9.40E−03	13.2	1.30E+12
1981	8.80E−03	12.8	1.27E+12
2011	8.60E−03	12.8	1.29E+12
2041	8.60E−03	13.1	1.35E+12
2072	8.80E−03	13.6	1.42E+12
2102	8.70E−03	13.8	1.46E+12
2131	8.50E−03	13.8	1.48E+12
2161	8.20E−03	13.5	1.47E+12
2191	7.80E−03	13.1	1.44E+12
2222	7.40E−03	12.6	1.41E+12
2251	7.00E−03	12.2	1.38E+12
2282	6.50E−03	11.4	1.31E+12
2311	6.20E−03	10.8	1.25E+12
2342	5.80E−03	10.2	1.20E+12
2372	5.60E−03	9.9	1.18E+12
2403	5.80E−03	10.2	1.24E+12
2431	6.30E−03	11.2	1.37E+12
2461	7.20E−03	12.7	1.57E+12
2493	8.20E−03	14.6	1.83E+12

Table 4–11a
Grating G270M, 2.0 Aperture

λ	Eff.	Sens.	Sens.
(Å)		(photons)	(flux)
2000	1.66E−02	30.8	3.10E+12
2099	1.44E−02	28.5	3.01E+12
2205	1.23E−02	26.1	2.90E+12
2240	1.27E−02	27.6	3.12E+12
2275	1.34E−02	29.4	3.36E+12
2310	1.36E−02	29.8	3.46E+12
2344	1.34E−02	29.6	3.50E+12
2381	1.32E−02	29.3	3.51E+12
2415	1.43E−02	31.8	3.87E+12
2450	1.69E−02	37.7	4.65E+12
2486	1.99E−02	44.4	5.56E+12
2520	2.17E−02	48.6	6.16E+12
2556	2.28E−02	51.1	6.57E+12
2590	2.30E−02	51.6	6.74E+12
2626	2.27E−02	51.1	6.76E+12
2661	2.20E−02	49.6	6.64E+12
2695	2.11E−02	47.6	6.46E+12
2730	2.01E−02	45.2	6.21E+12
2765	1.87E−02	42.0	5.85E+12
2800	1.75E−02	39.4	5.55E+12
2835	1.63E−02	36.5	5.21E+12
2871	1.47E−02	33.0	4.77E+12
2906	1.33E−02	29.7	4.35E+12
2940	1.18E−02	26.4	3.92E+12
2976	1.01E−02	22.7	3.40E+12
3010	8.60E−03	19.2	2.91E+12
3046	6.90E−03	15.6	2.38E+12
3081	5.60E−03	12.4	1.93E+12
3116	4.30E−03	9.6	1.50E+12
3151	3.40E−03	7.6	1.20E+12
3186	2.40E−03	5.4	8.62E+11
3221	1.70E−03	3.9	6.27E+11
3255	1.30E−03	2.8	4.60E+11
3291	9.00E−04	2.0	3.23E+11
3326	7.00E−04	1.4	2.42E+11

Table 4–12a
Grating G140L, 2.0 Aperture

λ	Eff.	Sens.	Sens.
(Å)		(photons)	(flux)
1200	2.16E−02	158	9.81E+12
1220	2.29E−02	180	1.16E+13
1240	2.22E−02	181	1.18E+13
1260	4.53E−02	372	2.42E+13
1280	5.08E−02	410	2.68E+13
1300	4.50E−02	357	2.34E+13
1320	3.93E−02	313	2.08E+13
1340	3.52E−02	281	1.90E+13
1360	3.03E−02	242	1.66E+13
1380	2.67E−02	214	1.49E+13
1400	2.66E−02	215	1.51E+13
1499	2.51E−02	200	1.51E+13
1588	1.85E−02	143	1.14E+13
1689	1.24E−02	95	8.10E+12
1790	4.30E−03	36	3.26E+12
1892	4.00E−04	3	3.32E+11

Table 4-13a
Grating ECH-A, 2.0 Aperture

λ	Eff.	Sens.	Sens.
(Å)		(photons)	(flux)
1170	3.40E−02	4.66	2.75E+11
1195	2.50E−02	3.68	2.21E+11
1221	1.20E−02	1.95	1.20E+11
1248	1.29E−02	2.25	1.41E+11
1277	1.41E−02	2.60	1.67E+11
1307	1.28E−02	2.43	1.60E+11
1338	9.54E−03	1.86	1.25E+11
1370	7.19E−03	1.43	9.89E+10
1405	7.30E−03	1.51	1.07E+11
1441	7.30E−03	1.54	1.12E+11
1478	7.90E−03	1.70	1.27E+11
1518	7.60E−03	1.67	1.27E+11
1561	7.10E−03	1.57	1.27E+11
1605	5.90E−03	1.33	1.08E+11
1652	5.40E−03	1.21	1.01E+11
1702	4.10E−03	1.00	8.55E+10
1756	2.60E−03	0.67	5.90E+10

Table 4–14a
Grating ECH-B, 2.0 Aperture

λ	Eff.	Sens.	Sens.
(Å)		(photons)	(flux)
1711	4.10E−03	0.98	8.45E+10
1764	9.50E−03	2.46	2.19E+11
1821	1.07E−02	3.06	2.80E+11
1882	1.12E−02	3.57	3.38E+11
1946	1.24E−02	4.39	4.30E+11
2016	1.45E−02	5.71	5.80E+11
2091	1.71E−02	7.37	7.76E+11
2171	1.91E−02	9.08	9.93E+11
2258	2.07E−02	10.9	1.24E+12
2352	2.14E−02	12.0	1.42E+12
2454	2.10E−02	12.5	1.54E+12
2566	2.04E−02	12.9	1.68E+12
2688	1.84E−02	12.4	1.68E+12
2822	1.47E−02	10.5	1.50E+12
2971	9.50E−03	7.28	1.09E+12
3136	3.60E−03	2.89	4.57E+11
3285	7.00E−04	0.65	1.07E+11

Table 4-8b
Grating G140M, 0.25 Aperture

λ	Eff.	Sens.	Sens.
(Å)		(photons)	(flux)
1160	2.12E−02	10.3	5.99E+11
1180	1.45E−02	7.34	4.36E+11
1200	1.14E−02	6.21	3.75E+11
1220	6.96E−03	3.98	2.44E+11
1240	5.96E−03	3.52	2.20E+11
1260	2.43E−02	14.7	9.35E+11
1280	2.72E−02	16.6	1.07E+12
1300	2.12E−02	13.0	8.52E+11
1320	1.78E−02	10.9	7.27E+11
1340	1.48E−02	9.12	6.15E+11
1360	1.18E−02	7.29	4.99E+11
1380	9.94E−03	6.15	4.27E+11
1400	1.01E−02	6.27	4.42E+11
1420	1.07E−02	6.59	4.71E+11
1442	1.06E−02	6.54	4.75E+11
1460	1.05E−02	6.43	4.73E+11
1480	1.03E−02	6.30	4.70E+11
1502	9.90E−03	6.04	4.57E+11
1520	9.50E−03	5.71	4.37E+11
1600	5.80E−03	3.38	2.72E+11
1700	3.30E−03	1.99	1.66E+11
1800	8.00E−04	0.54	4.93E+10
1900	1.00E−04	0.04	3.51E+09

Table 4–9b
Grating G160M, 0.25 Aperture

λ	Eff.	Sens.	Sens.
(Å)		(photons)	(flux)
1150	9.38E−03	6.07	3.52E+11
1175	1.18E−02	7.44	4.40E+11
1200	8.31E−03	5.66	3.42E+11
1225	6.90E−03	5.00	3.08E+11
1250	9.04E−03	6.96	4.38E+11
1275	2.12E−02	16.7	1.07E+12
1300	1.66E−02	13.2	8.61E+11
1324	1.29E−02	10.2	6.82E+11
1351	1.02E−02	8.17	5.56E+11
1375	8.17E−03	6.50	4.50E+11
1400	7.77E−03	6.19	4.36E+11
1424	9.50E−03	7.57	5.43E+11
1450	9.70E−03	7.68	5.61E+11
1475	9.30E−03	7.35	5.46E+11
1501	9.20E−03	7.22	5.45E+11
1525	1.01E−02	7.83	6.01E+11
1550	1.12E−02	8.56	6.71E+11
1575	1.19E−02	9.09	7.21E+11
1600	1.23E−02	9.25	7.45E+11
1626	1.23E−02	9.11	7.46E+11
1650	1.17E−02	8.52	7.08E+11
1675	1.13E−02	8.41	7.09E+11
1700	1.14E−02	8.61	7.37E+11
1725	1.13E−02	8.72	7.58E+11
1750	1.15E−02	9.03	7.96E+11
1775	1.14E−02	9.27	8.29E+11
1800	1.10E−02	9.19	8.33E+11
1825	1.03E−02	8.87	8.15E+11
1850	9.70E−03	8.55	7.96E+11
1900	8.30E−03	7.73	7.39E+11
2000	6.00E−03	6.21	6.25E+11
2101	5.00E−03	5.53	5.85E+11

Table 4–10b
Grating G200M, 0.25 Aperture

λ	Eff.	Sens.	Sens.
(Å)		(photons)	(flux)
1501	8.40E−03	7.85	5.93E+11
1601	9.90E−03	8.82	7.11E+11
1650	1.06E−02	9.16	7.61E+11
1680	1.00E−02	8.86	7.50E+11
1710	1.00E−02	9.11	7.84E+11
1741	1.15E−02	10.7	9.34E+11
1770	1.31E−02	12.6	1.12E+12
1800	1.36E−02	13.5	1.23E+12
1831	1.33E−02	13.7	1.26E+12
1860	1.24E−02	13.2	1.23E+12
1891	1.12E−02	12.4	1.18E+12
1921	1.02E−02	11.6	1.12E+12
1950	9.40E−03	11.0	1.08E+12
1981	8.80E−03	10.7	1.06E+12
2011	8.60E−03	10.7	1.08E+12
2041	8.60E−03	11.0	1.13E+12
2072	8.80E−03	11.4	1.19E+12
2102	8.70E−03	11.6	1.23E+12
2131	8.50E−03	11.6	1.24E+12
2161	8.20E−03	11.4	1.24E+12
2191	7.80E−03	11.0	1.22E+12
2222	7.40E−03	10.7	1.19E+12
2251	7.00E−03	10.3	1.17E+12
2282	6.50E−03	9.63	1.11E+12
2311	6.20E−03	9.13	1.06E+12
2342	5.80E−03	8.65	1.02E+12
2372	5.60E−03	8.40	1.00E+12
2403	5.80E−03	8.71	1.05E+12
2431	6.30E−03	9.51	1.16E+12
2461	7.20E−03	10.8	1.34E+12
2493	8.20E−03	12.5	1.57E+12

Table 4–11b
Grating G270M, 0.25 Aperture

λ	Eff.	Sens.	Sens.
(Å)		(photons)	(flux)
2000	1.66E−02	25.8	2.59E+12
2099	1.44E−02	24.0	2.53E+12
2205	1.23E−02	22.0	2.45E+12
2240	1.27E−02	23.3	2.63E+12
2275	1.34E−02	24.8	2.85E+12
2310	1.36E−02	25.2	2.93E+12
2344	1.34E−02	25.2	2.97E+12
2381	1.32E−02	24.9	2.98E+12
2415	1.43E−02	27.1	3.29E+12
2450	1.69E−02	32.1	3.96E+12
2486	1.99E−02	37.9	4.75E+12
2520	2.17E−02	41.5	5.26E+12
2556	2.28E−02	43.7	5.62E+12
2590	2.30E−02	44.2	5.77E+12
2626	2.27E−02	43.8	5.79E+12
2661	2.20E−02	42.6	5.70E+12
2695	2.11E−02	40.9	5.55E+12
2730	2.01E−02	38.8	5.34E+12
2765	1.87E−02	36.1	5.03E+12
2800	1.75E−02	33.9	4.77E+12
2835	1.63E−02	31.4	4.48E+12
2871	1.47E−02	28.4	4.10E+12
2906	1.33E−02	25.6	3.74E+12
2940	1.18E−02	22.7	3.37E+12
2976	1.01E−02	19.5	2.92E+12
3010	8.60E−03	16.5	2.50E+12
3046	6.90E−03	13.3	2.04E+12
3081	5.60E−03	10.7	1.66E+12
3116	4.30E−03	8.24	1.29E+12
3151	3.40E−03	6.53	1.04E+12
3186	2.40E−03	4.62	7.42E+11
3221	1.70E−03	3.32	5.39E+11
3255	1.30E−03	2.41	3.96E+11
3291	9.00E−04	1.68	2.78E+11
3326	7.00E−04	1.24	2.08E+11

Table 4–12b
Grating G140L, 0.25 Aperture

λ	Eff.	Sens.	Sens.
(Å)		(photons)	(flux)
1200	2.16E−02	125	7.80E+12
1220	2.29E−02	144	9.27E+12
1240	2.22E−02	145	9.38E+12
1260	4.53E−02	297	1.93E+13
1280	5.08E−02	329	2.14E+13
1300	4.50E−02	286	1.87E+13
1320	3.93E−02	251	1.67E+13
1340	3.52E−02	226	1.53E+13
1360	3.03E−02	195	1.34E+13
1380	2.67E−02	173	1.20E+13
1400	2.66E−02	174	1.22E+13
1499	2.51E−02	163	1.23E+13
1588	1.85E−02	117	9.34E+12
1689	1.24E−02	78	6.68E+12
1790	4.30E−03	30	2.70E+12
1892	4.00E−04	3	2.76E+11

Table 4–13b
Grating ECH-A, 0.25 Aperture

λ	Eff.	Sens.	Sens.
(Å)		(photons)	(flux)
1170	3.41E−02	3.70	2.18E+11
1195	2.50E−02	2.92	1.76E+11
1221	1.20E−02	1.56	9.57E+10
1248	1.29E−02	1.80	1.13E+11
1277	1.41E−02	2.08	1.34E+11
1307	1.28E−02	1.95	1.28E+11
1338	9.55E−03	1.50	1.01E+11
1370	7.19E−03	1.16	7.97E+10
1405	7.30E−03	1.22	8.61E+10
1441	7.30E−03	1.25	9.03E+10
1478	7.90E−03	1.38	1.03E+11
1518	7.60E−03	1.36	1.04E+11
1561	7.10E−03	1.28	1.01E+11
1605	5.90E−03	1.09	8.80E+10
1652	5.40E−03	0.99	8.28E+10
1702	4.10E−03	0.82	7.03E+10
1756	2.60E−03	0.55	4.87E+10

Table 4–14b
Grating ECH-B, 0.25 Aperture

λ	Eff.	Sens.	Sens.
(Å)		(photons)	(flux)
1711	4.10E−03	0.81	6.96E+10
1764	9.50E−03	2.03	1.81E+11
1821	1.07E−02	2.54	2.36E+11
1882	1.12E−02	2.97	2.81E+11
1946	1.24E−02	3.66	3.59E+11
2016	1.45E−02	4.79	4.86E+11
2091	1.71E−02	6.19	6.52E+11
2171	1.91E−02	7.66	8.37E+11
2258	2.07E−02	9.21	1.05E+12
2352	2.14E−02	10.2	1.20E+12
2454	2.10E−02	10.7	1.32E+12
2566	2.04E−02	11.0	1.43E+12
2688	1.84E−02	10.7	1.44E+12
2822	1.47E−02	9.07	1.29E+12
2971	9.50E−03	6.26	9.36E+11
3136	3.60E−03	2.49	3.93E+11
3285	7.00E−04	0.56	9.20E+10

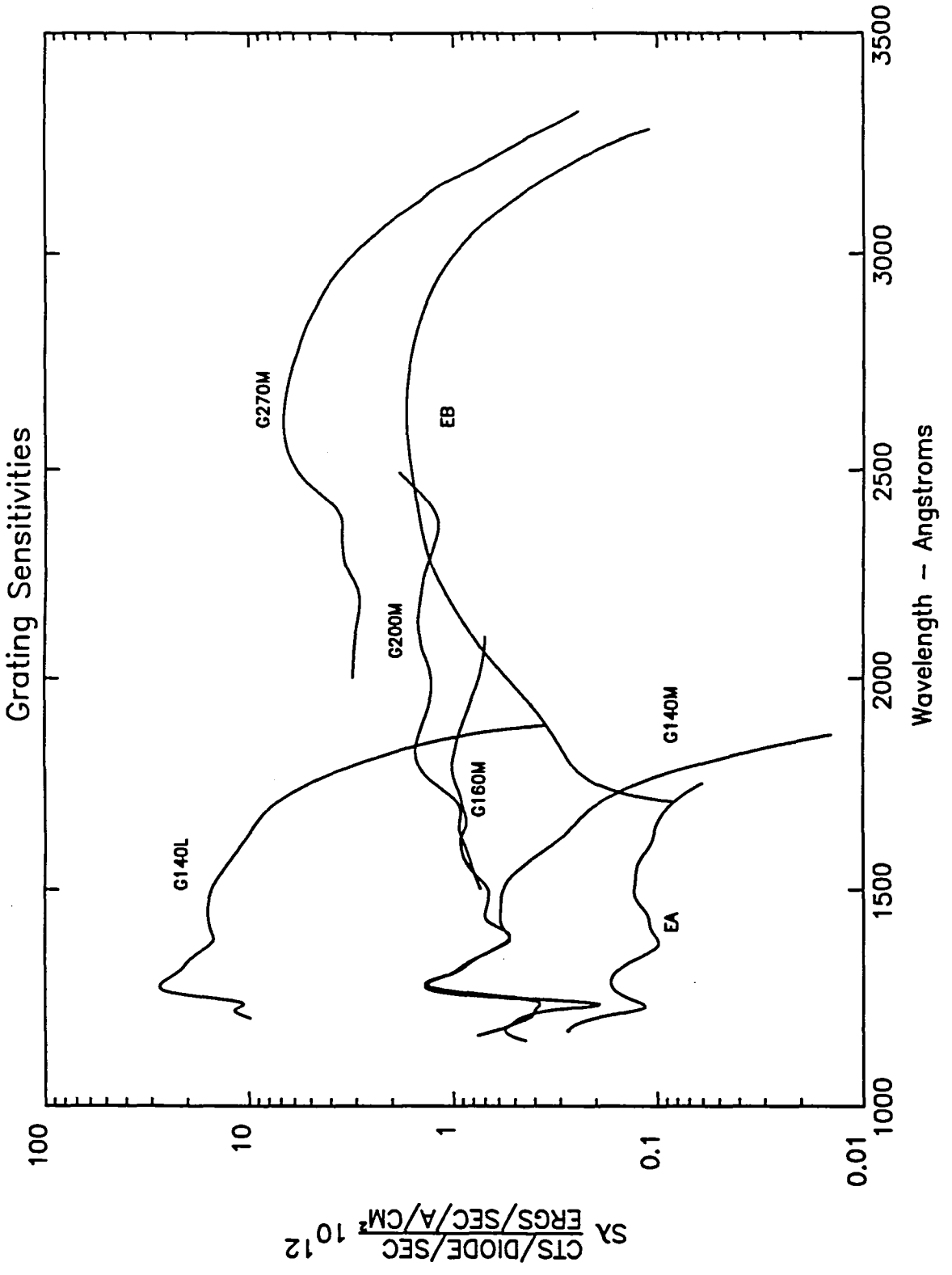

Figure 4-9. Combined GHRS and OTA Sensitivities
Based on Measured GHRS Efficiencies

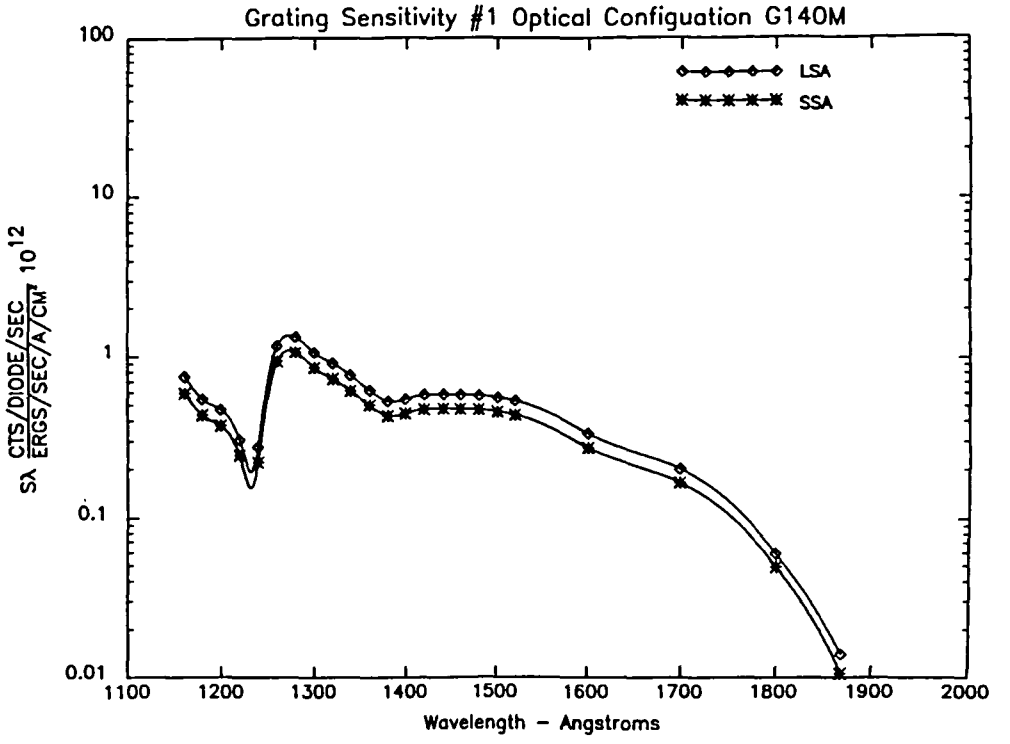

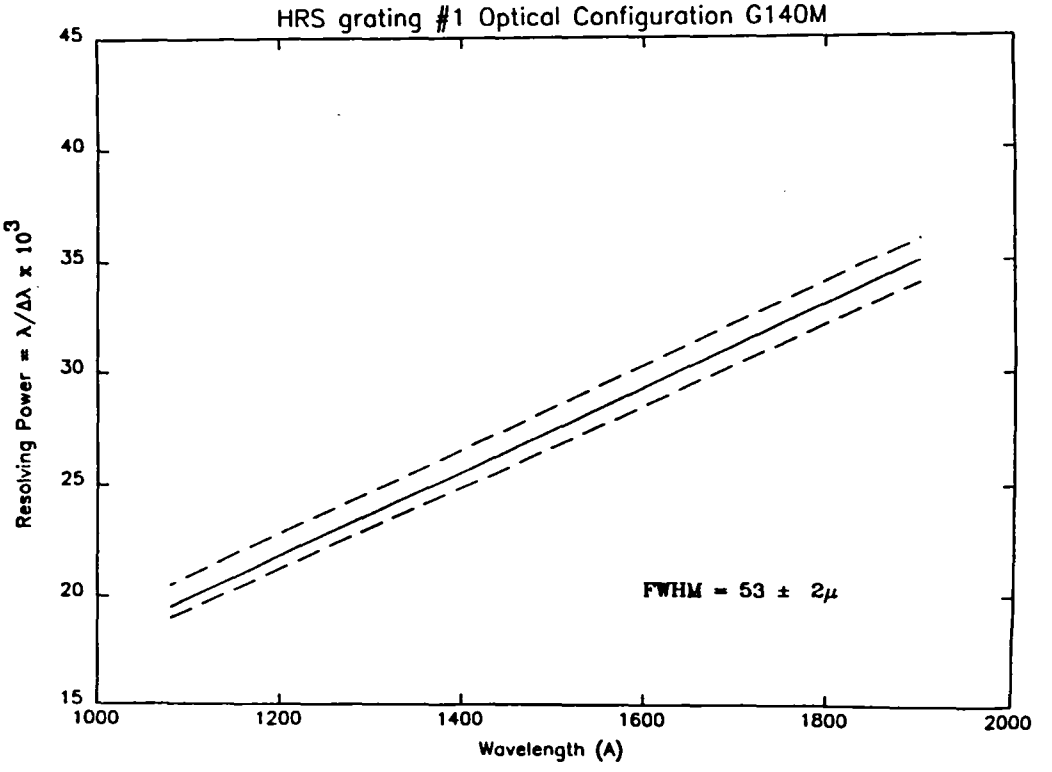

Figure 4-10. GHRS Grating One Optical Configuration G140M

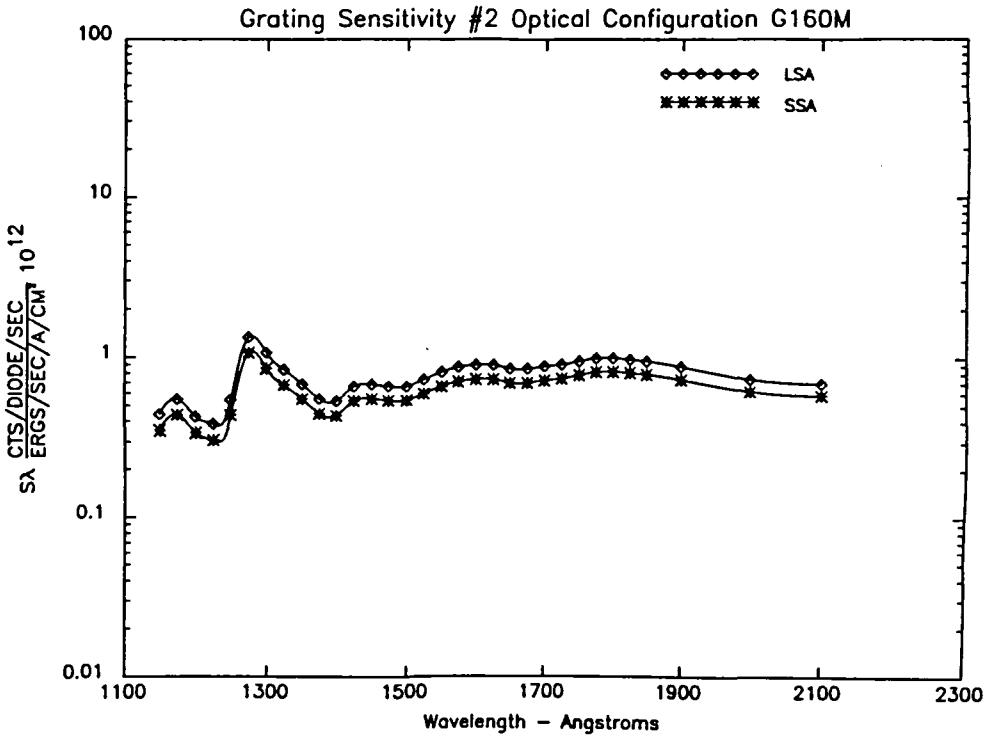

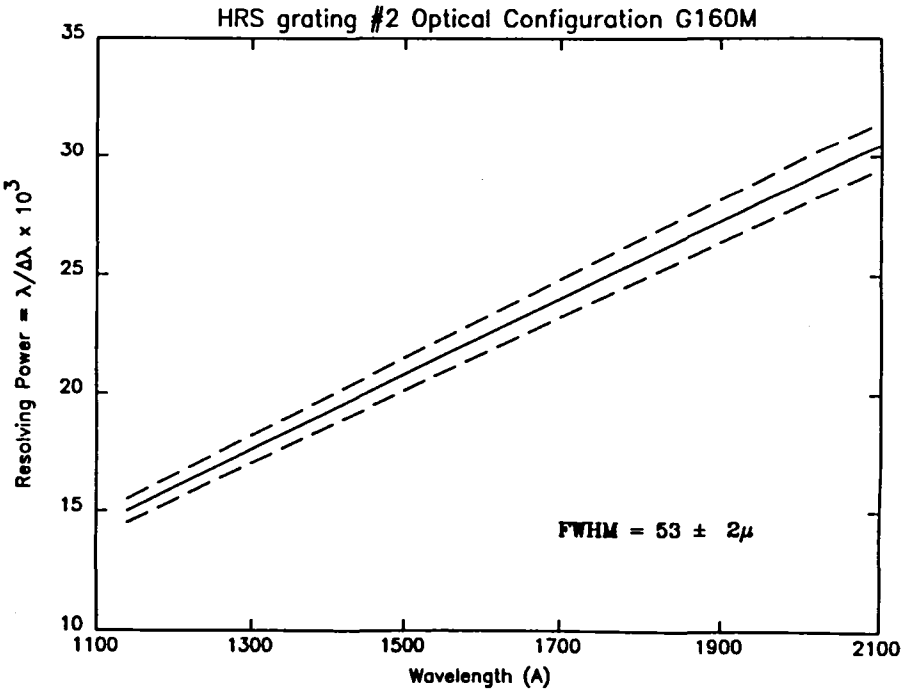

Figure 4-11. GHRS Grating Two Optical Configuration G160M

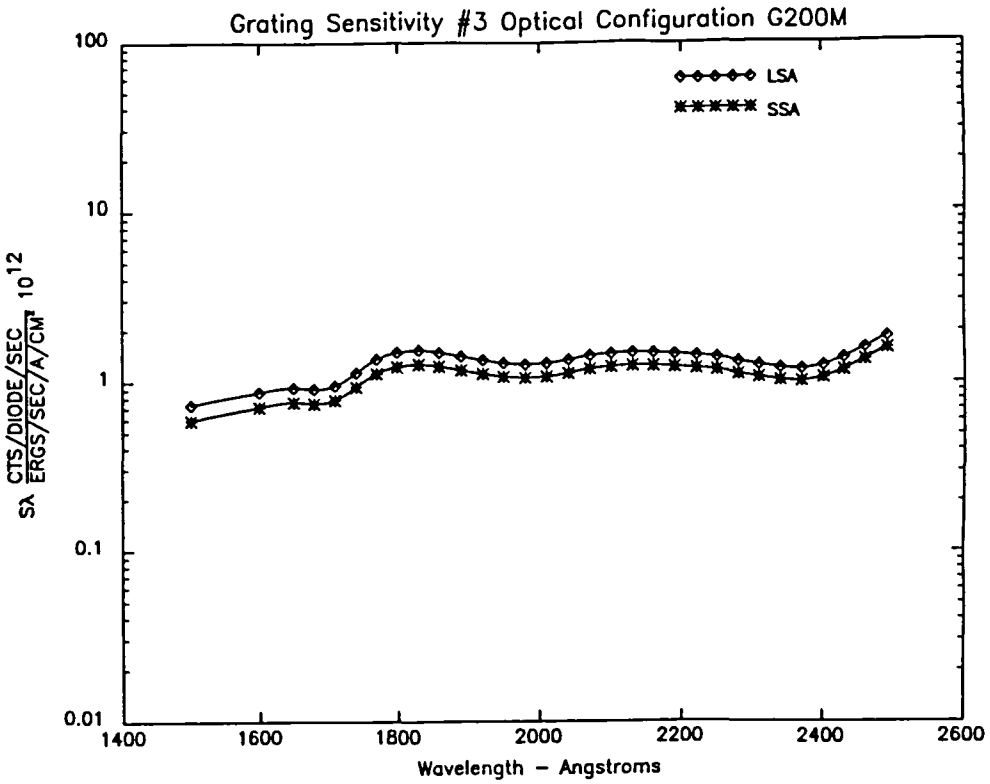

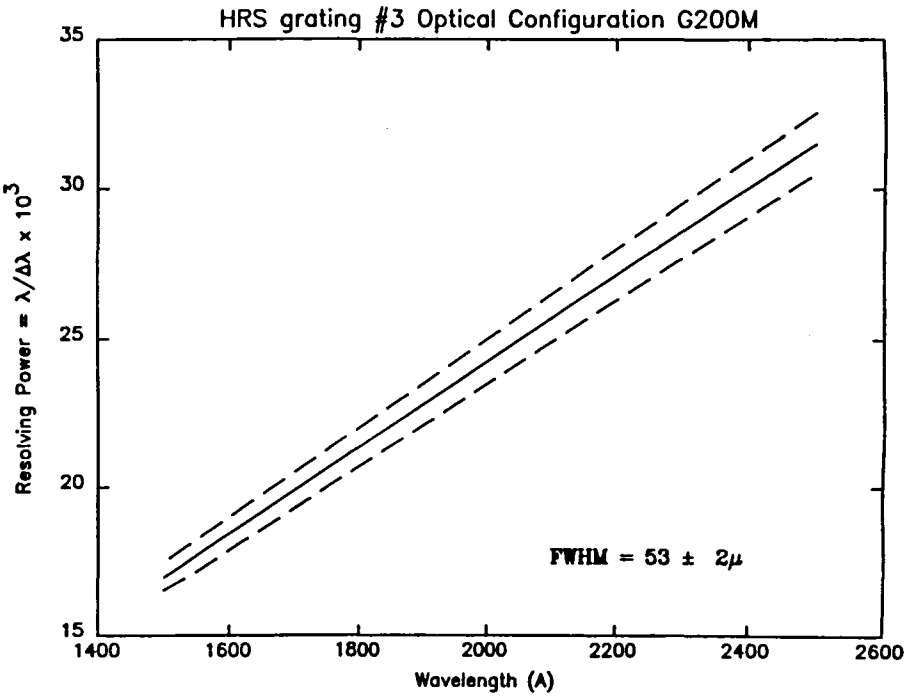

Figure 4-12. GHRS Grating Three Optical Configuration G200M

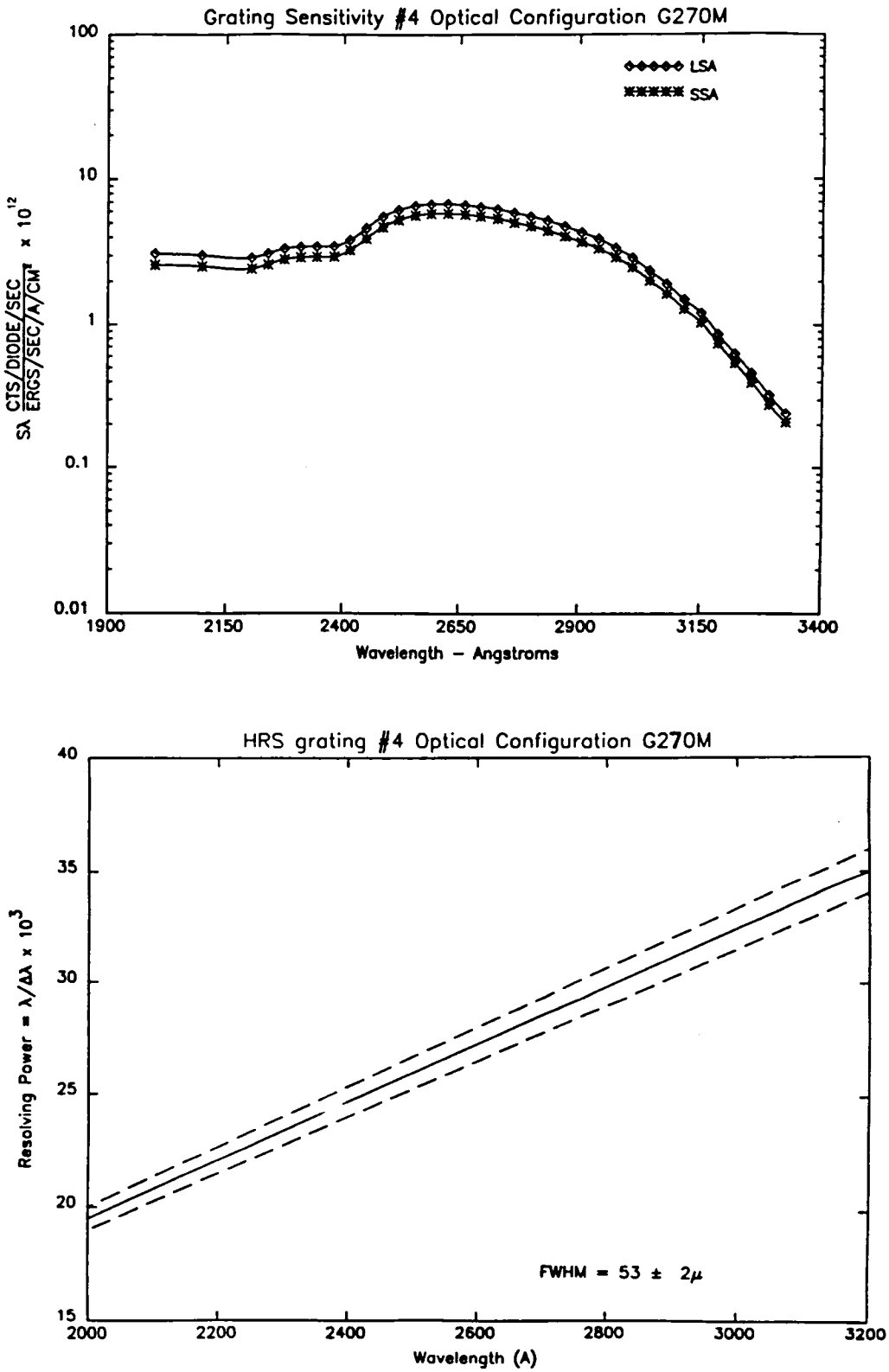

Figure 4-13. GHRS Grating Four Optical Configuration G270M

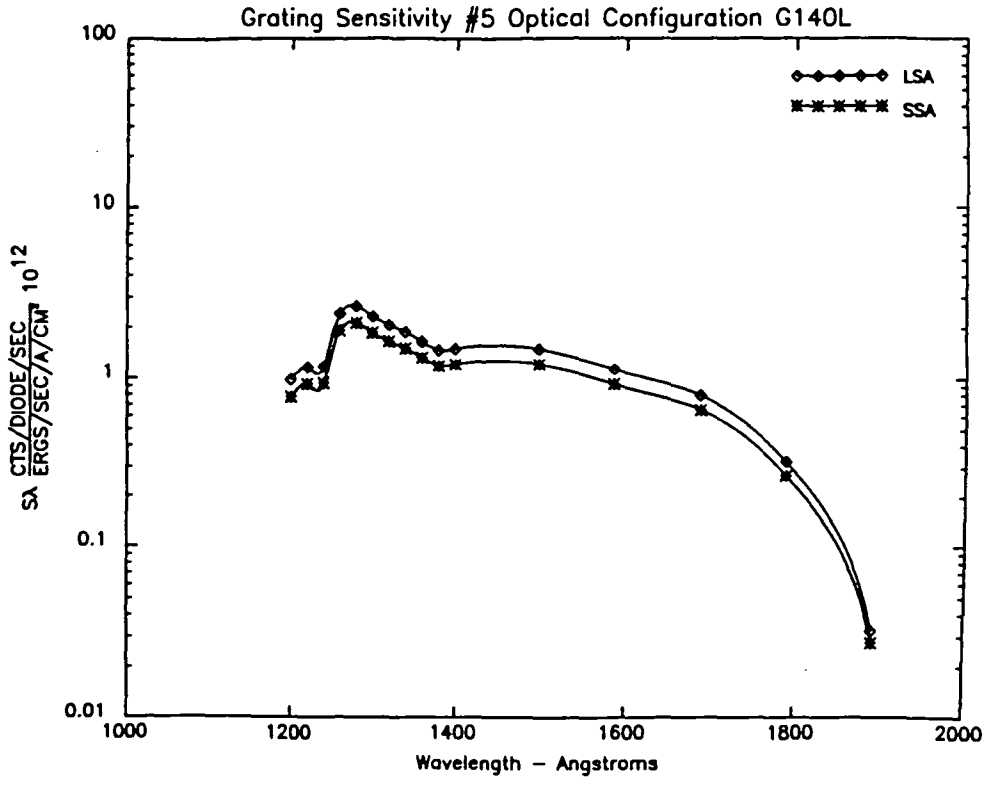

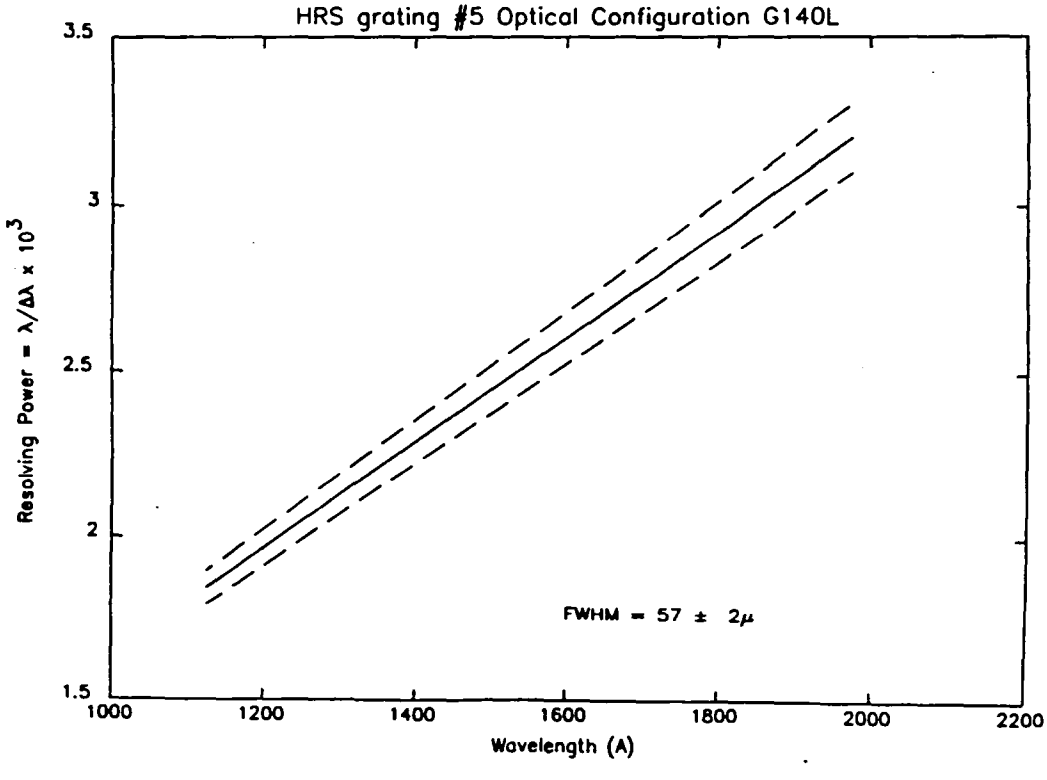

Figure 4-14. GHRS Grating Five Optical Configuration G140L

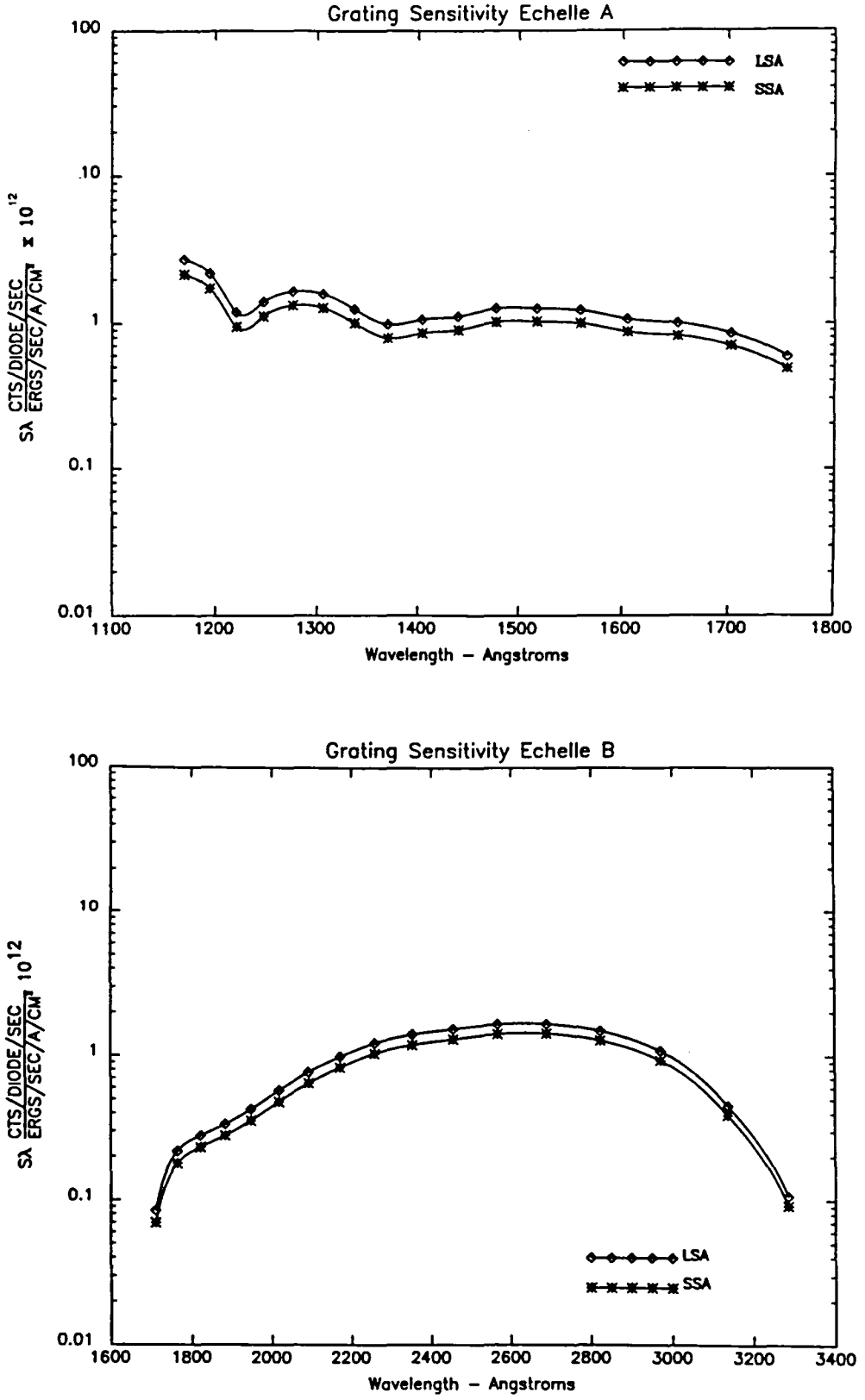

Figure 4-15. GHRS Echelle Gratings A and B

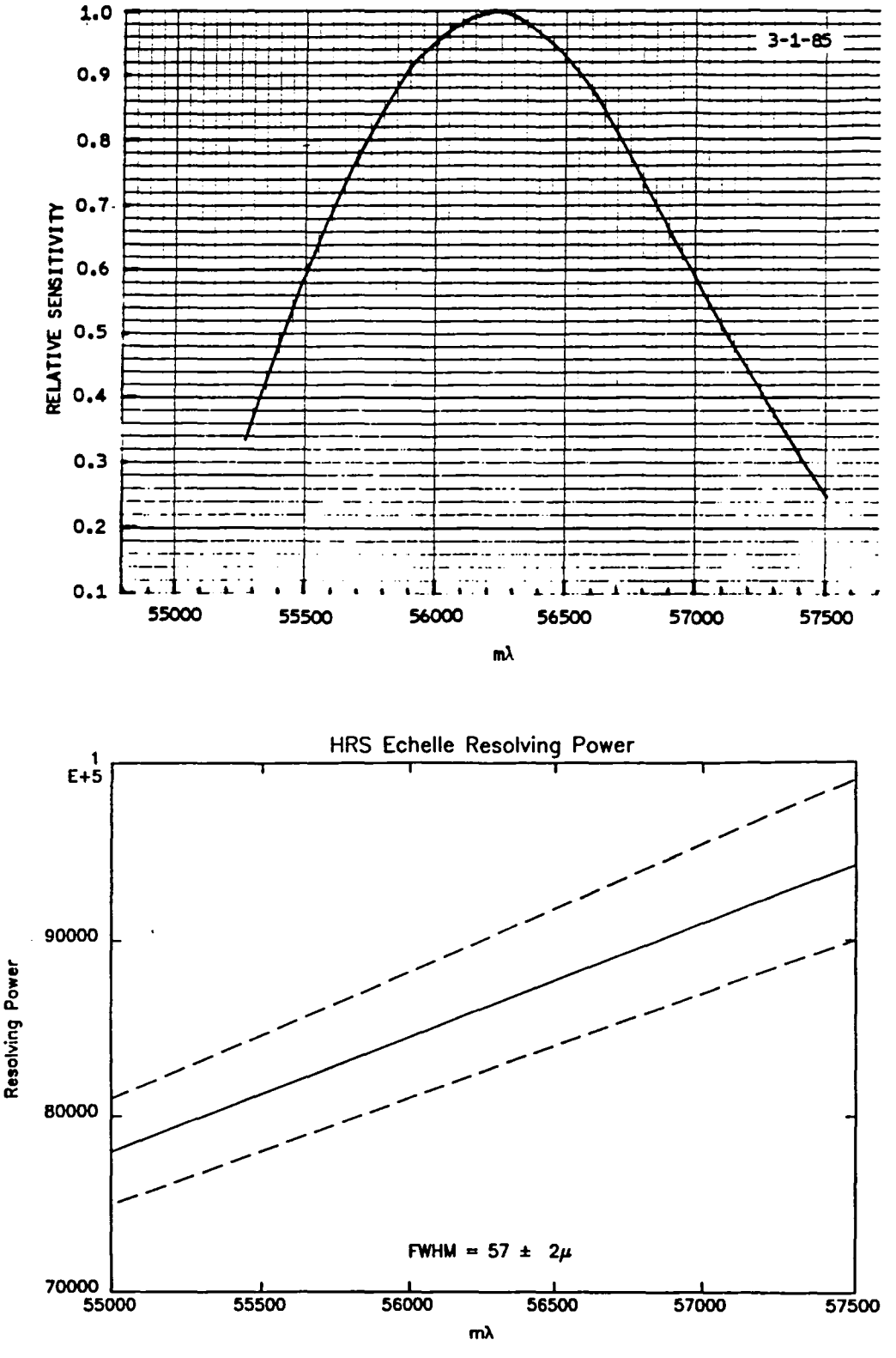

Figure 4-16. GHRS Echelle Normalized Blaze Function and Resolving Power

4.3.6 Scattered Light

The presence of stray and scattered light in a spectrograph is an effect which can influence the planning and execution of an observation, as well as the reduction and interpretation of the data. None of the optical configurations which include first order gratings has any serious problem with scattered light. The high quality of the imaging optics and diffraction gratings and the effectiveness of the baffles have successfully minimized the stray light. There are no special planning or observing strategies required. In the Echelle configurations, both the Echelle and the cross-dispersers are ruled gratings. This fact, plus the presence of light from sixteen orders simultaneously on the photocathode, results in a detectable level of background radiation. The irradiance on the photocathode due to scattered light (measured as count rate per unit area) is of the order of a few percent of the signal in the order. Two factors complicate this effect. The first is a geometrical effect caused by the fact that the science diodes are 400 μm tall, while the image of the spectrum is only about 55 μm wide. About $\frac{1}{8}$ of the diode is illuminated by the spectrum, while the rest is measuring background. Thus, a weak background irradiance is multiplied to the point that a significant fraction (15–20%) of the gross count rate on a diode is actually background. The measured scattered light background is the quantity listed in Tables 4-6 and 4-7. It varys significantly with order number, and is generally greater in Echelle A than in Echelle B. Its impact on data quality will be discussed in Section 4.5. The second complication arises from the fact that the background is the superposition of contributions from both the Echelle and cross-disperser. This means that the background is rather non-uniform, and has spatial structure which reflects the emission and absorption features in the nearby spectral orders. The background must therefore be measured and removed from the raw data with some care. The recommended strategy for echelle observations is to sample the signal in the inter-order region with the 500 science diodes, using deflection offsets which are calculated to precisely center that region on the diode array. An additional complication arises at the short wavelength ends of both echelle formats. Below approximately λ = 1100 Å in Echelle A and λ = 1800 Å in Echelle B, the spacing between orders is comparable to the length of the diodes, and it is difficult to make a clean measurement. The diode array has four large "corner diodes" which are long (1mm) in the direction of dispersion, but narrow (100 μm) in the cross-dispersion direction. These diodes may be used to sample the inter-order background without the problem of contamination by in order light, but they do not provide any spatial resolution. At a minimum, the time spent measuring the background should be about 10% of the time spent on the spectrum. If the goal is to achieve a very high signal to noise ratio in the net spectrum, it may be necessary to devote a greater fraction of time to the background measurement. Suggestions for estimating signal to noise ratios are made in Section 4.5 of this document.

4.4 DETECTORS

4.4.1 Background Count Rates

There are several potential sources of background counts, including detector dark count, electrical interference or cross talk with devices either within the GHRS or the spacecraft, and effects caused by the charged particle radiation environment of the ST orbit. During "thermal vacuum" testing at Lockhead, the detector dark count rates have been observed to be approximately 0.0003 counts per diode per second for the both detectors. The counts

appear to be randomly distributed in time, so that the "noise" in the dark count is the square root of the total counts accumulated during the observation. If one were observing very faint objects with low count rates, or the environment is noisier than expected, the background count rate can influence the signal to noise ratio of the data. A quantitative estimate is made in Section 4.5. At the present time there are no known sources of interference or cross talk which affect the detector count rates. The GHRS is equipped with both hardware and software capabilities to recognize and respond to cosmic ray and trapped particle events. Although the functioning of the hardware and validity of the software logic have been verified, a true assessment of the suppression of these events will be made after launch.

An external source of background which can potentially be a problem during the acquisition (not the observation) of faint targets is geocoronal background light. This problem and what to do about it is discussed in the *GHRS Target Acquisition Guidelines* Manual.

4.4.2 Photometric Linearity

The pulse counting digicon detectors have an extremely well behaved relationship between the detected count rate and the true photon event rate. At low count rates the relationship is linear, with unit slope and no threshold or bias level. At very high count rates, the intervals between photon events may become comparable to the response time of the electronics, and not every pulse will be counted. This so called "paired pulse effect" has been calibrated, and observed counting rates can be corrected up to a maximum of approximately 150,000 counts per diode per second true input event rate. The calibration is not valid for input rates higher than this. The relationship defined by the paired pulse effect is shown in Figure 4-17. A simple expression which fits the observed relationship well enough to be used for planning purposes is

$$y = \frac{1 - e^{-tx}}{t} \qquad (4-7)$$

where

x = true input event rate
y = observed counting rate
t = response time $\approx 10\mu$ seconds

Above 150,000 counts per second true input event rate, the output rate actually *decreases* slightly.

4.4.3 Photocathode Granularity

Since the optical image is focused directly onto the photocathode, spatial non-uniformities in the quantum efficiency show up as irregularities in the measured spectrum. Both detectors exhibit small scale granularity, somewhat analogous to the graininess in a photographic emulsion. The effect is far more pronounced in the D1 (LiF+ CsI) detector and must be considered in planning an observation. It is less serious in D2 (MgF_2+ CsTe), and will not be a problem unless you need high S/N data.

Figure 4-18 illustrates the D1 situation. Each plot shows the percent deviation from a perfectly uniform response. The top panel shows the entire diode array, while the middle and bottom panel show enlargements of the lower and upper 100 diodes. There are patterns of faintly visible "sleeks" on the photocathode faceplate, which are more pronounced on the

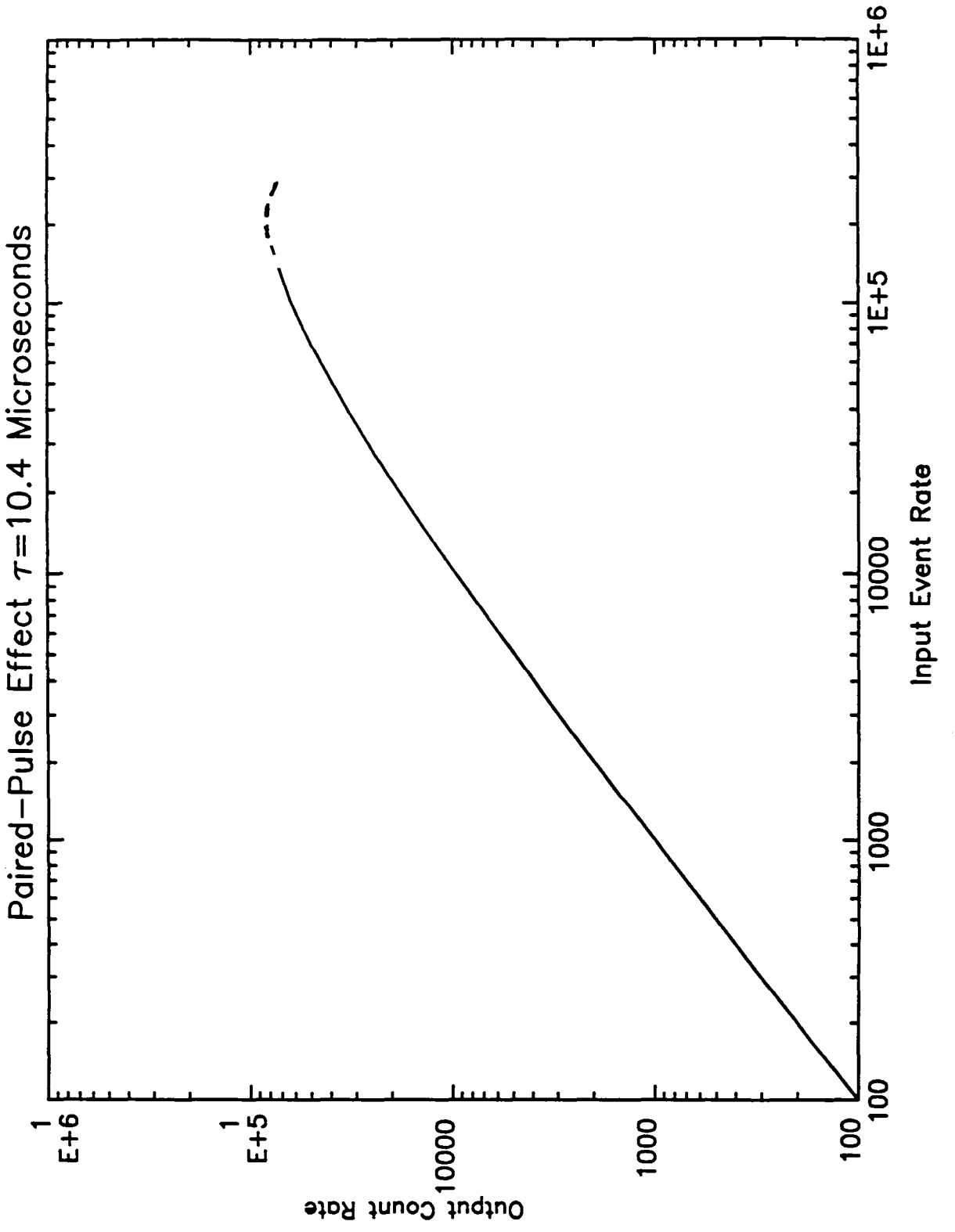
Paired–Pulse Effect τ=10.4 Microseconds
Output Count Rate
1 E+6
1 E+5
10000
1000
100
Input Event Rate
100
1000
10000
1E+5
1E+6

Figure 4-17

left side (low diode numbers, shorter wavelengths). The nonuniformities shown in Figure 4-18 have the following characteristics: (1) they have a characteristic spacing of about 6 diode widths (300 μm), (2) each feature has a width of 3-diodes, (3) the maximum peak to valley difference is about 8% and (4) averaged over the entire diode array, the RMS deviation is approximately 2%.

Figure 4-19 shows the same kind of data for detector D2. There is no sleeking on the MgF_2 faceplate, and no evidence of quasi-periodic irregularities on the response. The maximum deviations from uniformity are about 1%, with an RMS scatter of less than 0.5%. There are no significant variations in these statistics across the photocathode. However, there are a few isolated blemishes, whose response differs by 5% or more from the local average. There is presently no way of avoiding the isolated blemishes on the photocathode a priori.

If one intends to study spectral features whose characteristic widths and depths are comparable to the granularity, the following suggestions should be considered: (1) make a long enough exposure so that the photon noise is much smaller than the expected amplitude of the feature, (2) if at all possible, use detector D2, (3) if using D1, choose a central wavelength that will place important features on the right hand side of the detector and (4) **this is important:** break a long exposure into a series of subexposures, with the carousel position changed slightly between subexposures. This will move the spectrum along the photocathode and allow features with constant detector coordinates (granularity) to be distinguished from features with constant wavelengths (spectral lines). This can be requested via the FP-SPLIT optional parameter on the Exposure Logsheet during Phase II. One carousel step moves the spectrum approximately 5.2 diode widths.

4.4.4 Larger Scale Photocathode Nonuniformities

If a scientist wishes to study a longer part of the spectrum than can be recorded in a single observation, several of the shorter segments will be observed separately and combined afterwards. Any large scale nonuniformities in the detector response will show up as imprecise overlaps of adjoining spectral regions. The existence of such gradients was confirmed during the ground based testing, but a thorough analysis of the calibration data will not be completed until after the "science verification" period following launch. Hopefully, these large scale effects can be removed as part of the standard photometric calibration.

Both detectors exhibit nonuniformities in at least some wavelength regions. Figure 4-20 illustrates a particularly good region and an annoyingly worse region of the D2 detector. Shortward of $\lambda = 2500$ Å this detector shows quite good uniformity, and splicing together separate observations will not not pose any unusual problems. Between 2500 and 3200 Å the CsTe photocathode shows variations with both spatial and spectral dependencies. The lower panel of the figure shows that near 2800 Å the left side of the photocathode is about 5% more sensitive than the center and right side.

4.4.5 Diode Array

The 500 science diodes exhibit very little nonuniformity in their responses to photoelectrons. Precise measurements have revealed a small effect, which amounts to a nearly constant offset of about 1% between all of the odd numbered diodes compared to the even numbered channels. This is likely due to the way the electrical connections between the diodes and preamps are made. The effect can be almost entirely suppressed by use of a

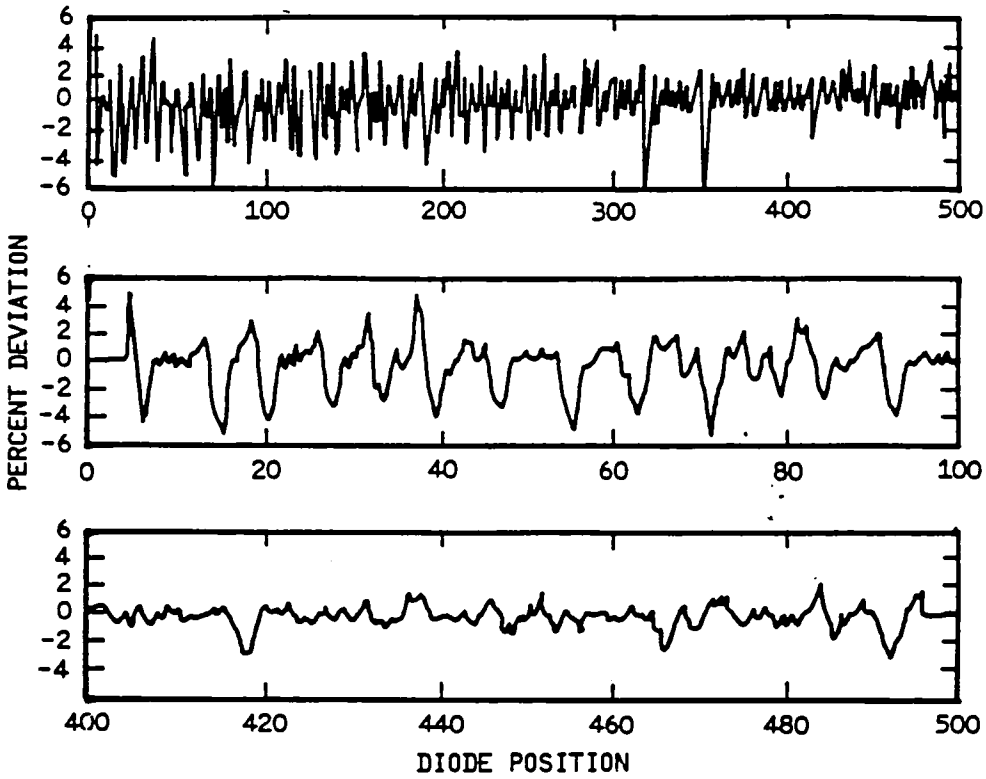

Figure 4-18. D1 Photocathode Granularity

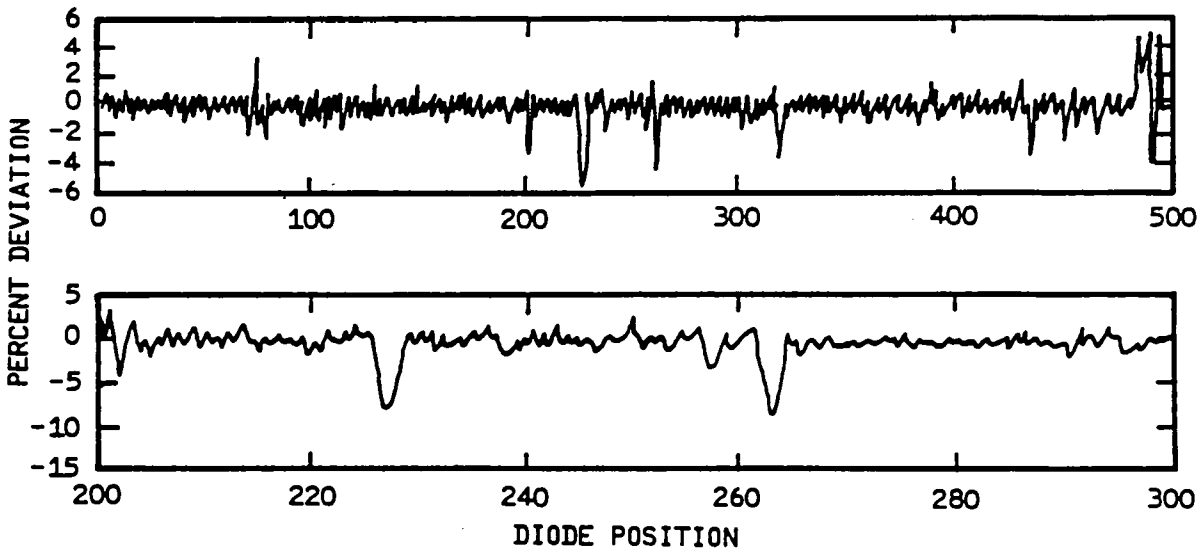

Figure 4-19. D2 Photocathode Granularity

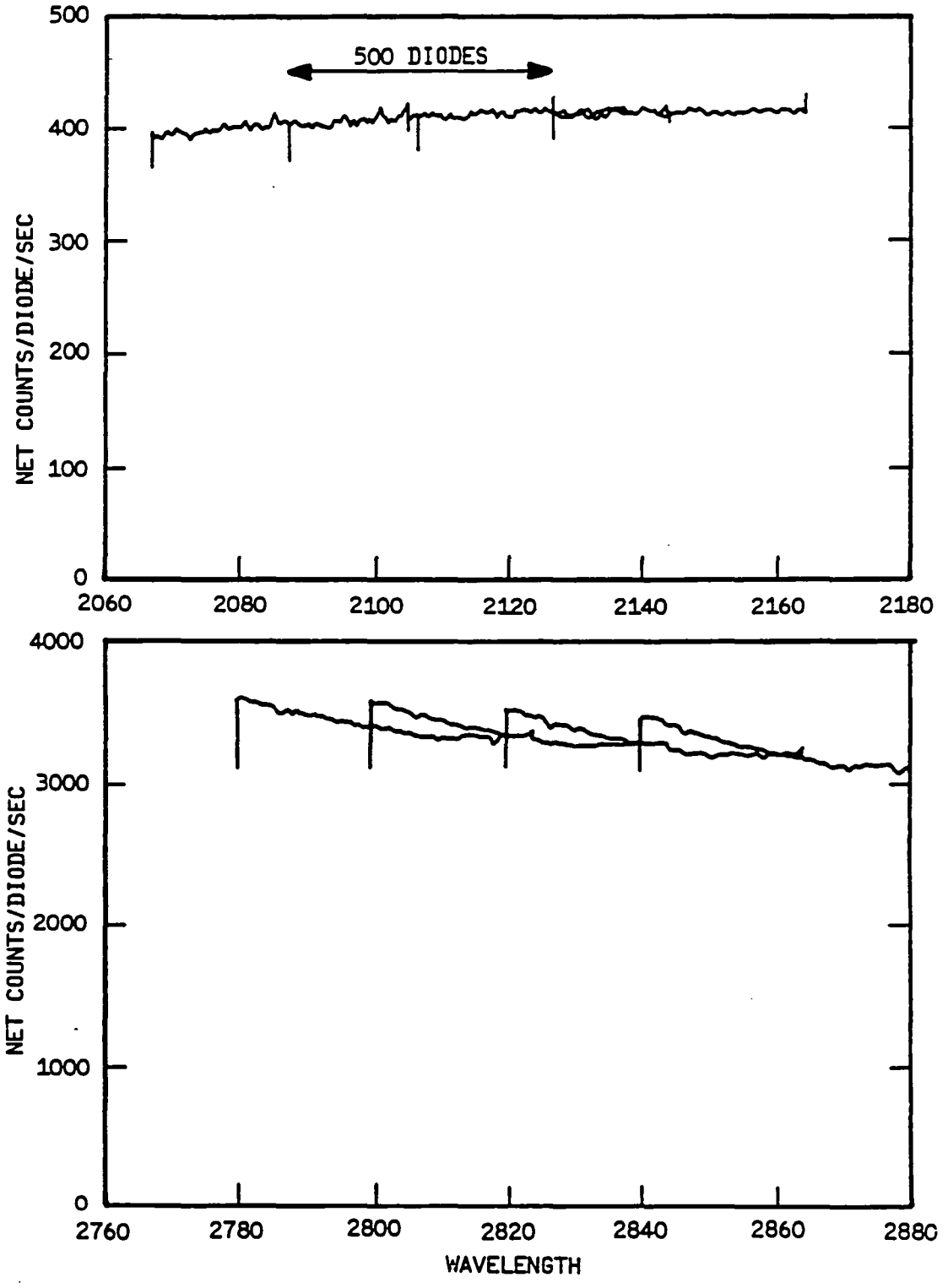

Figure 4-20. D2 Photocathode Non-Uniformity

"comb-addition" process, whereby each "pixel" on the photocathode is sampled by several adjacent diodes during an observation. This will be explained in Section 4.4.6.

Each science diode has a width of 40 μm and a height of 400 μm, corresponding to 0.2 × 2.0 arc seconds on the sky. They are spaced on 50 μm centers. The gap between diodes is not completely insensitive but contributes slightly to both neighboring channels. The response profile of an individual diode resembles a trapezoid with a 40 μm top and a 60 μm base, with the same effective area as a 50 μm wide rectangle. The Large Science Aperture projects onto 8 diodes width, the small Science Aperture onto one diode width.

At the four corners of the diode array there are large, horizontal "corner diodes" which are used to measure the background while the spectrum is being recorded by the science diodes. Each is 100 μm wide and 1000 μm long, and has approximately five times the effective collecting area of the science diodes.

At each end of the diode array is a gold plated "radiation diode." The conductive coating, in conjunction with a high discriminator threshold, renders these diodes insensitive to 23kV photoelectrons. They do respond to higher energy particles though, and are used to monitor the radiation environment during an observation.

There are five small "focus diodes" which are used to produce the field maps for target acquisition and Image Mode observations. Each is a 25 μm square, and has roughly 15% of the response to a point source image that a science diode has. Figure 4-21 shows the layout of the diodes.

4.4.6 Substepping Strategies

Substepping is the detailed procedure by which the spectrum and background are sampled by the diode array. The monochromatic image of the small Science Aperture is a spot approximately 50μm in diameter. A continuous spectrum forms a linear image 50μm wide and several cm long. The location of the image on the photocathode is different for each grating, and varies as a function of wavelength and order. The diode array is fixed to the back end of the digicon tube. A pair of magnetic deflection coils is used to select the area of the photocathode which is sampled by the diode array. One coil steers the electron image parallel to the diode array (the "x" direction), while the second deflects the image perpendicular to the diodes (the "y" direction). The deflections are commanded with 12 bits (0–4095) in each axis. One step moves the image by 6.25μm, or $\frac{1}{8}$ of a diode width (which corresponds to $\frac{1}{32}$ of an arc second at the HST focal plane).

Since the image of the small science aperture has the same width as the detector resolution element (one diode width), a single integration undersamples the spectrum. A proper measurement requires at least two samples per resolution element. The requirement is met by a procedure called substepping. Each integration produces a total of 524 words of data: the counts from the 500 science diodes, the 12 auxiliary diodes, and 12 words of engineering data, such as the integration time and grating configuration. There is enough memory available in the on-board computer to accommodate seven independent integrations. These buffers are referred to as the "substep bins". One observation consists of all the data taken with the carousel at a fixed position, and stored in from one to seven bins. Each bin will usually represent a different pair of deflection coordinates, so that slightly different areas of the photocathode are sampled. The usual practice is to make either two or four integrations with the spectrum centered on the diode array, but offset from each other by $\frac{1}{2}$ or $\frac{1}{4}$ diode width in the x coordinate ("half-stepping" or "quarter-stepping").

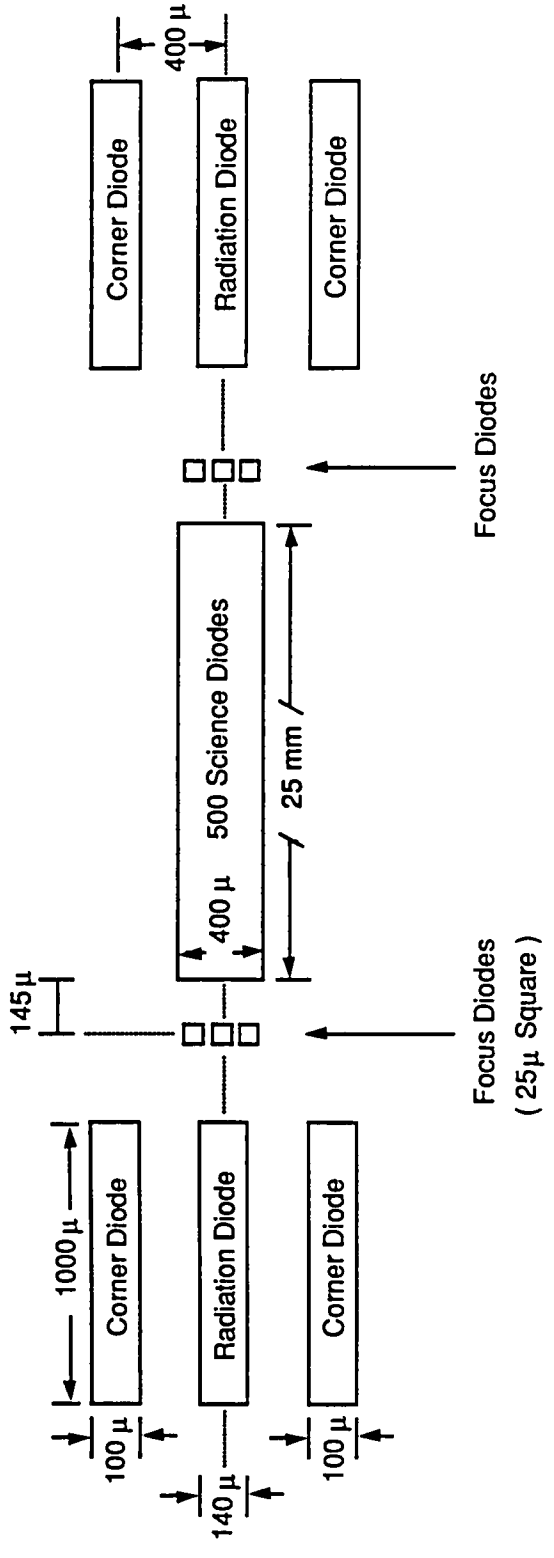

Figure 4-21. Layout of Digicon Diodes, **Not to Scale**

This produces a spectrum with two or four samples per resolution element, and satisfies the requirement for proper sampling. All bins which sample the spectrum usually have the same total exposure time. The data from the separate bins are merged into a single spectrum during the data reduction process. Two additional bins can be used to sample the background adjacent to the spectrum. In the Echelle configurations, the deflections are adjusted to sample the background precisely midway between adjacent orders. This process gives a detailed measurement of the background, which can be averaged, filtered and subtracted from the gross spectrum. The exposure time on the background does not have to be the same as the time on the spectrum. A parameter called the "repeat code" may have values of 1, 2, 4 or 8. A background bin with repeat code r will have an exposure time of $\frac{1}{r}$ of the bin(s) with the spectrum.

Substep patterns are sequences of deflections and integrations that fill the bins to produce an observation. The integration time at each deflection coordinate is short—typically 200 milliseconds. Each deflection pair is issued, and the counts obtained at that position are coadded into the appropriate bin. A long observation will cycle through the pattern dozens or hundreds of times to accumulate the required exposure time. The pattern must be completed at least once, which limits the duration of the shortest possible exposure. The standard use of comb addition (see below) means that each pattern must be repeated a minimum of four times. The flight software can accommodate a wide variety of patterns. A few useful patterns which have been adopted as standards are summarized in Table 4-15. The columns labeled Spectrum Bins and Background Bins show the number of samples on each region. Background Diodes indicate whether the background is measured with the main array of 500 science diodes or with the larger corner diodes. The number "f" is the fraction of the total observing time spent measuring the spectrum. Since all integrations are made up of substep pattens, they are effectively "quantized" in units of time equal to one pass through the substep pattern. Actual exposure time will be slightly less than requested if not an exact multiple of the "quantized"time. The next column indicates with which gratings each pattern is most appropriately used. The observer may select one of these standard patterns with the STEP-PATT optional parameter on the exposure logsheet during Phase II. In the absence of any choice, the default pattern (numbers 4 and 6) will make two samples per resolution element on the spectrum, and background measurements above and below the spectrum each with a repeat code of 8 (*i.e.*, about 11% of the time will be spent measuring the background). Remember that at least two samples per diode are needed to take advantage of the instrumental resolution.

An additional process usually used as part of the substepping strategy is "Comb Addition." After each complete cycle through the substep pattern, the initial x deflection is changed by an integral number of diode widths. The pattern is then repeated around the new position. The result is that each pixel on the photocathode is sampled by several different diodes. The small diode to diode gain variations are averaged out, and holes in the spectrum due to a few inoperative channels are avoided. As the data are stored into the various substep bins, adjustments are made to ensure that each data point refers to the same photocathode pixel, not the same diode number. The usual practice is to cycle through four initial deflections, each offset by one diode width. There is nothing on the Phase I proposal for comb-addition; it is programmed automatically. If any changes to the standard technique are needed they can be specified on a Phase II form. The "Shortest Exposure Times" in

TABLE 4-15
Standard Substep Patterns

Pattern Number	Spectrum Bins	Background Bins	Background Diodes	f	Used With	Shortest Exposure (seconds)
1	1	0		1.00	all	0.8
2	2	0		1.00	all	1.6
3	4	0		1.00	all	3.2
4	2	2	Science	0.89	1st order	14.4
5	4	2	Science	0.94	1st order	27.2
6	2	2	Science	0.89	Echelle	14.4
7	4	2	Science	0.94	Echelle	27.2
8	2	2	Corner	0.89	Echelle	14.4
9	4	2	Corner	0.94	Echelle	27.2
10	2	2	Science	0.50	1st order	3.2
11	4	2	Science	0.67	1st order	4.8
12	2	2	Science	0.50	Echelle	3.2
13	4	2	Science	0.67	Echelle	4.8
14	2	2	Corner	0.50	Echelle	3.2
15	4	2	Corner	0.67	Echelle	4.8

Table 4-15 are calculated assuming Comb Addition = 4. Specifying Comb-Addition = 2 would reduce them $\times 1/2$; no Comb Addition would reduce them $\times 1/4$.

Any individual bin will overflow if it accumulates more than 65,536 counts.

4.5 SIGNAL TO NOISE CHARACTERISTICS

There are several factors which influence the signal to noise, including statistical (photon) noise in the detected spectrum, dark count noise in the detector, scattered light in the spectrograph, diode to diode gain variations, and granularity in the photocathode sensitivity. For signal to noise ratios up to approximately 60, statistical fluctuations in the signal and background will dominate. Diode to diode variations are extremely small, and are accounted for in the routine calibration procedures. Cathode granularity will become important if signal to noise greater than 60 is required, and must be treated separately. For sources observed through the small aperture the sky background should not contribute significantly to the noise.

4.5.1 Photon Noise

The following equations may be use to estimate signal to noise ratio, depending on the relative importance of scattered light and dark count.

(1) Neither Scattered Light nor Dark Count is important

Let:
s = signal strength—counts per diode per second—estimated by multiplying the stellar flux by the sensitivity at the desired wavelength.
t = duration of the observation—seconds. This total time will be divided among the separate substep bins.
n_s = the number of adjacent diodes that will be binned together to produce an effective resolution element. Usually $n_s = 1$. This is *not* the merging of substep bins, but the deliberate averaging to increase signal to noise at the expense of resolution.

$$(S/N)^2 = sn_st \qquad (4-8)$$

This formula would be appropriate for relatively bright objects observed with any first order grating, when substep pattern 1, 2, or 3 is used.

(2) Dark Count is important, Scattered Light is not

Let:
d = dark count rate—counts per diode per second.

$$(S/N)^2 = \left(\frac{s/d}{s/d+1}\right)sn_st \qquad (4-9)$$

If the signal is less than about ten times the dark count rate, the factor in parentheses should be included in the estimate. This formula would be useful if patterns 1, 2, or 3 were used with a first order grating to measure a faint source.

(3) Scattered Light is important, Dark Count is not

Let:
f = fraction of time spent measuring the spectrum. Column 5 of Table 4-15.
b = scattered light as a fraction of the signal in the adjacent orders. Column 6 of Tables 4-6, 4-7.

$$(S/N)^2 \approx \left(\frac{f}{1+b}\right)sn_st \qquad (4-10)$$

This formula gives a good estimate of the performance for observations with the Echelles when patterns 6, 7, 8 or 9 are used. This formula assumes that the background bins are heavily smoothed. Most of the high frequency statistical noise in the background bins is thus suppressed.

(4) Both Scattered Light and Dark Count are important

Let:

n_b = number of adjacent diodes to smooth the background bins over before subtracting. Experiments with ground-based data indicate that $n_b \approx 10$ gives the best results.

$$(S/N)^2 = \frac{s^2 t}{s\{\frac{1+b}{n_s f} + \frac{b}{n_b(1-f)}\} + d\{\frac{1}{n_s f} + \frac{1}{n_b(1-f)}\}} \qquad (4-11)$$

There are two ways to use these formulae. If you need a certain S/N to do the scientific analysis, use the appropriate equation to solve for the required exposure time t. Alternately, you can decide to devote a fixed length of time to the observation, and use the equations to estimate what S/N will be achieved.

4.5.2 Fixed Pattern Noise

The formulae just presented suggest that the signal to noise ratio increases in proportion to the square root of the exposure time. These relations should hold true until S/N $\sim$ 60 or so is reached. At higher signal levels the photocathode granularity described in Section 4.4.3 will become the limiting factor. Observing standard stars to provide a precise "flat field" observation is unlikely to be an efficient or common practice. There is no on-board continuum lamp that illuminates the optics and detectors in exactly the same way as the stellar spectrum. The best practice is expected to be using the FP-SPLIT option (sec. 4.4.3), or at least several carousel settings. Simulations suggest the following: For D2 the granularity is small, and plays no significant role for S/N $\lesssim$ 80. For higher values the actual S/N will be approximately 80% of the photon noise limited value for a single observation. If four subexposures are used, the ultimate S/N reaches about 95% of its theoretical value. For the D1 detector the granularity limits the ultimate S/N for a single observation to $\sim$ 60. Using four subexposures increases the ultimate value to about 80% of pure photon noise case. The improvement appears to increase roughly as the square root of the number of subexposures, so that 16 segments must be averaged to reach 90% of the theoretical S/N. One caution is that the granularity was modeled as additional random noise in these simulations.

4.5.3 Exposure Control Strategies

Having made an estimate of the time required to obtain the data, it is necessary to specify the exposure control parameters. There are two ways for an observer to control the length of an observation—by time, and by the number of counts accumulated. All observations must have a maximum duration specified by the astronomer. This will be the exposure time, t, which is found from the S/N estimate. As a practical matter you might want to specify an exposure time somewhat longer than the estimate to allow for errors in the flux, efficiencies, background rate etc., or to let an observation fill a block of time such as one full orbit. Since the exposure time refers to the total observation, the time per bin measuring the spectrum will be shorter. When the exposure time has been satisfied the observation will terminate normally and the next observation in the sequence will begin.

The flight software has an exposure meter capability which can be used to control the length of an observation. Both overexposure and underexposure tests are available. Both tests are optional, and may be enabled or disabled as requested. The overexposure test is a way to terminate an observation when a pre-determined number of counts has been accumulated, rather than waiting for a fixed length of time to elapse. This is useful if the flux is poorly known or variable. To calculate the number of counts, use the S/N equations to estimate the exposure time, t. The total counts collected on the spectrum in time t is then

$$N = sft$$

This number can be used as a threshold for the overexposure test. If the limit is exceeded, the exposure is judged to be sufficient and the observation will terminate. As long as the limit is not exceeded, the observation will continue until the specified exposure time ends. You can also protect against a useless underexposure by using the S/N equations to calculate the minimum acceptable count rate. Decide what the minimum useful S/N would be, assume that the observation continues for the full exposure time, and calculate the minimum. After 10% of the observation has passed, the software will calculate the average count rate. If the rate exceeds the minimum, the observation will continue without further underexposure tests. If the threshold is not exceeded, an underexposure condition is declared and that observation will terminate prematurely.

An important feature of both tests is that they use only a restricted segment of the spectrum—between 1 and 64 contiguous channels anywhere in the diode array. This allows the observer to control the observation with a clearly defined section of the spectrum, either a region of clear continuum, or an absorption or emission line. The wavelength at any diode can be estimated from the central wavelength and the linear dispersion.

As a default, the central 64 diodes will be checked. If you wish to use the exposure meter, it is only necessary to use the optional parameter METER = YES on the Phase I proposal. The details discussed here will be specified during the Phase II process, since the observing time actually allocated may influence the exposure time per observation.

4.6 INSTRUMENTAL OVERHEAD TIMES

In addition to actually counting photons, all instruments spend some fraction of the time performing "overhead" functions such as moving mechanisms, reading out data, performing internal calibrations, etc. Table 4-16 contains rough estimates of some of the major time consuming activities within the overhead in the ground system on other spacecraft functions. None is a hard and fast number, but they represent typical times suggested by ground based experience.

Note that you have some control over the amount of overhead time lost in switching detectors. Unless you have other scientific considerations, you should order your observations to group all observations with a given detector together. This includes target acquisitions: mirrors N1 and A1 use Digicon 1; mirrors N2 and A2 use Digicon 2. Avoid unnecessary side switches!

TABLE 4-16
GHRS Overhead Times

Activity	Typical Time
Guide Star acquisition	(course track; the 10 minute default)
Guide Star acquisition (fine lock)	20 minutes
Target Acquisition	See GHRS Target Acquisition Manual
Switching Detectors (includes time for thermal stabilization)	30 minutes
Carousel Motions	60 seconds
Spectral Lamp Observations	1 minute + exposure time
Data Readout	8 seconds

5.0 A GUIDE TO PLANNING OBSERVATIONS

5.1 THE PHASE I PROPOSAL

Chapters 3 and 4 presented all of the information about operating modes and performance characteristics which is needed to plan an observation. This chapter will be a quick summary of the proposal process with guidelines for use of the various instrumental modes and configurations. You should, of course, also make use of the *Proposal Instructions* Handbook when preparing to submit your initial (Phase I) proposal, and the *Phase II Proposal Instructions* during Phase II.

Table 5-1 summarizes some basic calibrations which will be maintained by the Institute and available to all astronomers without any special requests.

5.1.1 Specifying A Target Acquisition Observation

For the Phase I proposal only a very basic amount of information is needed. You must decide which of the instrument modes is most appropriate (see section 3.3) and identify any Special Requirements such as Early Acquisition or Interactive Acquisition. You must specify which mirror you intend to use, and calculate exposure times using the sensitivities given in Section 4.3.5. Many other details will either be filled in automatically using routine procedures, or will be requested during the Phase II process, for proposers who are allocated telescope time. Try to avoid unnecessary side switches (section 4.6) when choosing your target acquisition mirror.

5.1.2 Selecting A Spectral Element And Aperture

There are three basic factors to consider when choosing a spectral element: (1) spectral resolving power, (2) spectral range and coverage, and (3) sensitivity. The resolving power should be matched to the characteristic width of important features in the spectrum being studied. If the purpose is to study gross spectral morphology, continuum fluxes, broad spectral line features (stellar wind P Cygni profiles), or to measure emission fluxes in well separated lines, then grating G140L would be the appropriate choice. Remember that this

Table 5-1
Expected Calibration Accuracies—HRS

Individual Calibration	Accuracy	Comments
Wavelength Calibration	±1 diode ±0.2 diodes	with accompanying calibration-lamp observation
Carousel Repeatability	0.05 diodes	
Point-Spread Function	1.0–1.2 diodes	
Paired-Pulse Correction	$\leq 1\%$	up to 150,000 cts s^{-1}
Absolute Flux Calibration	$\leq 10\%$	may be slightly worse when piecing together echelle orders

Notes:

1. Scattered-light contribution will have been measured for all dispersers, except for echelle inter-order background below 1200 Å .

2. Signal-to-noise ratios higher than 30, especially when using detector D1, should be obtainable with the FP-SPLIT option of multiple carousel settings to average out photocathode non-uniformities.

grating is useful between 1050 Å and 1800 Å, and has a plate scale of 0.57 Å per resolution element (approximately 150 km/sec). Nearly 300 Å can be recorded with one observation.

If you plan to study narrower spectral line features such as chromospheric emission lines in cool stars, photospheric absorption lines, interstellar or nebular lines, the first order configurations G140M, G160M, G200M and G270M would be better suited. All have a plate scale of approximately 15 km/sec per resolution element. The entire wavelength region of 1050–3200 Å is accessible with these gratings. All have excellent image quality, and are free from problems with scattered light. The spectral range recorded by a single observation ranges from 27 to 45 Å with increasing wavelength.

Projects demanding the highest spectral resolution or the most precise wavelength /velocity measurements may be well suited to the Echelle configurations. The resolving power is approximately R = 100000, with plate scale of 3 km/sec per resolution element. With care, the wavelength scale will be accurate to at least ± 1 km/sec. The Echelle configurations have several drawbacks which must be weighed against the need for high resolution. The spectral coverage is very restricted, recording only 5–17Å at a time. Surveys of many lines could become a time consuming program. The sensitivity is lower than with the first order gratings, requiring substantially longer exposure times to reach a given count level. The rapid variation of the blaze functions with wavelength and the presence of scattered light complicate the reduction and analysis of data. The ability to study the details of line profiles of weak and narrow features in stellar, interstellar and planetary spectra may nevertheless make an Echelle configuration the appropriate choice.

If an Echelle is selected, the order may also be specified. Tables 4-6 and 4-7 list the free spectral range for each order, and should be consulted for the initial choice. If you are really after the ultimate resolution, working in the next higher order, m+1, might be possible. Figure 4-16 shows that the resolving power increases with mλ, but that the efficiency decreases rapidly. If you do not specify an order the one which includes your wavelength within its free spectral range will be used.

In addition to the grating, you need to specify which of the two apertures to use. The issues are the following: the Small Science Aperture passes only the central peak of the stellar image, clipping the diffraction rings and wings of the telescope point spread function. The instrumental profile, spectral purity, resolving power and wavelength scale precision are all better when a point source is observed in the small aperture. The disadvantage of the small aperture is that, since the opening is matched to a point source image, the centering is critical. Any mispositioning or movement of the image will cause a (presumably unknown) fraction of the light to be vignetted. If you are interested in spectrophotometric measurements where the absolute number of photons detected is important, the small aperture is not recommended. If you are mainly interested in relative flux measurements over narrow wavelength intervals (line profiles) this loss of light will not create any serious problems. Basically, resolution and wavelength scales are better when the small aperture is used; flux measurements are more reliable when the large aperture is used.

5.1.3 Estimating the Counting Rate and Exposure Time

An optical configuration having been selected, it is possible to estimate the count rate. For the first order gratings, multiply the flux from the star by the sensitivity and aperture transmission at the chosen wavelength. The flux can be taken from existing data (OAO, IUE, etc.), or estimated from black body or power law distributions, with allowances for extinction (reddening), if needed. The *Bibliography of IUE Atlases and Catalogues*, IUE NASA Newsletter *37* (Feb. 1989), is a good reference to sources of UV fluxes for a wide variety of objects. The *IUE Ultraviolet Spectral Atlas*, IUE NASA Newsletter *22* (Nov. 1983), gives UV spectra for a wide range of stellar sources. If your desired target has been observed with IUE, an IUE spectrum is an excellent source for a flux measurement. Otherwise you may have to estimate UV flux from spectra of a similar object or a black-body or power law distribution, a much more uncertain process. Do not forget extinction (reddening) which is much more important in the UV than in the visible. Table 5-2, due to Savage and Mathis [*Ann. Rev. Astron. Astr.* **17**, 1979], gives the UV extinction at various wavelengths λ, expressed as a ratio of reddenings, E(λ-V)/E(B-V). For example, extinction sufficient to cause a difference of 1 magnitude between B and V wavelengths, E(B-V) = 1.00, will cause a magnitude difference of 5.02 magnitudes between λ1600Å and V. Additional discussion of extinction is contained in the FOS Instrument Handbook.

The sensitivity curves for each grating are shown in Figures 4-9 through 4-14 and in Tables 4-8 through 4-12. For the Echelle configurations, use the curves in Figure 4-15 adjusted by the relative blaze efficiency shown in Figure 4-16. The result of this calculation should be the count rate s, in counts per diode per second. You can list your calculated rate in section 5 of your Phase I Proposal, the section which says, "Justify your exposure time....". Also briefly describe how you estimated the UV flux of your target. This reference will allow the planning process at the Science Institute to double check your estimates using the most current instrument calibration information.

Table 5-2
Average Normalized UV Extinction as a Function of Wavelength

Wavelength (A)	E(λ-V)/E(B-V)	Wavelength (A)	E(λ-V)/E(B-V)
1000	11.30	1900	4.90
1050	9.80	2000	5.52
1110	8.45	2100	6.23
1180	7.45	2190	6.57
1250	6.55	2300	5.77
1390	5.39	2400	4.90
1490	5.05	2500	4.19
1600	5.02	2740	3.10
1700	4.77	3440	1.80
1800	4.65	4000	1.30

Once you have an estimate of the signal level s, you can use the information in section 4.5 to derive the exposure time required to achieve a desired signal to noise level. What signal to noise ratio is required depends on the strength of the spectral features being studied, and the precision with which they must be measured.

5.1.4 Selecting the Observing Mode: Rapid Readout vs. Accumulation Mode.

Rapid Readout is recommended only when time resolution faster than 10 seconds is required. It may be appropriate for studying the flickering of an accretion disk, emission line changes during stellar flares, or the occultation of a star by a planetary atmosphere. For spectroscopy of non-varying sources, or even time resolved studies with longer time scales, Accumulation Mode is recommended. Refer to section 3.3.2 for descriptions of the features of the modes.

5.1.5 Specifying a Rapid Readout Observation

If you use Rapid Readout Mode, there are three additional items that may be specified: the central wavelength, the sample time, and the duration of the observation. The sample time is the duration of each short integration and may be any multiple of 50 milliseconds up to 12.75 seconds. There is virtually no dead time between integrations, so that, for example, 50 msec integrations are accurately spaced on 50 msec centers. Each integration is tagged with a time from the spacecraft clock for use during data analysis, and correlation of events with observations from other sites. Since none of the primary flight software processors is active during Rapid Readout Mode, an observation cannot be terminated by an exposure time or level test. The absolute duration of the sequence must be specified, so that a special command to the instrument can be issued to stop the data flow.

5.1.6 Specifying an Accumulation Mode Observation

If you use Accumulation Mode there are several additional choices to make and parameters to specify.

5.1.6.1 Central Wavelength Range

The first is the wavelength to be centered on the diode array. The specification of the grating, aperture, and central wavelength allows the precise position of the carousel to be calculated. An observer may choose any wavelength within the operational range of the grating. The carousel drive mechanism is such that each step moves the image along the diode array approximately 5 diode widths. The requested wavelength will be placed within approximately 10 diodes of the center. The desired wavelength, in Angstroms, should be entered on the Exposure Logsheet.

5.1.6.2 Exposure Time and Signal to Noise Ratio

Calculate this using the information in Sections 4.3.5 and 4.5. They exposure time is the total time spent on the observation, and will be split up among the various substep bins. The signal to noise ratio refers to the total signal collected by the bins which contain the spectrum. The signal to noise per bin will be less by the square root of the number of bins.

5.1.6.3 Exposure Control Parameters

(The following discussion is intended mainly for Phase II Proposers.)

The two basic ways to control the length of an observation — by time and by the number of counts accumulated — were described in section 4.5.3. However, you only need to make a choice if you get to Phase II. The flight software actually uses the number of completed substep patterns, and not the elapsed time directly, as a measure of the exposure time. The conversion from exposure time to number of patterns is a simple operation that will be done at the Science Institute. One of the advantages of using the Exposure Meter is making optimum use of your observing time. It should eventually permit an event-driven sequence rather than a sequence specified by time: as soon as one exposure finishes (receives the number of counts you have specified), the next one starts. Most other instrument observations, and all HST maneuvers, must be pre-planned to occur at specific clock times. The Phase II instructions will permit you to specify a sequence of observations which formally take more time than the observing time you have been allocated. Your sequence would then act as a priority list, with the latter observations being taken only if the previous ones finish. However, this capability is not yet implemented, and will not be during the first year of operation.

Users of Exposure Metering in a sequence of observations must be very careful in asking for additional restrictions. This is because <u>all</u> observations grouped in an event-driven sequence are affected by any restrictions placed on any exposure in the sequence. For instance, suppose that exposures #3 and 4, in a sequence of 5 exposures running under Exposure Meter control are specified to be done "within 15 minutes." (One might be a calibration for the other, for instance.) The ground system will not schedule exposures 3 and 4 unless there is enough time not interrupted by earth occultation to do both. However, the ground system does not know in advance how long exposures #1 and 2 will take, since they are under Exposure Meter control. It only knows the maximum time they can take. Only if there is an uninterruped block of time equal to the maximum time you have specified for exposures 1–4 can your sequence be scheduled. Long meter-controlled sequences containing restrictions are therefore not recommended.

5.1.6.4 Internal Spectral Calibrations

When wavelengths more accurate than the standard calibrations are required, one may request additional calibrations as described in Section 4.3.2. On the Exposure Logsheet, the Target Name should be WAVE; the Instrument Configuration is GHRS; and only ACCUM mode can be used. The lamps are identified by their apertures SC1 and SC2. For targets in the LSA the following lamp use is recommended: G200M, G270M, Ech B - SC1; G140L, G140M, G160M, Ech A - Sc2. For targets in the SSA the shutter cannot be used to prevent interference in the calibration lamp image by the target so special provisions must be considered. For first order gratings, SC1 is offset in Y-deflection and can be used for wavelength calibration without interference. Use of SC1 is recommended for all first order gratings when the target is in the SSA. For echelle modes, SC2 will overlay the target spectrum and SC1 will be between orders of the target spectrum. SC1 is recommended for use with the echelle modes.

The spectral element, central wavelength and substep pattern should be identical to the observation for which the calibration is being obtained. The exposure meter should not be used. Tables of optimum exposure times will be maintained at the Science Institute, and DEF may be given for the exposure time. Alternatively, exposure times may be determined using the count rates from the pt Atlas in the Appendix. When using either echelle, we suggest that you calculate the optimum exposure time yourself. The observation should be explicitly identified as a calibration for particular lines on the Exposure Logsheet by using the Special Requirement CALIB FOR ⟨ lines ⟩.

When using the Echelle Mode it is recommended that users do <u>not</u> specify DEF for the exposure time. The wavelength coverage is small, and the number and strength of comprison lines varies significantly with wavelength, so it is better to calculate an exposure time by looking at the Pt Atlas. If necessary to get enough comparison lines, one may observe adjacent echelle orders with the same value of $m\lambda$ (without moving the carousel).

The following are currently default exposure times for the wavecal observations:

G1 - 2 minutes
G2 - 1 minute
G3 - 40 seconds
G4 - 40 seconds
G5 - 30 seconds

[EA - 2 minutes for a single order. If you are doing multiple orders (eg OSCAN), 30 seconds per order.

EB - 1 minute for a single order. If you are doing multiple orders, 30 seconds per order.]

5.1.7 <u>Series of Observations</u>

Items to consider in Phase II besides those mentioned in the section on Exposure Control, when planning a series of observations:

(1.) Each change in the carousel position requires approximately 1 minute.

(2.) Wavelength calibrations are needed only if the investigation requires precision greater than about ± 1 diode width. Standard calibrations will be at least that good.

(3.) Avoid unnecessary side (detector) switches.

There are three basic ways to specify series of observations. The first and most direct approach is to simply fill in a separate line on the Exposure Logsheet for each observation, explicitly specifying each parameter. For short and simple cases this may be the easiest way to proceed. The second option is to use one of the Optional Parameters that provide a short hand way to specify the most common series. Breaking an observation into a series of subexposures at closely adjacent carousel positions to overcome fixed pattern noise can be requested with the FP-SPLIT parameter. Observations at a number of successive carousel positions to scan a longer wavelength range can be specified using the WSCAN Optional Parameter. This may be used with any of the first order gratings, or to scan along any one order of the Echelle. The same substep pattern and exposure control parameters will be used for each of the individual observations. In the Echelle configuration, it is often convenient to observe several orders at a fixed carousel position. An "order scan" can be requested by using the OSCAN-MIN and OSCAN-MAX optional parameters. All of the orders between and including the minimum and maximum will be observed in ascending numerical order, using the same substep pattern and exposure control. These optional parameters have some restrictions and other details, given in the Phase II Instructions. The third way to specify a series of observations is to define a SEQUENCE in the Exposure Logsheet, as explained in the Proposal Instructions.

5.1.8 Sample Target Lists and Exposure Logsheets

The Phase I or initial proposal submission now only requires an Observation Summary Form—see the Proposal Instructions. Sample filled-out Target Lists and Exposure Logsheets are given with the *Phase II Proposal Instructions.*

5.1.9 References to other Useful Documents

(1) SI System Description and User's Handbook for the High Resolution Spectrograph (GHRS) for the Space Telescope (ST). GHRS-2176-050 B (SE-01). This is a detailed engineering document which contains technical descriptions of all aspects of the hardware and software. It was prepared by the prime contractor, Ball Aerospace Systems Division. Copies are available in the ST ScI library and in the files of the Telescope and Instrumentation Branch at the ST ScI.

(2) Preliminary SI Pre-launch Calibration Report for the High Resolution Spectrograph (GHRS) for the Space Telescope (ST). GHRS-2176-051. This document contains the results of the ground-based calibration effort. Many performance characteristics in addition to the ones summarized in the Handbook are described. It is also available in the library and the TIB.

(3) SO-11 Calibration Data Base Operator's Guide Goddard High Resolution Spectrograph, Volume 2. This document describes the various instrumental signatures which are calibrated and removed in the data reduction process.

(4) Instrument Science Reports. The Instrument Support Branch maintains files of reports dealing with specific performance characteristics and operational issues.

6.0 DATA PROCESSING

Having worked hard to develop an understanding of the HST and its instruments, to formulate a competitive scientific program, and to submit a feasible and properly specified proposal, most astronomers will eagerly await the return of their data. This chapter outlines how the data will be processed, and what kinds of output products an observer might expect. There will be facilities at the Science Institute for analysis and interpretation of data, and for repeating the "pipeline" processing for yourself, using different calibrations if desired. Although ample documentation on the hardware and software is available, the final section will summarize those capabilities which may be useful for GHRS users.

6.1 CALIBRATIONS MAINTAINED BY THE ST ScI

Most of the calibrations needed to configure and operate the GHRS and to reduce the data will be established and maintained by the Science Institute. These include the following:

Calibrations required to configure and operate the GHRS:

(1) Detector functions
   (a) electro-optic focus
   (b) discriminator thresholds
   (c) deflection coordinates

(2) Carousel functions
   (a) encoder positions vs central wavelengths
   (b) encoder positions for target acquisition mirrors

(3) Aperture functions
   (a) plate scale
   (b) effective areas
   (c) location and orientation in HST focal plane

Calibrations required to reduce raw data

(1) Geometrical corrections
   (a) detector mapping function
   (b) dispersion constants
   (c) spectral lamp aperture offsets
   (d) instrumental profile (point spread functions)

(2) Photometric corrections
   (a) count rate non-linearity
   (b) diode to diode variations
   (c) photocathode non-uniformities
   (d) Echelle blaze function
   (e) absolute sensitivities
   (f) target acquisition mirror sensitivities

Calibrations used to monitor the performance

(1) Background signals
    (a) detector dark count
    (b) radiation count rates
    (c) cross-talk, interference, etc.
    (d) stray and scattered light
(2) Stability and repeatability
    (a) carousel mechanical performance
    (b) detector deflection system
    (c) photometric stability
    (d) thermally induced image motion

Data bases maintained for calibration monitoring

(1) Spectral lamp wavelength libraries
(2) Spectrophotometric standard stars
(3) Interstellar wavelength/velocity standards

6.2 STANDARD DATA REDUCTION PROCESS

The data arrive at the Science Institute within minutes of the completion of an observation. An automatic "pipeline" type processing system, called RSDP (Routine Science Data Processing) subjects each data set to a standardized reduction process. For the GHRS data reduction is fairly straightforward and the routine processing is expected to produce satisfactory results most of the time. The basic steps are as follows:

(1) Compute a linearized count rate for each data point
    (a) divide raw counts by the exposure time
    (b) correct for count rate non-linearity
    (c) correct for diode array non-uniformity
(2) Assign a wavelength to each data point
    (a) compute detector line and sample coordinates
    (b) find appropriate dispersion constants
    (c) adjust for location of star in aperture if necessary
    (d) solve dispersion equation for vacuum wavelengths
(3) Compute the incident flux
    (a) correct for photocathode non-uniformity
    (b) subtract background
    (c) correct for the Echelle blaze function
    (d) apply absolute photometric calibration
    (e) correct for light loss at aperture if necessary
(4) Produce final products
    (a) merge the substep bins
    (b) convert to air wavelengths if $\lambda > 2000$ Å
    (c) remove Doppler shifts to produce heliocentric wavelengths

6.3 OUTPUT PRODUCTS FOR GENERAL OBSERVERS

As the pipeline processing proceeds standard output products are generated from the raw data, certain intermediate steps, and the final results. One set of output products is retained for the permanent archive and one set is provided to the General Observer. Each set consists of a magnetic tape, written in FITS format, and some hard copy graphic output. The tape will contain raw as well as calibrated data. The hard copy will be a plot of only the fully calibrated data. One plot will be generated for each observation, except in Rapid Readout Mode. The format will be a high quality, high resolution laser plot, pen plot or glossy photograph, approximately 8×10 inches. Each will be annotated with wavelength and flux scales, and enough information to identify the target, observer, program and instrument mode. The tape output may be analyzed further at ST ScI, or taken to one's home institution for further work. The graphic products may be used to make preliminary assessments, show to friends and tape to office doors.

6.4 SPACE TELESCOPE SCIENCE DATA ANALYSIS SYSTEM (STSDAS)

The Science Institute has developed a comprehensive interactive software system to facilitate further analysis and interpretation of data. It is built within the environment of IRAF, the Image Reduction Facility developed by the National Optical Astronomy Observatories, which is familiar to many astronomers. Summary information is available from the STSDAS Group at the Science Institute.

ACKNOWLEDGEMENTS

This handbook has particularly benefitted from the work of and the engineers of Ball Aerospace, builders of the GHRS, especially Harry Garner at the Science Institute. Ken Carpenter of the IDT has made contributions too numerous to mention individually. Thanks are also due to Ron Gilliland, GHRS Instrument Scientist.

The GHRS Investigation Definition Team is: J. C. Brandt, P.I., S. R. Heap, Co–P.I., A. Boggess, K. G. Carpenter, S. P. Maran, A. M. Smith, E. A. Beaver, J. B. Hutchings, M. A. Jura, J. L. Linsky, B. D. Savage, L. M. Trafton, F. M. Walter, R. J. Weymann, D. C. Ebbets.

APPENDIX

The appendix consists of an Atlas of the Pt Spectral Calibration Lamps made with the GHRS medium resolution gratings. The spcetra are presented twice, with two different scales. **Note that the first scale is logarithmic!**. Units are **counts per second.**

You can expect the count-rates given to be accurate to a few tens of percent. (These lamps are not designed to be flux constant. They change with time and there are slight differences between SC1 and SC2.)

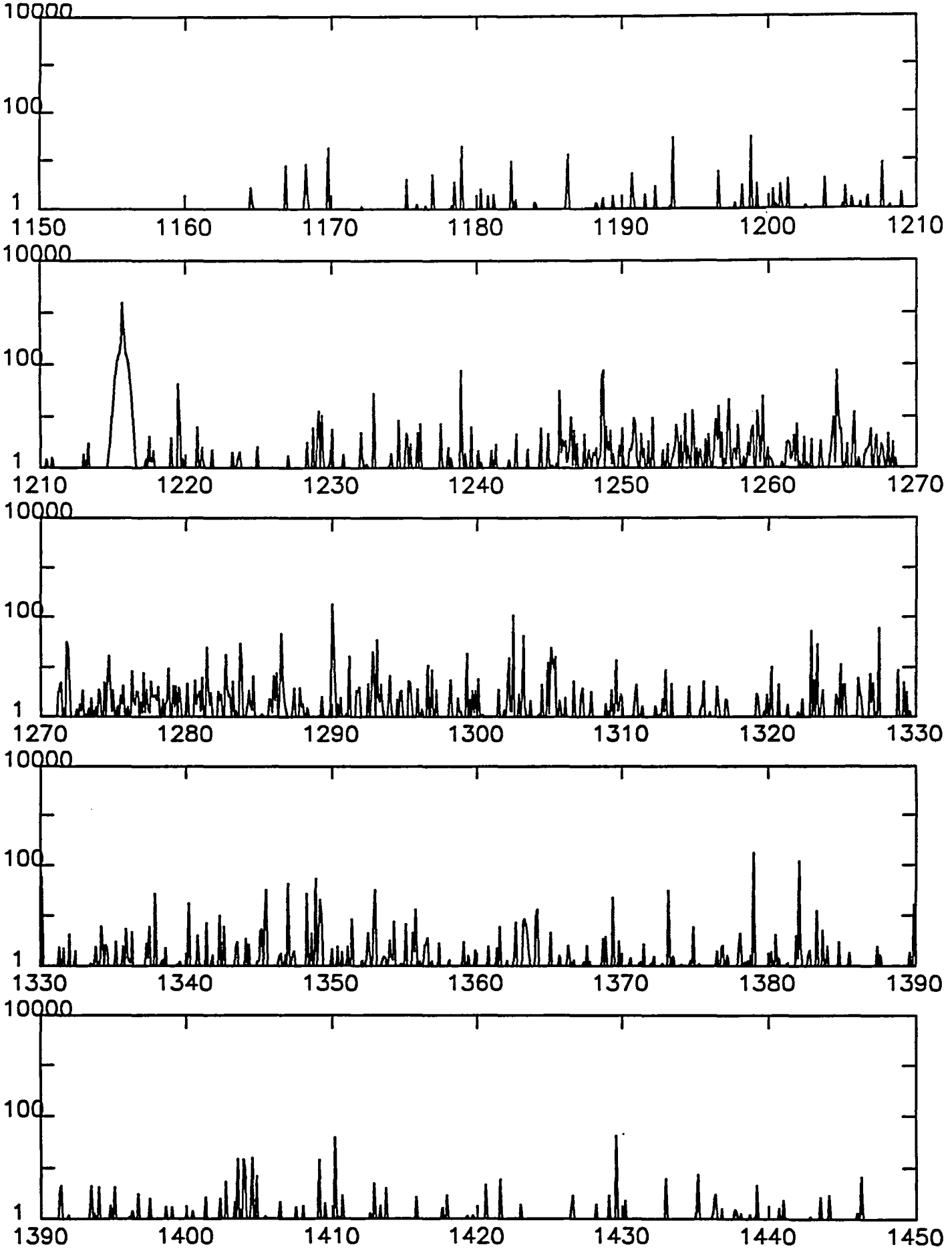
10000
100
1
1150
1160
1170
1180
1190
1200
1210
10000
100
1
1210
1220
1230
1240
1250
1260
1270
10000
100
1
1270
1280
1290
1300
1310
1320
1330
10000
100
1
1330
1340
1350
1360
1370
1380
1390
10000
100
1
1390
1400
1410
1420
1430
1440
1450

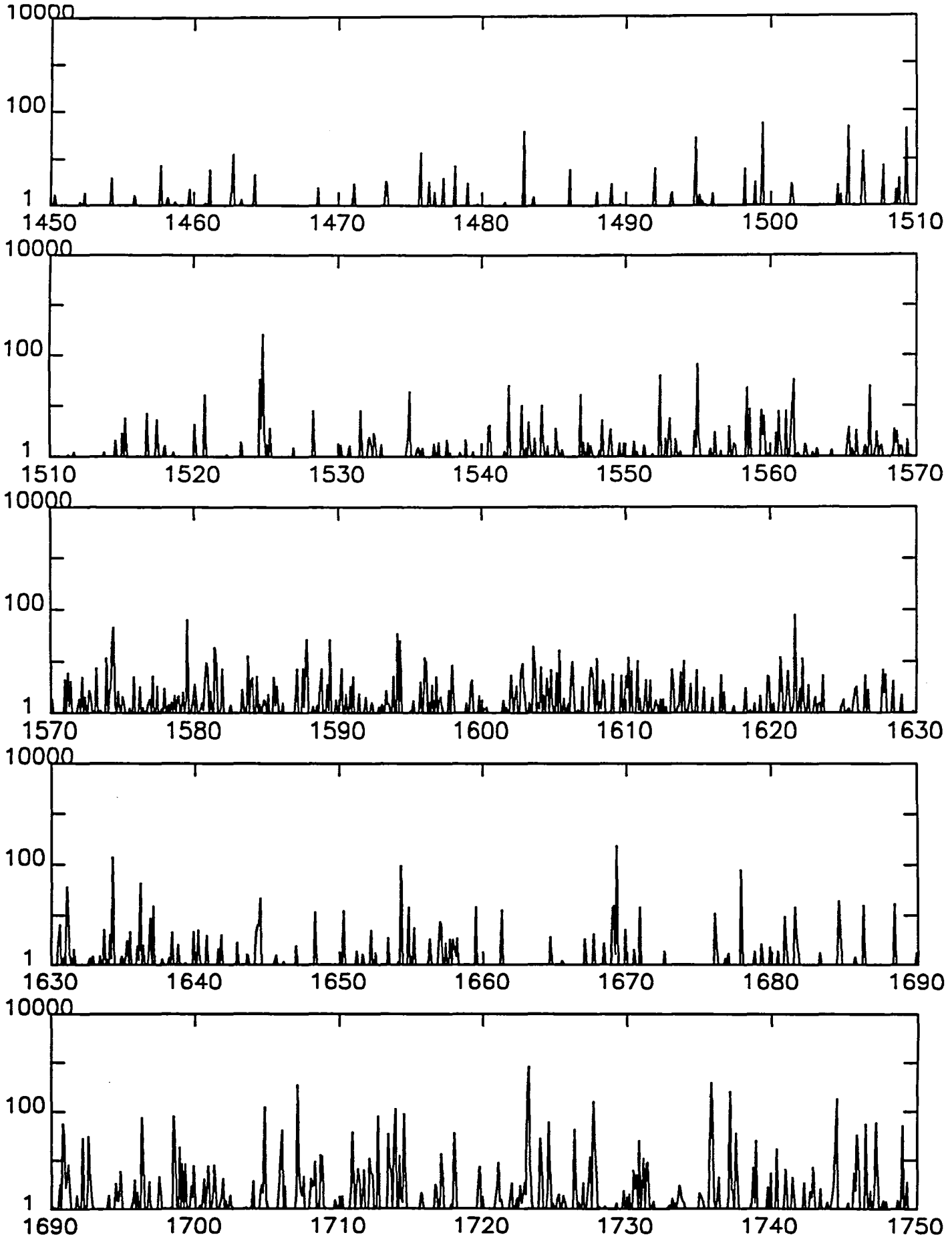
10000
100
1
1450
1460
1470
1480
1490
1500
1510
10000
100
1
1510
1520
1530
1540
1550
1560
1570
10000
100
1
1570
1580
1590
1600
1610
1620
1630
10000
100
1
1630
1640
1650
1660
1670
1680
1690
10000
100
1
1690
1700
1710
1720
1730
1740
1750

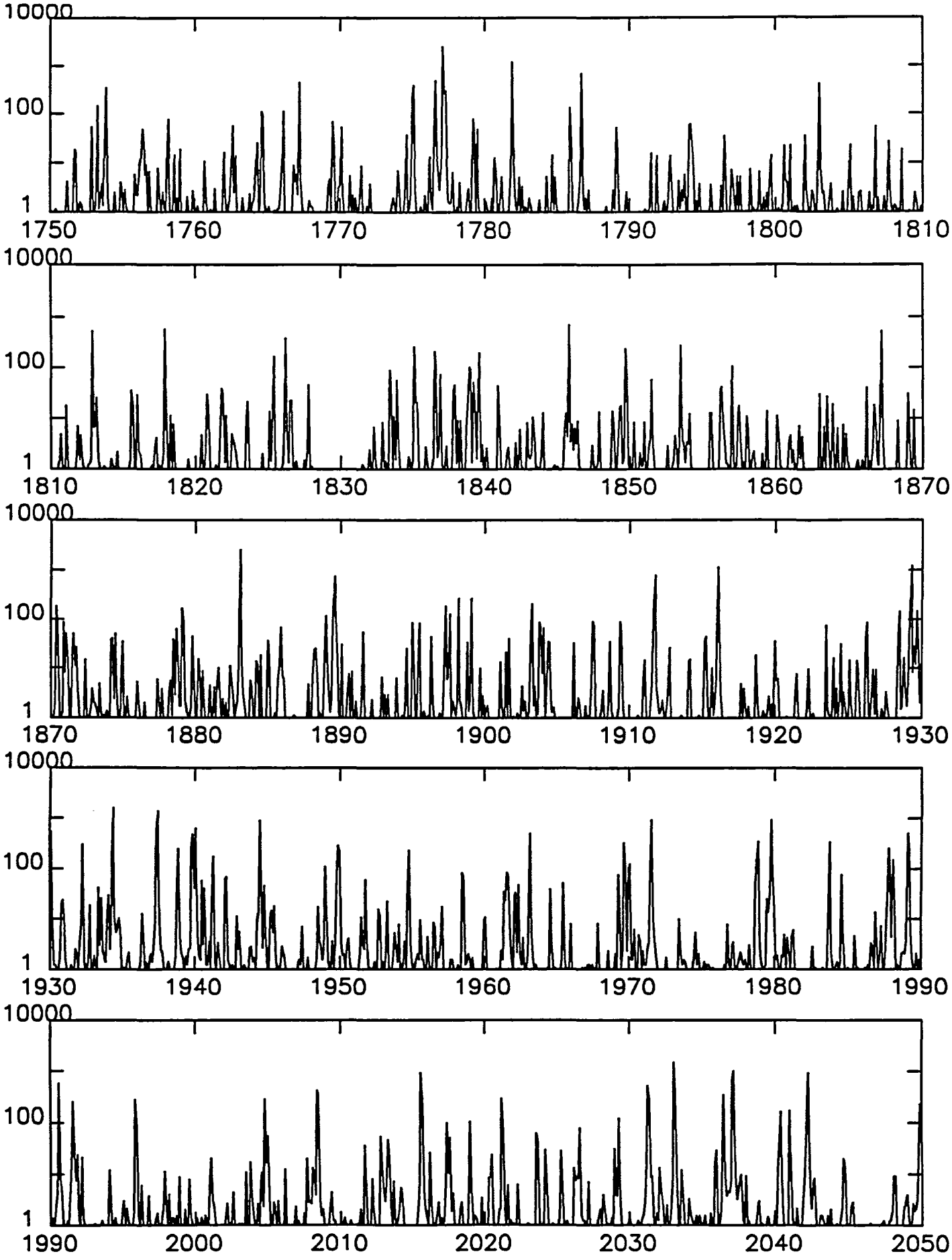
10000
100
1
1750
1760
1770
1780
1790
1800
1810
10000
100
1
1810
1820
1830
1840
1850
1860
1870
10000
100
1
1870
1880
1890
1900
1910
1920
1930
10000
100
1
1930
1940
1950
1960
1970
1980
1990
10000
100
1
1990
2000
2010
2020
2030
2040
2050

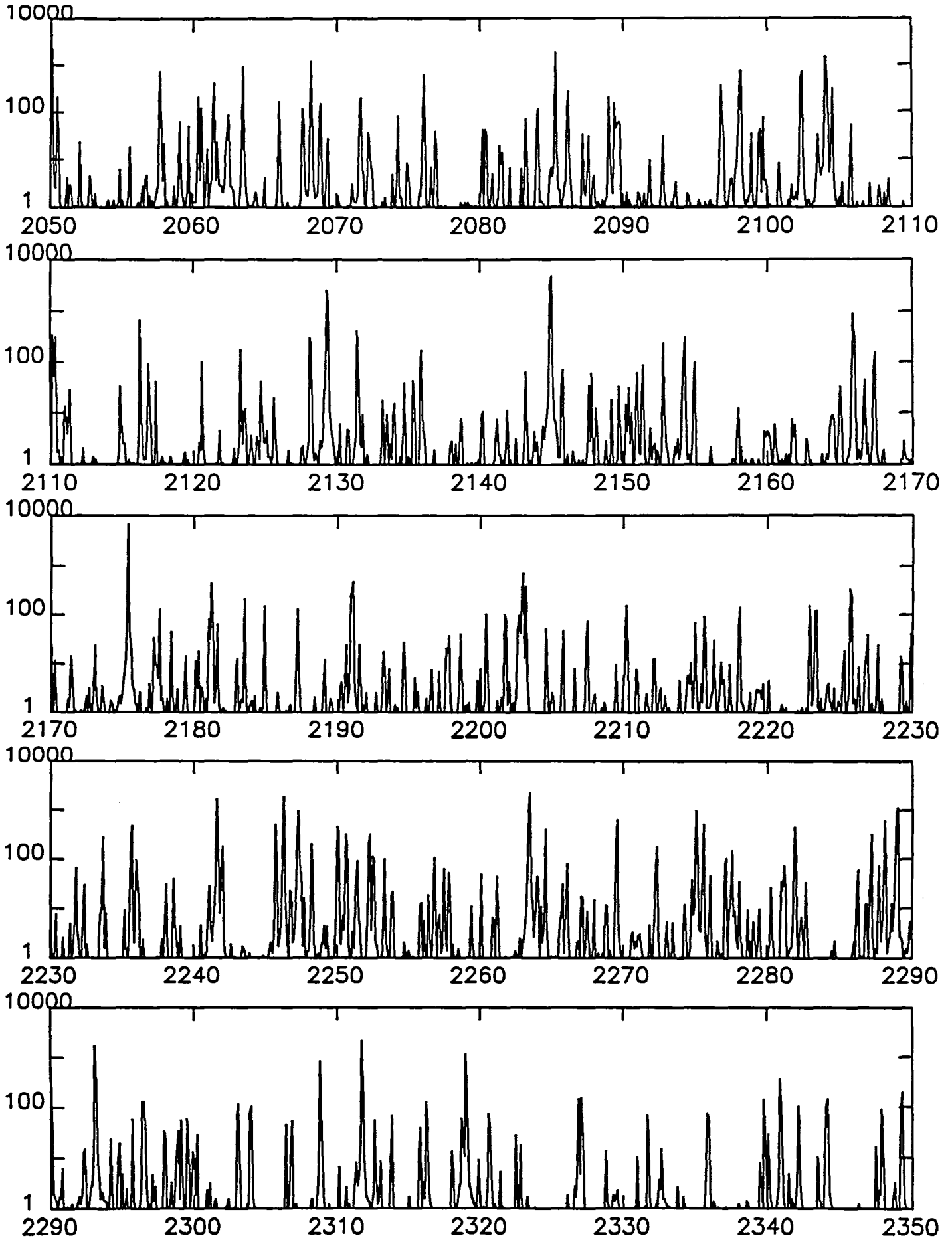
10000
100
1
2050
2060
2070
2080
2090
2100
2110
10000
100
1
2110
2120
2130
2140
2150
2160
2170
10000
100
1
2170
2180
2190
2200
2210
2220
2230
10000
100
1
2230
2240
2250
2260
2270
2280
2290
10000
100
1
2290
2300
2310
2320
2330
2340
2350

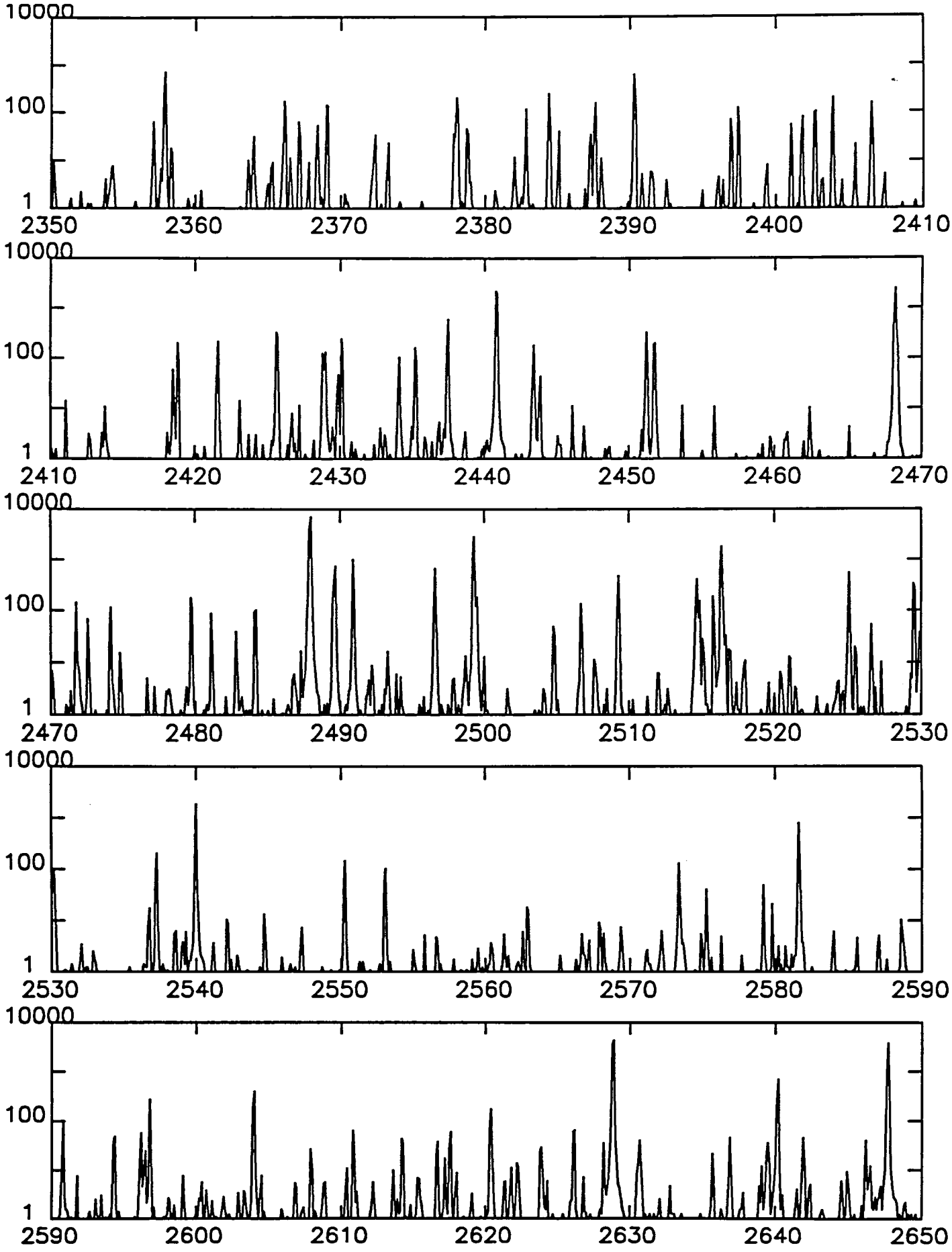
10000
100
1
2350
2360
2370
2380
2390
2400
2410
10000
100
1
2410
2420
2430
2440
2450
2460
2470
10000
100
1
2470
2480
2490
2500
2510
2520
2530
10000
100
1
2530
2540
2550
2560
2570
2580
2590
10000
100
1
2590
2600
2610
2620
2630
2640
2650

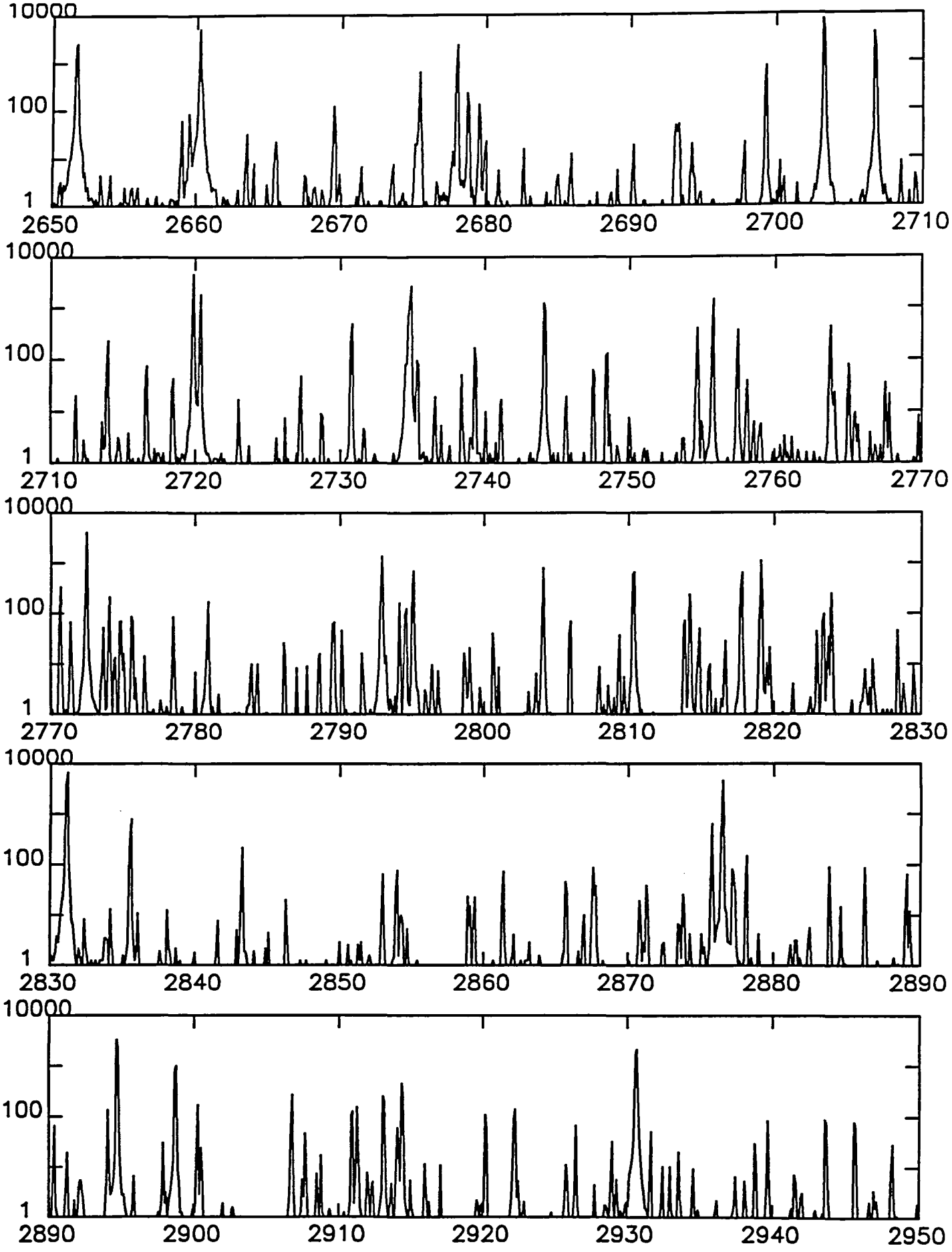
10000
100
1
2650
2660
2670
2680
2690
2700
2710
10000
100
1
2710
2720
2730
2740
2750
2760
2770
10000
100
1
2770
2780
2790
2800
2810
2820
2830
10000
100
1
2830
2840
2850
2860
2870
2880
2890
10000
100
1
2890
2900
2910
2920
2930
2940
2950

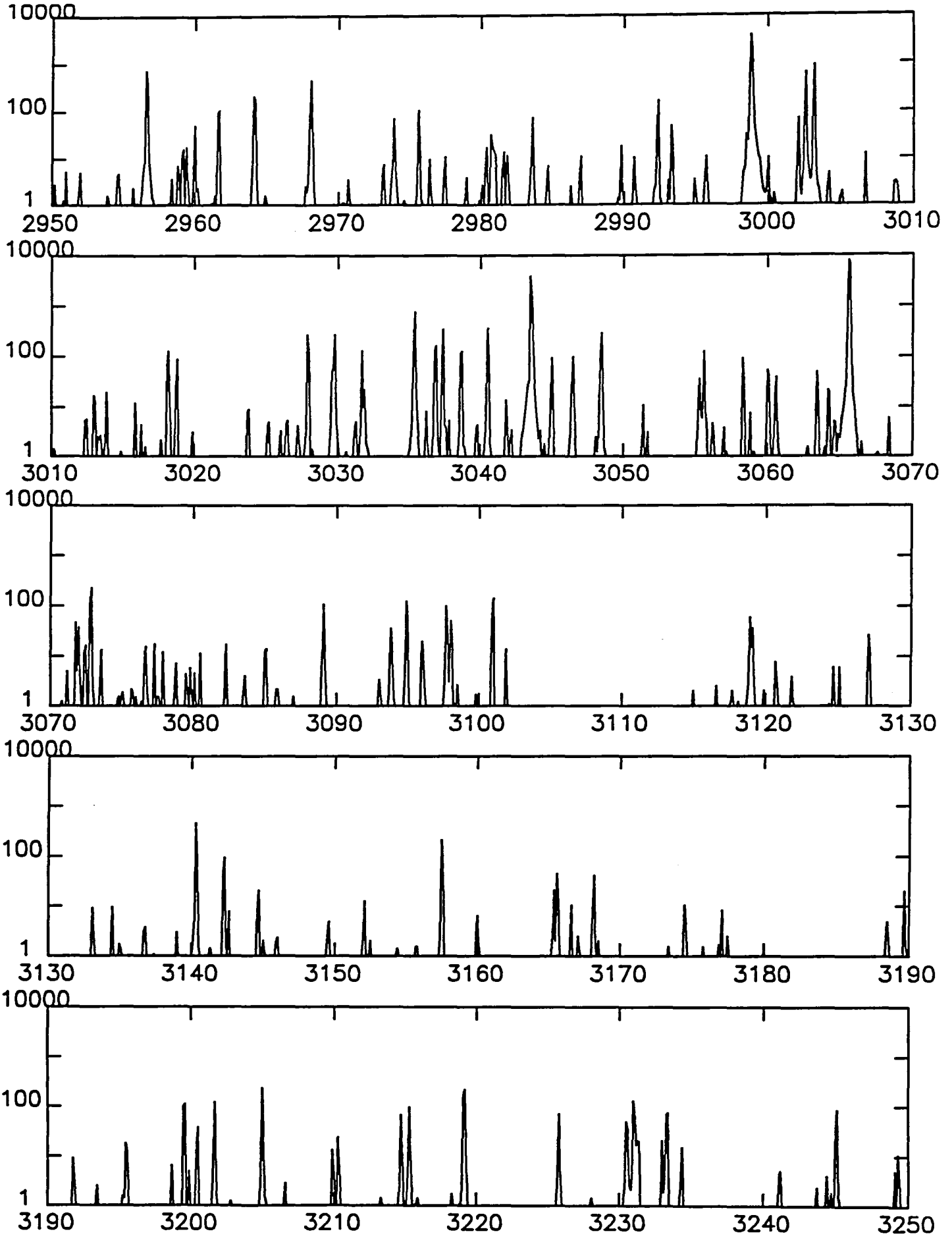
10000
100
1
2950
2960
2970
2980
2990
3000
3010
10000
100
1
3010
3020
3030
3040
3050
3060
3070
10000
100
1
3070
3080
3090
3100
3110
3120
3130
10000
100
1
3130
3140
3150
3160
3170
3180
3190
10000
100
1
3190
3200
3210
3220
3230
3240
3250

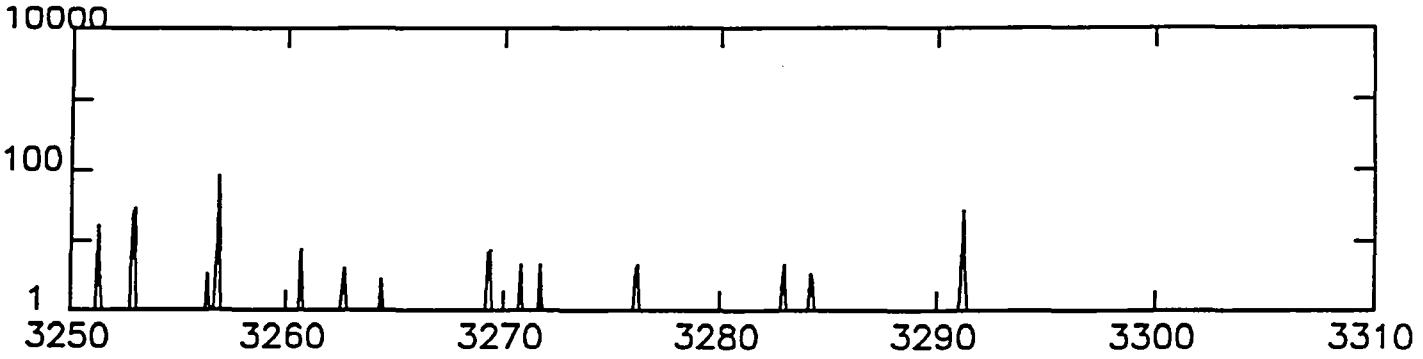
10000
100
1
3250
3260
3270
3280
3290
3300
3310

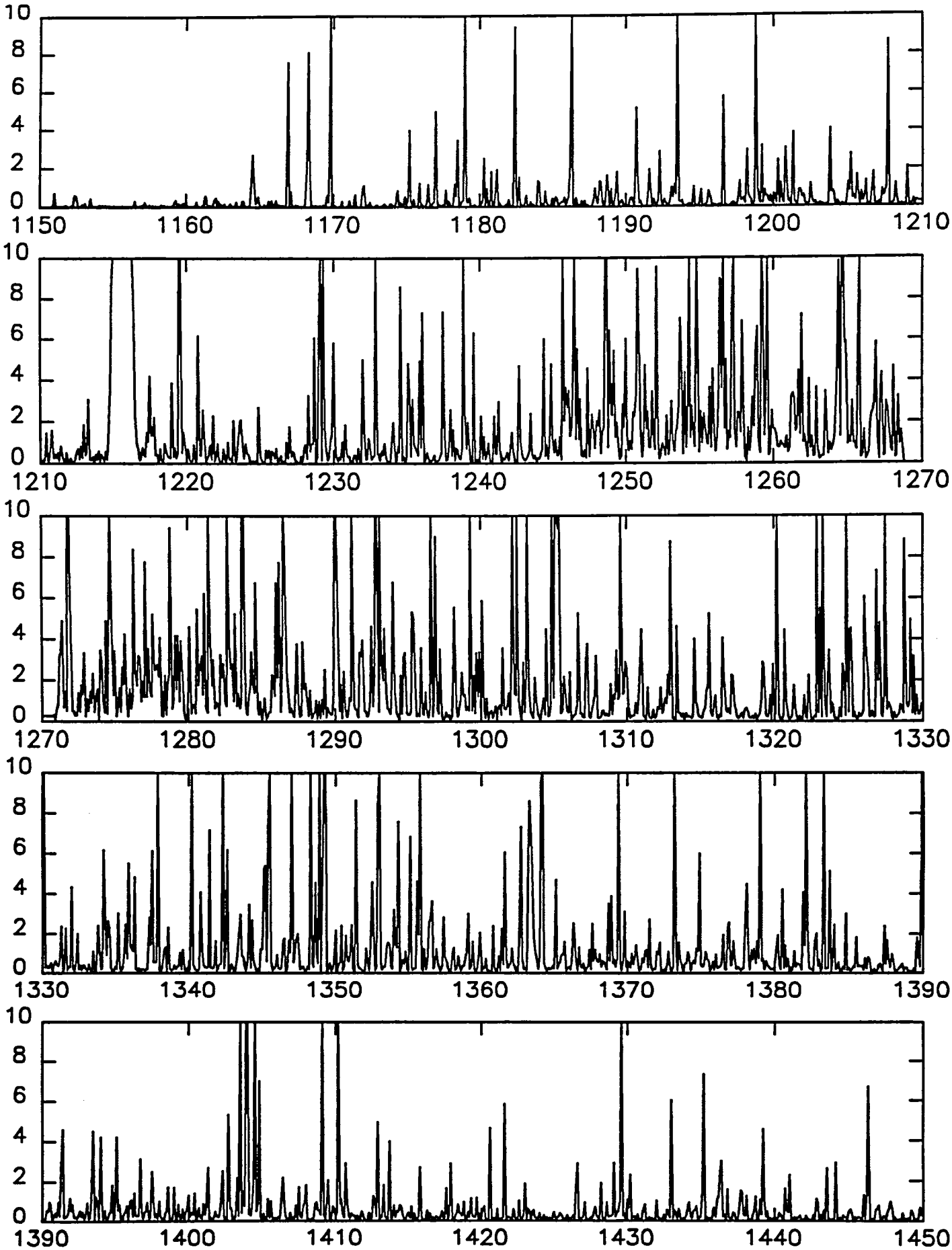
10
8
6
4
2
0
1150
1160
1170
1180
1190
1200
1210
1210
1220
1230
1240
1250
1260
1270
1270
1280
1290
1300
1310
1320
1330
1330
1340
1350
1360
1370
1380
1390
1390
1400
1410
1420
1430
1440
1450

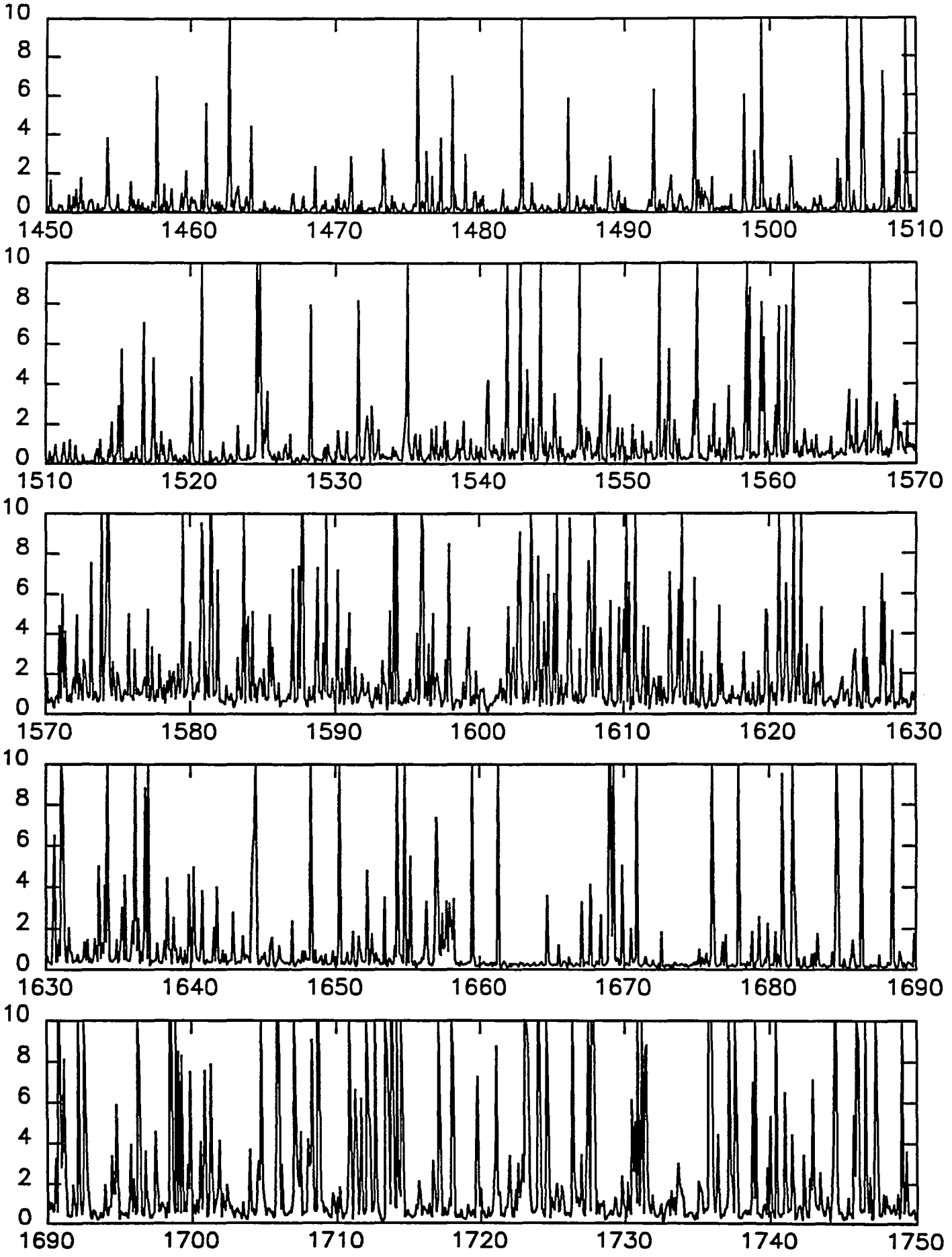
10
8
6
4
2
0
1450
1460
1470
1480
1490
1500
1510
1510
1520
1530
1540
1550
1560
1570
1570
1580
1590
1600
1610
1620
1630
1630
1640
1650
1660
1670
1680
1690
1690
1700
1710
1720
1730
1740
1750

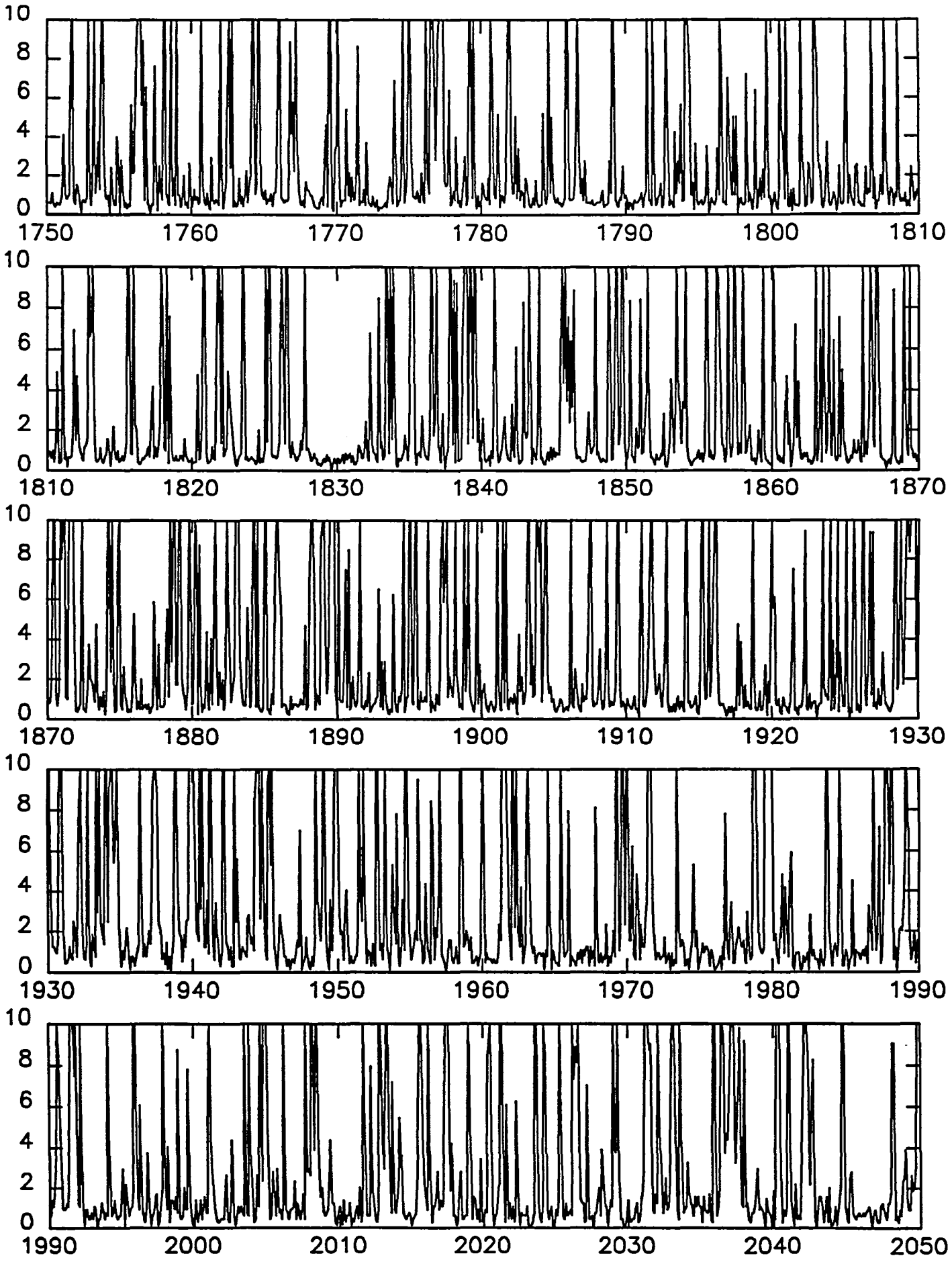
10
8
6
4
2
0
1750
1760
1770
1780
1790
1800
1810
10
8
6
4
2
0
1810
1820
1830
1840
1850
1860
1870
10
8
6
4
2
0
1870
1880
1890
1900
1910
1920
1930
10
8
6
4
2
0
1930
1940
1950
1960
1970
1980
1990
10
8
6
4
2
0
1990
2000
2010
2020
2030
2040
2050

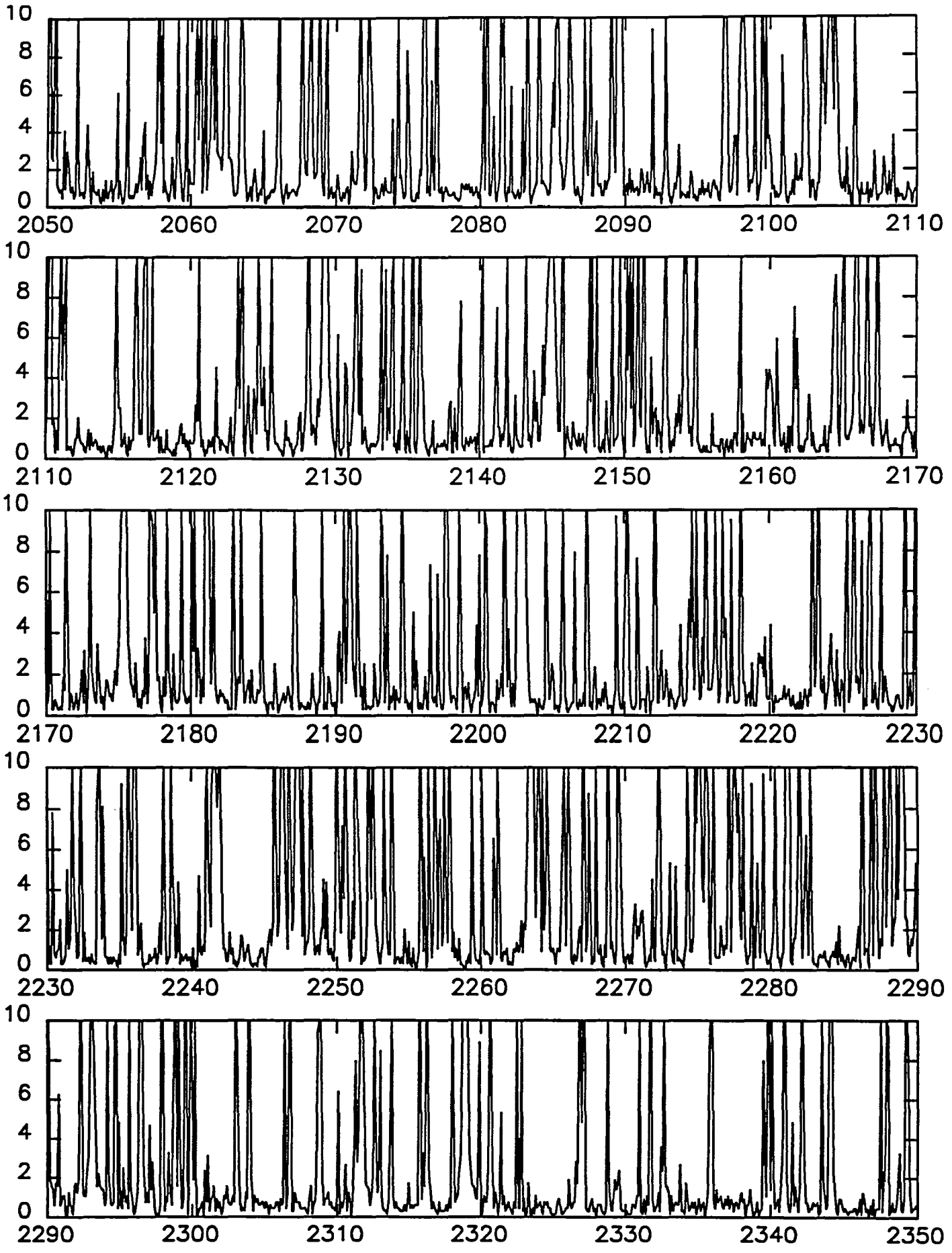
10
8
6
4
2
0
2050
2060
2070
2080
2090
2100
2110
10
8
6
4
2
0
2110
2120
2130
2140
2150
2160
2170
10
8
6
4
2
0
2170
2180
2190
2200
2210
2220
2230
10
8
6
4
2
0
2230
2240
2250
2260
2270
2280
2290
10
8
6
4
2
0
2290
2300
2310
2320
2330
2340
2350

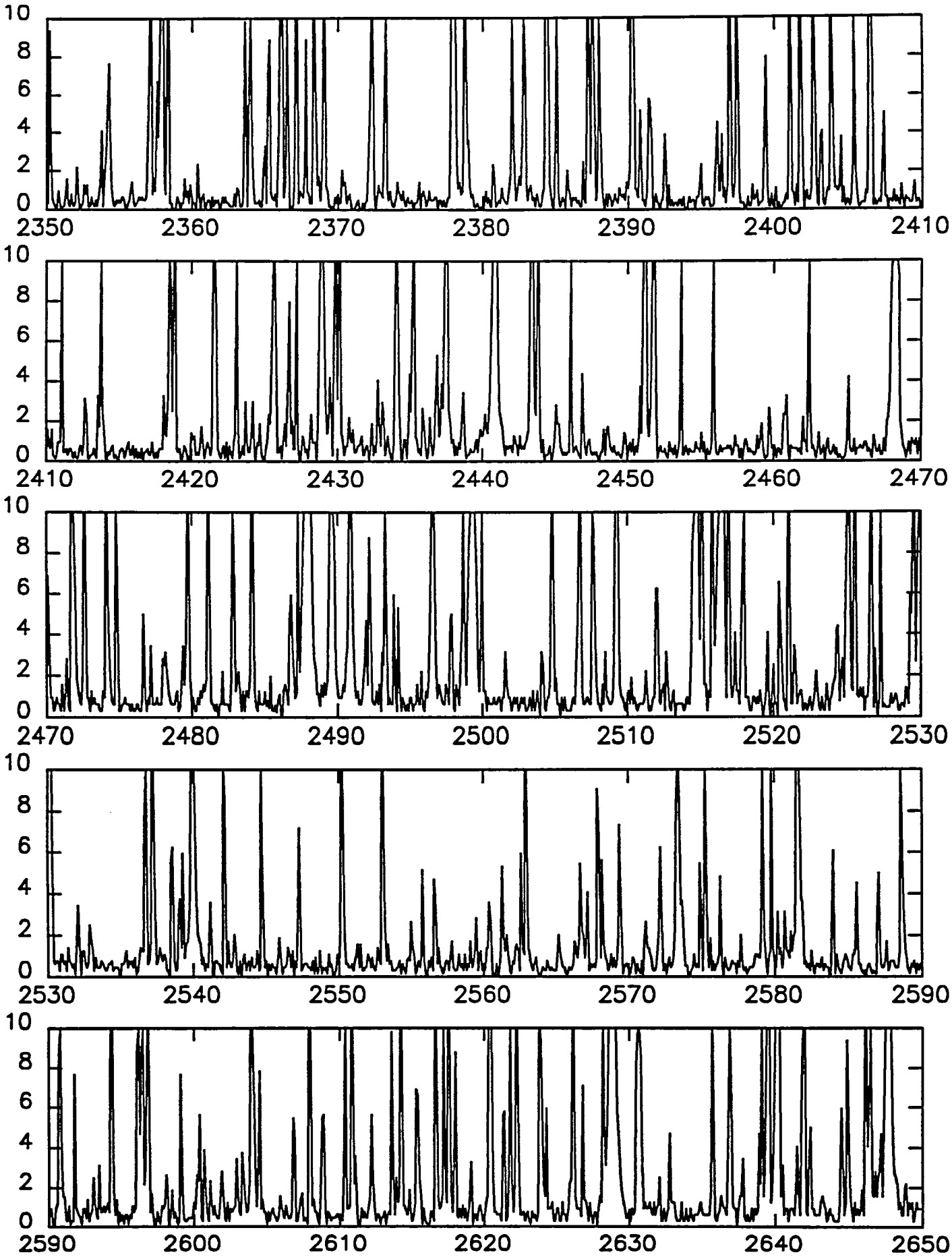
10
8
6
4
2
0
2350
2360
2370
2380
2390
2400
2410
10
8
6
4
2
0
2410
2420
2430
2440
2450
2460
2470
10
8
6
4
2
0
2470
2480
2490
2500
2510
2520
2530
10
8
6
4
2
0
2530
2540
2550
2560
2570
2580
2590
10
8
6
4
2
0
2590
2600
2610
2620
2630
2640
2650

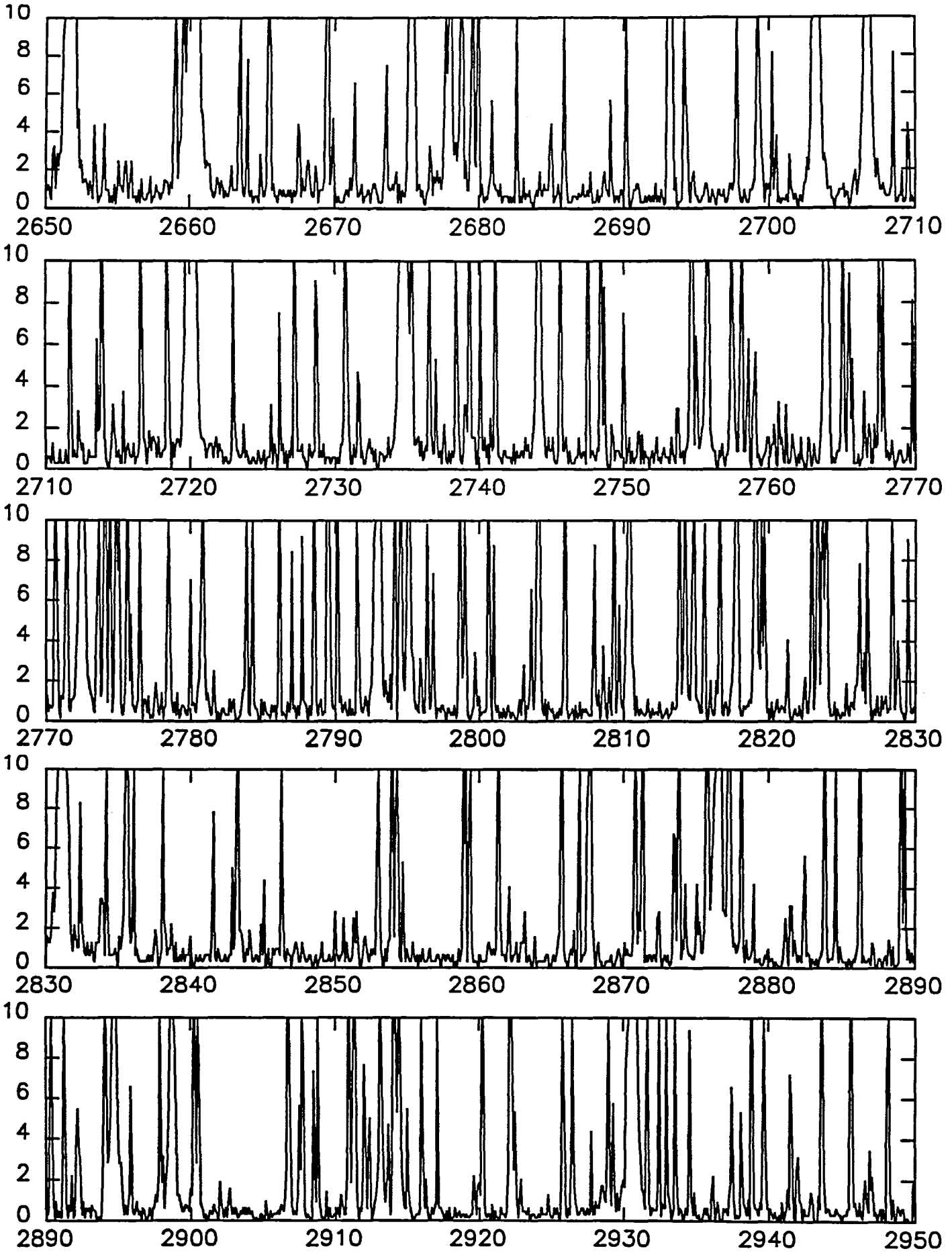
10
8
6
4
2
0
2650
2660
2670
2680
2690
2700
2710
2710
2720
2730
2740
2750
2760
2770
2770
2780
2790
2800
2810
2820
2830
2830
2840
2850
2860
2870
2880
2890
2890
2900
2910
2920
2930
2940
2950

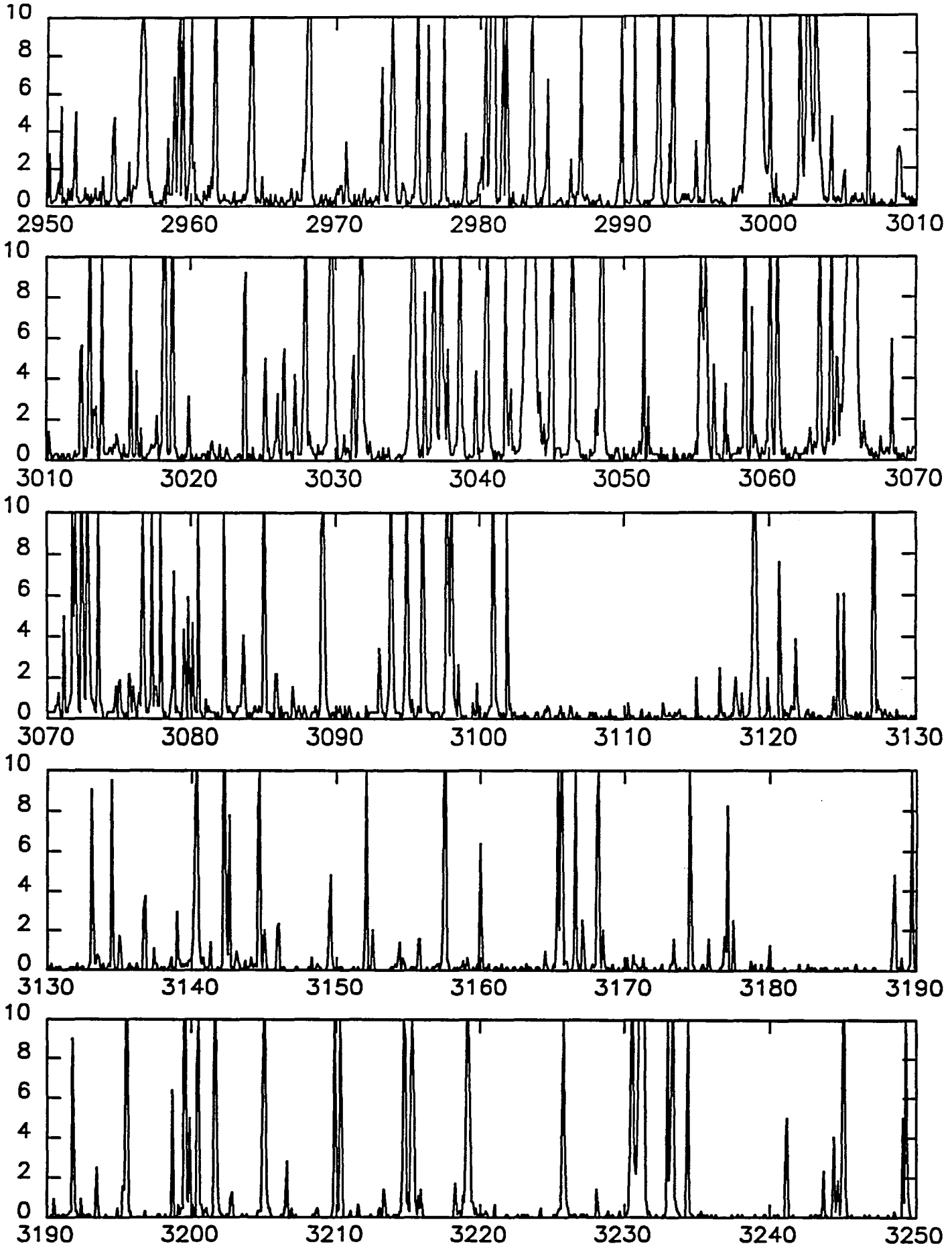
10
8
6
4
2
0
2950
2960
2970
2980
2990
3000
3010
3020
3030
3040
3050
3060
3070
3080
3090
3100
3110
3120
3130
3140
3150
3160
3170
3180
3190
3200
3210
3220
3230
3240
3250

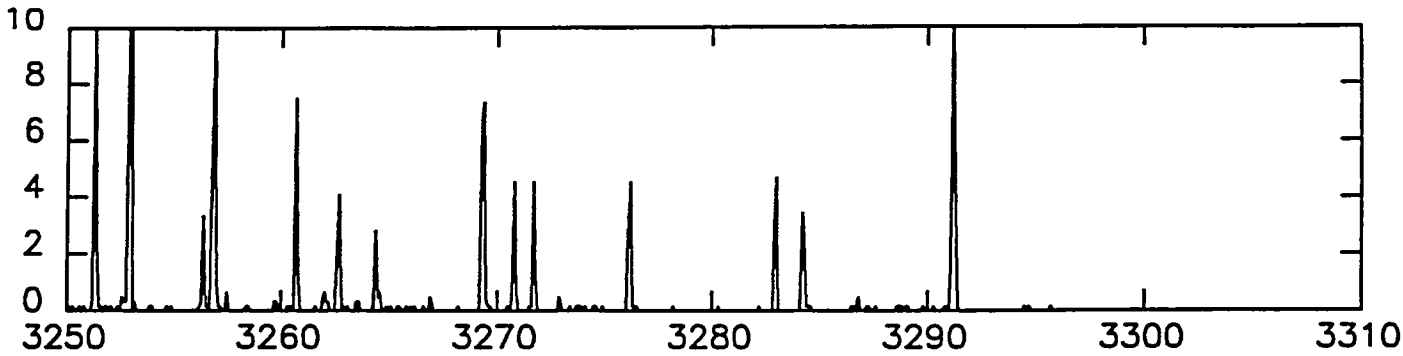
10
8
6
4
2
0
3250
3260
3270
3280
3290
3300
3310